NASA CONTRACTOR REPORT

NASA CR-1420

NASA CR-1420

CASE FILE COPY

EMISSIVITY COATINGS FOR LOW-TEMPERATURE SPACE RADIATORS

by G. R. Cunnington, J. R. Grammer, and F. J. Smith

Prepared by
LOCKHEED AIRCRAFT CORPORATION
Sunnyvale, Calif.

for Lewis Research Center

NATIONAL AERONAUTICS AND SPACE ADMINISTRATION • WASHINGTON, D. C. • SEPTEMBER 1969

NASA CR-1420

EMISSIVITY COATINGS FOR LOW-TEMPERATURE SPACE RADIATORS

By G. R. Cunnington, J. R. Grammer, and F. J. Smith

Prepared under Contract No. NAS 3-7630 by
LOCKHEED PALO ALTO RESEARCH LABORATORY
LOCKHEED MISSILES & SPACE COMPANY
Sunnyvale, Calif.

for Lewis Research Center

NATIONAL AERONAUTICS AND SPACE ADMINISTRATION

For sale by the Clearinghouse for Federal Scientific and Technical Information
Springfield, Virginia 22151 – CFSTI price $3.00

ABSTRACT

Studies were made on the effects of simulated solar ultraviolet radiation, temperature, and vacuum on the stability of solar absorptance and total hemispherical emittance of seven potential low-temperature space power system radiator coatings. A calorimetric in situ technique was used to measure broadband spectral and total absorptance and total hemispherical emittance as a function of time of exposure to an ultraviolet source (xenon lamp) at a 1-sun level.* Exposures were for durations varying from 500 to 10,000 hr and at temperatures from 300°K (80°F) to 533°K (500°F). The coatings investigated were titanium dioxide and zinc oxide pigments in methyl silicone binders; zinc oxide, zirconium silicate, and aluminum silicate in potassium silicate binders; and the Optical Solar Reflector. The Optical Solar Reflector was the most stable coating at 150°F; no change in its solar absorptance or total hemispherical emittance was observed during testing. Zinc oxide in potassium silicate (IITRI Z-93 system) showed the greatest stability for the paint-type coatings; total hemispherical emittance remained constant and solar absorptance increased 0.06 during 10,000 hr of exposure at 422°K (300°F).

*One sun is defined as the flux density of extraterrestrial solar radiation in the 0.20- to 0.40-μm wavelength region which is incident upon a flat plate oriented perpendicular to the solar vector at a distance of 1 astronomical unit (A.U.) from the sun.

FOREWORD

This document was prepared by the Lockheed Palo Alto Research Laboratory, Lockheed Missiles & Space Company, for the Lewis Research Center of the National Aeronautics and Space Administration as the final report of the research activities carried out under Contract NAS 3-7630. The NASA Project Manager was Mr. John A. Milko, Space Power Systems Division, Lewis Research Center.

CONTENTS

ILLUSTRATIONS

Figure		Page

Figure		Page

TABLES

Section 1
INTRODUCTION

The objective of this program is the evaluation of the environmental stability of coatings which would be used to obtain the maximum heat rejection efficiency for low-temperature spacecraft radiators. Several types of high thermal efficiency power systems being developed for use on spacecraft having long operational lifetimes present a problem regarding the optical properties of the radiator surface. To achieve maximum efficiency, this surface must have a high total hemispherical emittance over the radiator operating temperature range. However, to be consistent with high cycle thermal efficiency, the power systems reject heat at relatively low temperature. Therefore, for missions where the radiator is exposed to solar radiation, the surfaces must have a low absorptance to electromagnetic energy in the solar spectrum.

The stability of the radiative properties of the surface in the space environment is a critical factor since changes in either absorptance or emittance during a mission might result in severe problems with the power system operation. Changes in the radiative properties may occur because of exposure to temperature, vacuum, temperature cycling, and the complex radiation fields of the space environment. The requirement of high emittance and low solar absorptance precludes the use of bare metallic surfaces. Two classes of coatings or surface treatments meet the radiative properties requirement. These are the white pigmented paint-type coatings and the second surface mirror or Optical Solar Reflector (commonly referred to as the OSR). The white pigmented coatings typically show an increase in solar absorptance during prolonged exposure to simulated space radiation environment (Ref. 1). This change is a function of the energy and flux as well as the temperature and atmosphere during exposure. The OSR surface has been shown to be extremely stable in laboratory investigations (Ref. 2) for a wide range of environments.

A number of coatings have been developed which showed promise for the radiator application as their emittance is relatively high (greater than 0.80), solar absorptance is

low (0.20 or less), and in laboratory tests small changes in absorptance were observed during ultraviolet exposure in vacuum. Particulate (electrons and protons) radiation was not considered in this program because of the proposed orbit for this application, < 300 nm.

The program consisted of three phases. The initial phase had as its objective evaluation of the radiative properties and their stability for six candidate coatings under conditions of exposure (500 to 2000 hr) to ultraviolet radiation, vacuum of 1×10^{-7} Torr, elevated temperature, and temperature cycling. The second phase of the program was the long-term exposure (10,000 hr) of one coating selected on the basis of the result of Phase 1. The final phase of the program was the investigation of the second surface mirror for use at temperatures to 340°K (150°F). This material has been reported (Ref. 2) to have a solar absorptance of 0.06 or less with a total hemispherical emittance of 0.75 to 0.80. All ultraviolet exposure tests were conducted at a 1-sun level (0.20 to 0.40 μm).

The coatings investigated and their ultraviolet exposure conditions are:

- Titanium dioxide/methyl silicone (Thermatrol 2A-100, LMSC)
  395°K (250°F) – 550 hr
- Zinc oxide/methyl silicone (S-13, IITRI)
  395°K (250°F) – 500 hr
- Modified zinc oxide/methyl silicone (S-13G, IITRI)
  395°K (250°F) – 520 hr
- Zirconium silicate/potassium silicate (LMSC)
  533°K (500°F) – 500 hr
- Aluminum silicate/potassium silicate (Hughes)
  533°K (500°F) – 530 hr
- Zinc oxide/potassium silicate (Z-93, IITRI)
  300°K (80°F) – 2001 hr
  367°K (200°F) – 2024 hr
  422°K (300°F) – 500 hr

450 °K (350 °F) – 1004 hr
533 °K (500 °F) – 502 hr
422 °K (300 °F) – 4574 hr*
422 °K (300 °F) – 10,014 hr*

- OSR (LMSC)

  339 °K (150 °F) – 2040 hr

Of the paint-type coatings, the zinc oxide/potassium silicate system (IITRI No. Z-93) exhibited the greatest stability in solar absorptance at temperatures to 422 °K (300 °F). The change in solar absorptance observed during the three exposure tests at this temperature did not exceed 0.06. All other materials tested at 395 °K (250 °F) showed increases in solar absorptance of 0.08 or greater. At 533 °K (500 °F), the minimum increase in solar absorptance was 0.13, and this again was for the Z-93 material.

All of the coatings have initial values of solar absorptance of 0.12 or greater which drastically reduces radiator efficiency at temperatures of 339 °K (150 °F) or less. Thus it was decided to investigate the second surface mirror (OSR) concept, $\alpha_s \leq 0.06$, for the very low temperature radiator application. No change in solar absorptance was observed during a 2024-hr exposure test of this material at 339 °K (150 °F).

Detailed discussions of the experimental techniques and results are given in the following sections.

---

*Long-term exposure tests; first test terminated at 4574 hr due to vacuum system failure.

Section 2

LITERATURE SURVEY AND SELECTION OF COATING

2.1 BACKGROUND

A survey of the literature (Refs. 3 through 60) was conducted to provide the data for the selection of the candidate surfaces to be experimentally evaluated in this program. These findings are also applied to the evaluation and comparison of the experimental data of this program with those of other investigators.

The criteria for selection of the coatings were: solar absorptance $\leq$ 0.20 and total hemispherical emittance $\geq$ 0.80; long-term stability of optical properties, solar absorptance, and total hemispherical emittance; and adhesion and compatibility with the substrate material, 6061 aluminum. Coatings were evaluated for several environmental aspects considered to be potential sources of significant damage; i.e., ultraviolet irradiation, vacuum, elevated temperatures, and temperature cycling. The thermal-control coatings must be optically and physically stable at temperatures up to 533°K (500°F) for extended periods of time in the space environments.

Requirements of the space programs have resulted in the development of surface materials which have desirable thermal-control properties and which have some degree of resistance to degradation in the space environment (Refs. 1 through 13). These materials studies have for the most part been conducted at room temperature, with fewer studies at elevated and cryogenic temperatures. It has been a general observation that exposure to ultraviolet radiation degrades the properties of low α_s/ϵ surface materials by causing an increase in solar absorptance. The total hemispherical emittance of the more promising materials is not adversely affected by this environment. Changes in optical properties which occur during the vehicle lifetime may be accounted for in the vehicle thermal design when the extent of degradation is known as a function of exposure time and temperature.

Progress in the prediction of degradation rates and the development of stable materials has been hampered to a large extent by the lack of precise knowledge concerning the mechanisms of optical damage. A number of investigators have postulated various damage mechanisms (Ref. 14) in an attempt to understand the results on a specific material. However, the processes of degradation are complex, and for any given material several mechanisms appear to interact in producing the observed changes in spectral absorptance. While the postulated mechanisms have proved useful in guiding material development work, no complete picture is available which allows correlation from one exposure condition to another without experimental observations.

2.2 EFFECTS OF THE SPACECRAFT ENVIRONMENT

The radiation environment encountered by space vehicles is generally the most important source of damage to low α_s/ϵ thermal-control surfaces (Ref. 3). As the orbital conditions specified for this application were a near-earth orbit, 300 nm or less, the principal radiation environment considered was electromagnetic radiation in the ultraviolet spectrum. The candidate coatings were evaluated for the combined effects of ultraviolet radiation, vacuum, temperature, and temperature cycling. The selection of the initial coatings was based on the information available in 1966. A brief summary of space environmental effects on optical properties follows.

Ascent environment. The operational environment of a spacecraft begins with the ascent of the vehicle from the launch pad. The primary sources of damage during ascent are elevated temperatures (Ref. 15). However, it is very likely that the critical surfaces of low-temperature space radiators will be protected by a shroud or fairing during ascent, and consequently they will not be subjected to temperatures in excess of their maximum design operating temperatures during this phase of vehicle operation.

Vacuum. In addition to its role in the damage mechanisms, the extremely rarefied environment of vacuum makes volatilization of thermal-control coatings a

possible problem. However, coatings such as acrylics, silicones, and inorganic silicates that are used for thermal-control applications have been extensively studied in various environmental tests with no noted indications of instability due to vacuum alone.

Extraterrestrial solar radiation. In general, the continued exposure of many low α_s/ϵ materials to ultraviolet energy in a vacuum increases the solar absorptance until some saturation value is reached (Refs. 14 through 24). The total increase in solar absorptance is usually dependent upon temperature level and may or may not be a function of intensity of radiation. Figure 2-1 shows the solar absorptance of six coatings as a function of exposure time to ultraviolet radiation in sun-hours at room temperature (Ref. 24). The effect of ultraviolet radiation on the solar absorptance of several thermal-control materials at 530°K (495°F) is shown in Fig. 2-2 (Ref. 27). For several organic and inorganic systems the degradation has been observed to increase with increasing temperature as shown in Fig. 2-3. Spectral absorptance curves for a titanium dioxide/epoxy coating are shown in Fig. 2-4 to illustrate the change in spectral absorptance as a function of exposure temperature. An initial large change in absorptance due to exposure to ultraviolet radiation at 305°K (89°F) is observed. At increasing temperatures, the same exposure causes a general increase in absorptance with a fairly regular pattern. The shape of the curve at 530°K (495°F) appears to deviate considerably from the pattern for the lower temperature exposures which may indicate that a different process or a different rate of degradation has begun, so extrapolation of the data beyond this temperature would be unwise.

The spectral absorptance curves for the zirconium silicate/potassium silicate coating (Fig. 2-5) show a large initial change in absorptance due to exposure to ultraviolet radiation at 305°K (89°F). As the exposure temperature increases, the absorptance increases in the visible and infrared regions of the spectrum, but decreases in the ultraviolet region. The net result is an increase in the solar absorptance with increasing temperature.

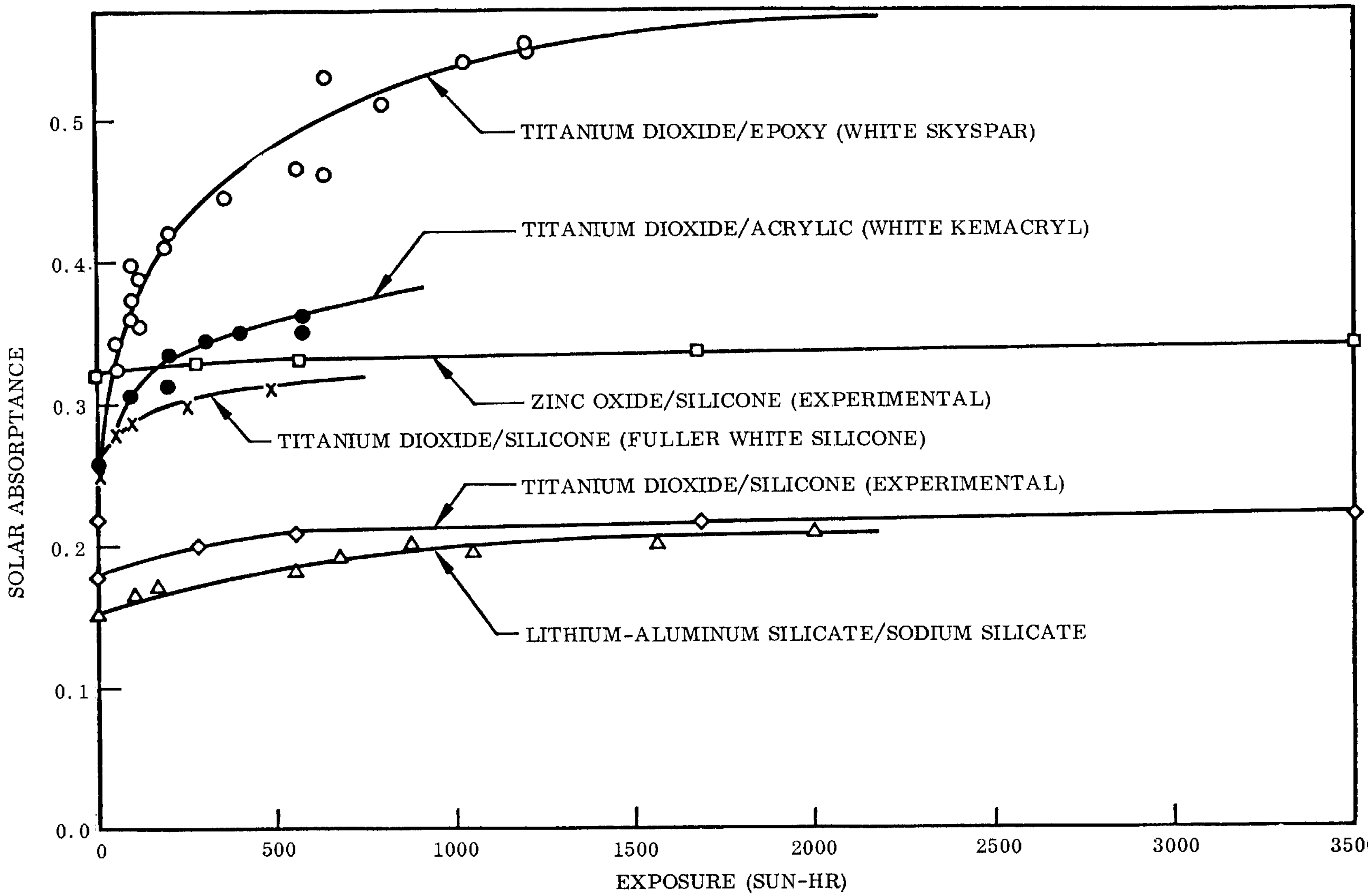

Fig. 2-1 Solar Absorptance Versus Ultraviolet Exposure at 300°K (80°F) (Ref. 24)

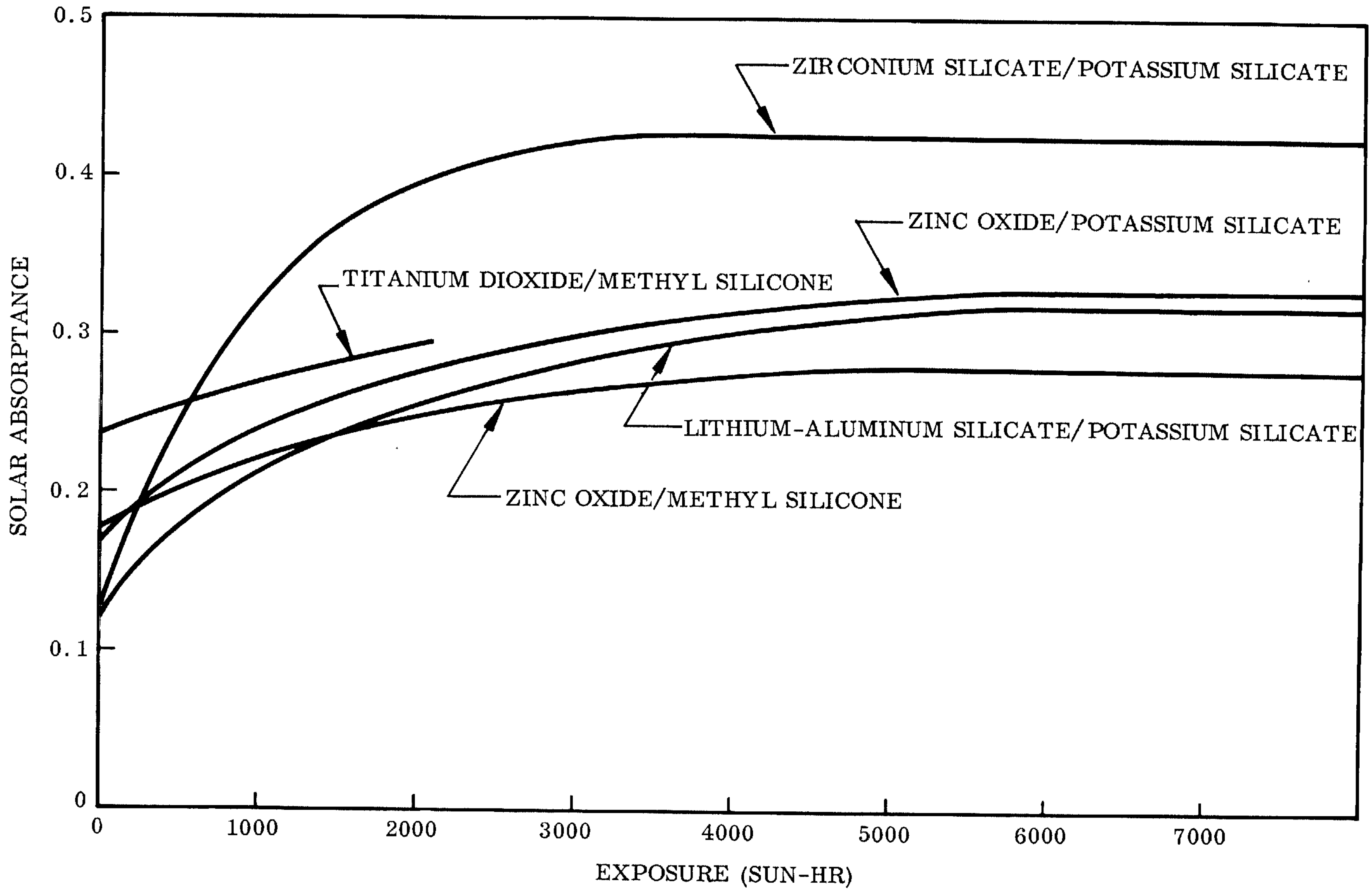

Fig. 2-2 Effect of Ultraviolet Radiation on Thermal-Control Surfaces at 530°K (495°F) and 10 Suns (Ref. 27)

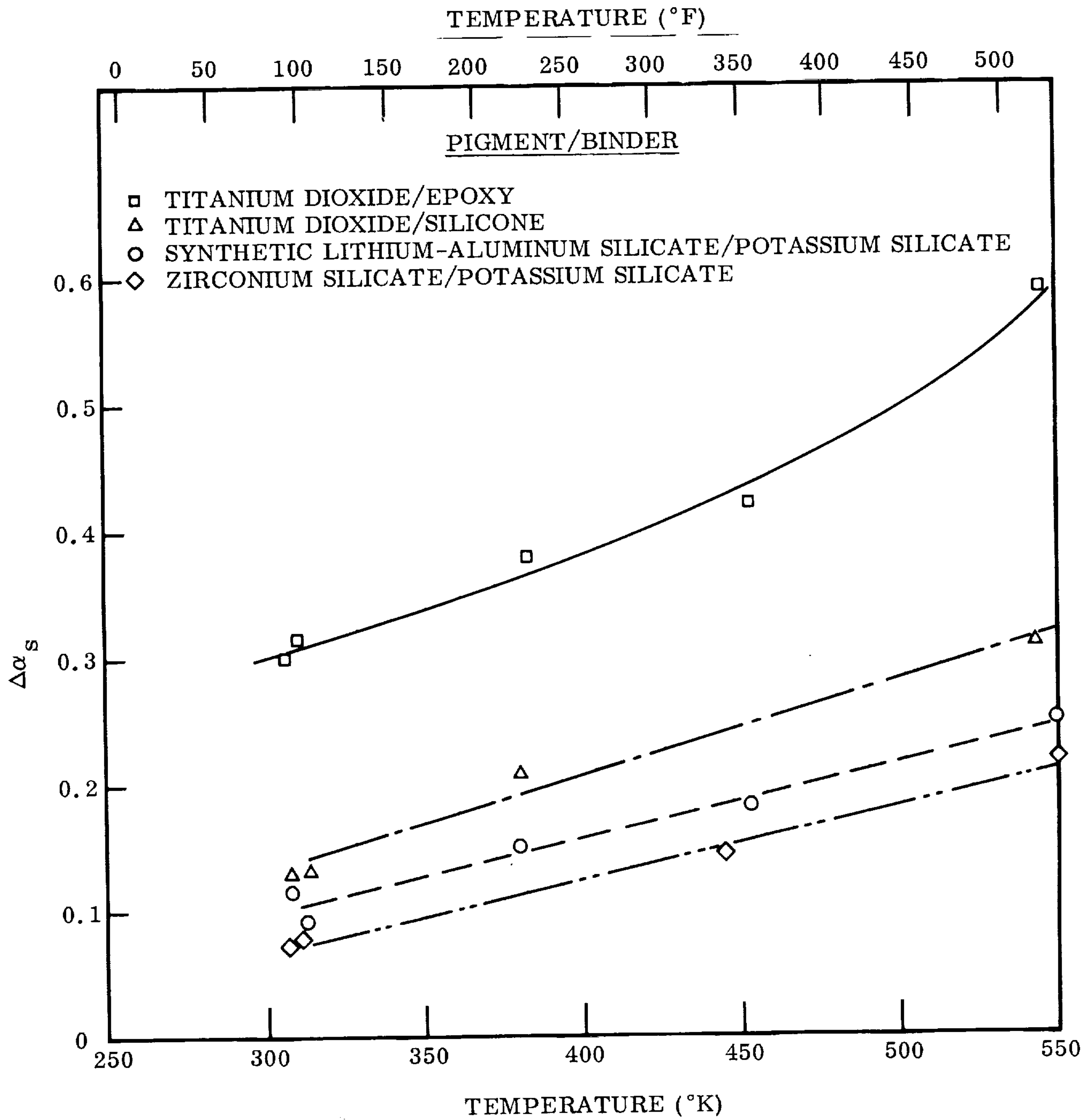

Fig. 2-3 Effect of Ultraviolet Exposure Temperature on Increase in Solar Absorptance of Four Thermal Control Coatings, 50-hr Exposure at 10-Sun Level (Ref. 24)

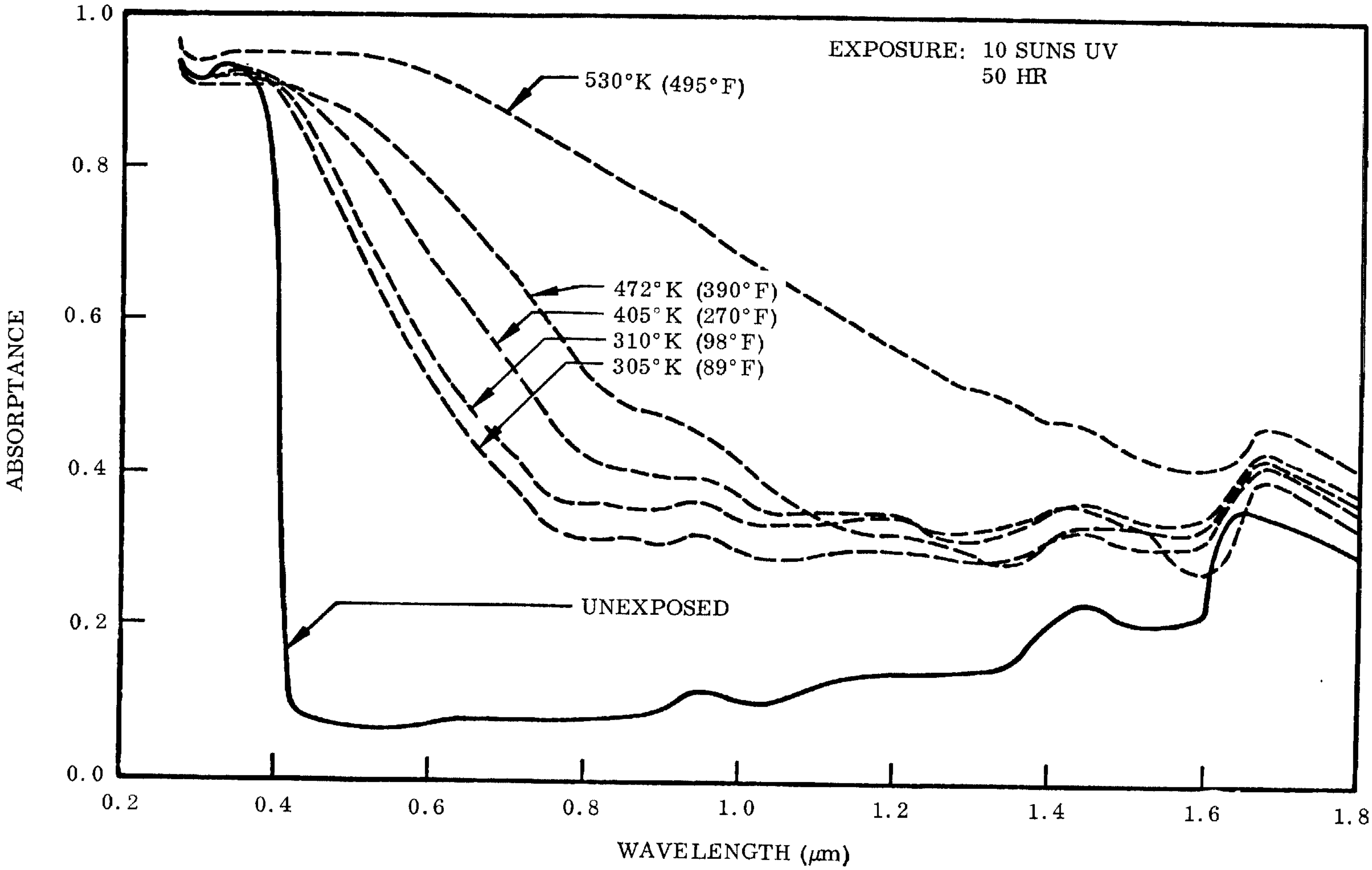

Fig. 2-4 Spectral Absorptance of Titanium Dioxide/Epoxy (Ref. 24)

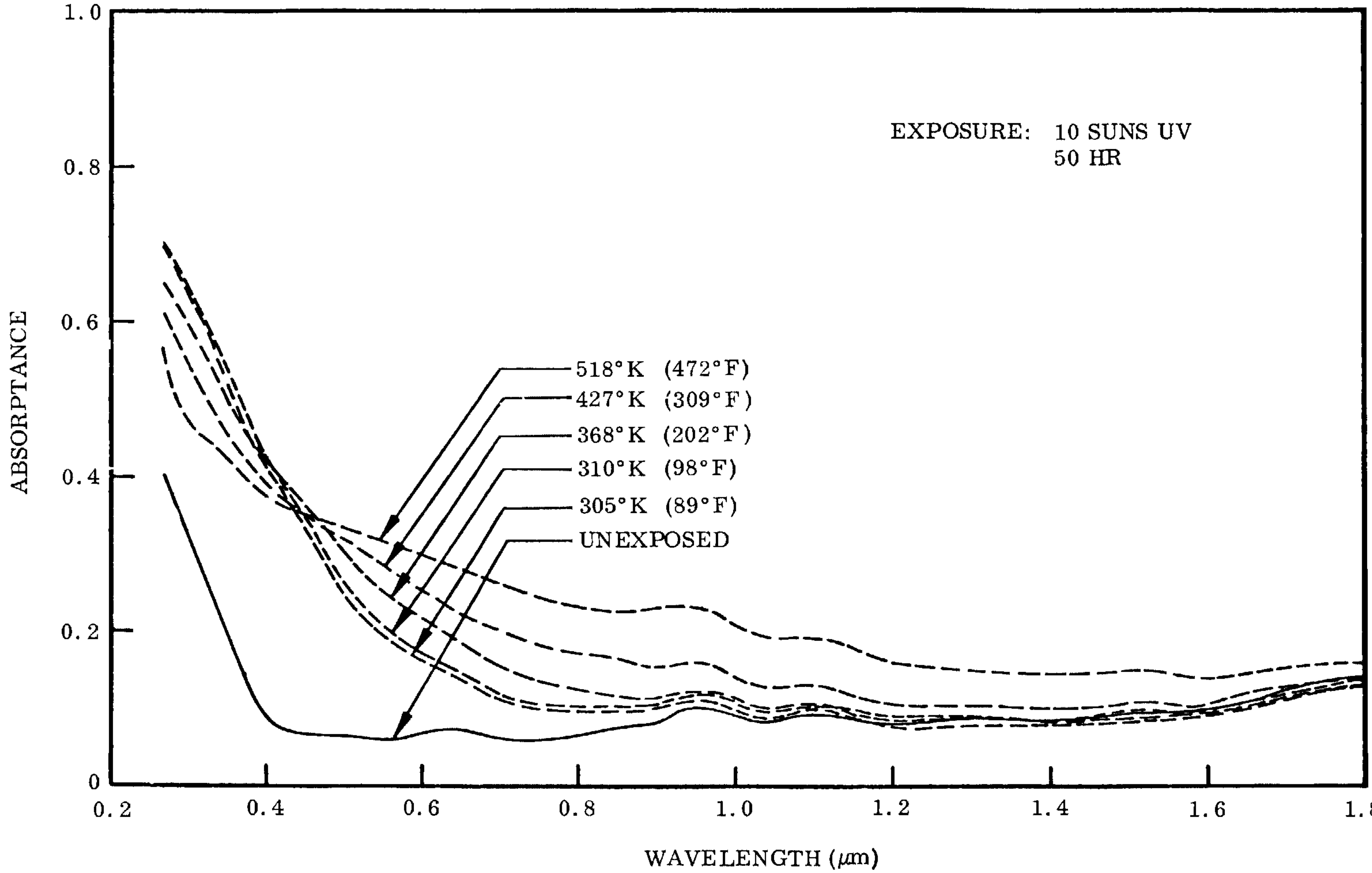

Fig. 2-5 Spectral Absorptance of Zirconium Silicate/Potassium Silicate (Ref. 24)

The ultraviolet radiation induced absorption of pigmented coatings may be related to the photolytic decomposition of the pigment material (Ref. 28). The liberation of oxygen from some pigments during irradiation has been postulated for materials such as zinc oxide (Refs. 14,30–33). At elevated temperatures in vacuum, the oxygen may then be physically desorbed creating a metal-rich surface. The metal diffusion into the bulk increases with increasing temperature resulting in increased absorption. Under a NASA-Marshall Space Flight Center contract (Ref. 14), LMSC has investigated solar radiation induced damage to the optical properties of zinc oxide. That program succeeded in demonstrating that the damage mechanism for zinc oxide pigments was based on a photochemical evolution of oxygen. Furthermore, on the basis of in situ measurements of ultraviolet radiation damage in vacuum, it was conclusively demonstrated that uv-degraded zinc oxide rapidly recovered its initial optical properties upon reexposure to air. This recovery phenomena has made much of the earlier exposure data suspect as degradation was evaluated on the basis of post-test reflectance measurements in air.

A second problem in evaluation of earlier data is that the assumption was made that a reciprocal relationship existed between the effects of time and ultraviolet irradiance, with regard to the damage produced; i.e., exposure to 1 sun for 10 hr will produce the same effect as exposure to 10 suns for 1 hr. Although this assumption served as a useful first approximation, it has not been proven to be valid for all of the materials under discussion. At the time of the coating selection, no long-term in situ exposures of thermal-control coatings at a 1-sun level and at elevated temperatures had been attempted to verify or disprove this assumption.

A final consideration is that the majority of exposure data had been obtained using a high pressure mercury lamp which has several very strong lines in the uv region and is not a good match to the solar spectrum.

Meteoroids. As no valid estimates had been made of the micrometeoroid flux at the time of the inception of this program, no evaluation was made of the effects of this environment on the candidate coatings.

Penetrating radiation. For prolonged mission exposure in a polar orbit or high-altitude (> 500 nm) trajectories, constituents of the space environment other than ultraviolet irradiation can induce first-order damage to optical surface materials; i.e., the intense high-energy electron and the low-energy proton portions of the geomagnetically trapped particle environment. In addition, for missions beyond the earth's geomagnetic field, the low-energy proton portion of the quiescent solar plasma (solar wind), galactic cosmic radiation, solar cosmic radiation from solar cosmic events, solar x-rays, and solar extreme ultraviolet radiation must be considered.

With regard to experimental techniques, in situ measurements on zinc oxide and titanium dioxide pigmented silicone paints (Ref. 53) specifically indicated that these paints exhibited the same damage and recovery phenomena as the free pigments. Also, results from the Ames emissivity experiment on OSO-II (Ref. 54) were in substantial agreement with the laboratory in situ results for these coatings. However, gross disagreement was observed between the flight data and conventional pre- and post-test measurements. The results of the in situ measurements coupled with the flight data lead to the incontestable conclusion that all prior uv radiation test data based on pre- and post-test measurements of optical properties performed in air must be critically reexamined. For this reason, considerable data of this nature which have been published prior to 1966 (during the period of this survey) have not been included in this report.

2.3 SELECTION OF COATINGS

The coatings to be evaluated in this program were selected on the basis of evidence available in the literature in 1966 which indicated high total hemispherical emittance, low solar absorptance, and stability in the space environment. The majority of

the exposure data available at the time of the selection was from post-exposure reflectance measurements in air and are therefore not reliable for some of the systems. In making the selection of materials recommended for study, the following criteria were considered:

- Thermal stability
- Stability under ultraviolet irradiation
- Solar absorptance and total hemispherical emittance
- Adhesion characteristics
- Compatibility with substrates

From the data compiled during the literature and technology survey, ten candidate coating materials were selected for detailed evaluation of the stability of optical properties under ultraviolet radiation in vacuum at elevated temperatures. These candidate coatings are tabulated in Table 2-1. Experimental data on the effects of ultraviolet radiation are shown in Table 2-2. Overall coating evaluations are presented in Table 2-3.

The sodium silicate coating systems were eliminated because of poor stability in ultraviolet radiation at elevated temperature, as shown in Fig. 2-3 and Table 2-2. Also, the titanium dioxide/polyvinyl butyral coating was eliminated because of its marginal ultraviolet stability even at room temperature and lower. The coatings listed in Table 2-4 were recommended as candidates for the 390° to 530°K range and the 295° to 390°K range. This recommendation was approved, and these coating materials were tested during the program. Complete descriptions of these coatings are contained in Appendix A.

Table 2-1

CANDIDATE COATING MATERIALS

Class	Binder	Pigment	Source
Inorganic	Potassium Silicate	Zirconium Silicate	LMSC
Inorganic	Sodium Silicate	Lithium-Aluminum Silicate	LMSC
Inorganic	Potassium Silicate	Lithium-Aluminum Silicate	LMSC
Inorganic	Potassium Silicate	Zinc Oxide	IITRI
Inorganic	Aluminum Phosphate	Chromium-Cobalt-Nickel Spinel with Stannic Oxide Overlay	AI
Inorganic	Potassium Silicate	Aluminum Silicate	Hughes
Organic	Methyl Silicone	Zinc Oxide	IITRI
Organic	Methyl Silicone	Titanium Dioxide	LMSC
Organic	Polyvinyl Butyral	Titanium Dioxide	American Cyanamid
–	Optical Solar Reflector[(a)]		LMSC

(a) This system consists of 6 to 8 mils of high purity fused silica with a vacuum-deposited silver second surface.

Table 2-2

EFFECT OF ULTRAVIOLET RADIATION

Pigment/Binder	Initial α_s	Final α_s	Exposure (sun-hr)	Temperature (°K)	Temperature (°F)	Data Reference	Coating Source
Zirconium Silicate/Potassium Silicate	0.13	0.42	7200	530	495	(27)	LMSC
	0.11	0.21	600	292	67	(10)	
Lithium-Aluminum Silicate/Sodium Silicate	0.16	0.49	280	530	495	(22)	LMSC
	0.13	0.19	600	292	67	(10)	
Lithium-Aluminum Silicate/Potassium Silicate	0.12	0.32	7200	530	495	(27)	LMSC
	0.11	0.15	440	292	67	(a)	
Zinc Oxide/Potassium Silicate	0.17	0.33	7200	530	495	(27)	IITRI
	0.16	0.18	1050	305	90	(23)	
Stannic Oxide Overlay on Chromium-Cobalt-Nickel Spinel/Aluminum Phosphate	0.35	0.46	3000	589	600	(55)[a]	AI
Aluminum Silicate/Potassium Silicate	0.17	0.22	1000	292	67	(9)	Hughes
Zinc Oxide/Silicone	0.18	0.27	7200	530	493	(27)	IITRI
	0.23	0.26	440	335	145	(27)	
Titanium Dioxide/Silicone	0.18	0.39	320	530	493	(27)	LMSC
	0.18	0.22	3500	292	67	(45)	
Titanium Dioxide/Butyral	0.19	0.27	2700	292	65	(a)	American Cyanamid
Optical Solar Reflector	0.05	0.05	430	292	65	(48)	LMSC

(a) LMSC Thermophysics Materials, Investigation Reports.

Table 2-3

OVERALL COATING EVALUATIONS

Pigment/Binder	Initial[a] α_s	Initial[a] ϵ	Thermal Stability 390°K (242°F)	Thermal Stability 530°K (495°F)	Adhesion	Substrate Compatibility (6061-T6)	Predicted Ultraviolet Stability 250°F	Predicted Ultraviolet Stability 500°F
Zirconium Silicate/ Potassium Silicate	0.11	0.85	Good	Good	Good	Good	Fair	Fair
Lithium-Aluminum Silicate/Sodium Silicate	0.13	0.85	Good	Good	Good	Good	Good	Poor
Lithium-Aluminum Silicate/Potassium Silicate	0.11	0.85	Good	Good	Good	Good	Fair	Fair
Zinc Oxide/Potassium Silicate	0.16	0.85	Good	Good	Good	Good	Good	Fair
Stannic Oxide Overlay, Chromium-Cobalt-Nickel Spinel/Aluminum Phosphate	0.35	0.91	Good	Good	Good	(b)	–	Fair
Aluminum Silicate/Potassium Silicate	0.17	0.85	Good	Good	Good	Good	Good	Fair
Zinc Oxide/Silicone	0.18	0.85	Good	Poor	Fair	Good	Good	–
Titanium Dioxide/Silicone	0.18	0.85	Good	Poor	Fair	Good	Fair	–
Titanium Dioxide/Butyral	0.19	0.85	Good	Poor	Fair	Good	Fair	–
OSR	0.05	0.80	Good	Good	Fair	Good	Good	Good

(a) Room Temperature
(b) 1100 Aluminum Substrate

Table 2-4

RECOMMENDED COATINGS

Temperatures to 533°K (500°F)	Coating Source
Zinc Oxide/Potassium Silicate	IITRI
Zirconium Silicate/Potassium Silicate	LMSC
Aluminum Silicate/Potassium Silicate	Hughes
Temperatures to 394°K (250°F)	
Zinc Oxide/Methyl Silicone	IITRI
Titanium Dioxide/Methyl Silicone	LMSC
Zinc Oxide/Potassium Silicate	IITRI
Temperatures to 339°K (150°F)	
Optical Solar Reflector	LMSC

Section 3
SAMPLE PREPARATION

The candidate coatings were applied by their manufacturers to disk substrates of 6061-T6 aluminum supplied by LMSC. The disks, 2.54-cm (1-in.) diameter by 0.050 in. thick, were polished on one side and edge to obtain an emittance of 0.03 ± 0.01. The emittance of each disk was inspected using a Lion Research Corporation Optical Surface Comparator to ensure conformance to the established standard. The surface to be painted was machined to a 30 ± 3 rms finish. A number of disks were randomly selected, and the surface roughness measured using a Micrometrical Manufacturing Company Proficorder. The results indicated that the machine surfaces were within the specified tolerance. The disks were instrumented for temperature measurement by inserting 1/4-in. long, 26-gage pins of constantan and chromel into the edge. The constantan-chromel combination was selected for its high thermoelectric emf and stability in the temperature range of interest. The pins were inserted 1/8 in. into the disk and were peened to ensure mechanical and electrical integrity. The pins were located 90 deg apart to give the sample stability when it is suspended in the chamber.

The calorimetric absorptance method requires that the specific heat of the substrate be accurately known. To provide these data, the specific heat of the 6061-T6 aluminum stock from which the substrates were cut was determined by LMSC. The method consisted of measuring the enthalpy of the material as a function of temperature using a flooded ice-mantle drop-type calorimeter. Enthalpy versus temperature data was fitted to the formula

$$\Delta H_{32} = a_o + a_1 T + a_2 T^2 + a_3 T^{-1}$$

using a least-square method. The computation was performed using a digital computer. Specific heat was calculated from the derivative with respect to temperature of the enthalpy equation. The specific heat and data are shown in Fig. 3-1. Maximum uncertainty in specific heat data is calculated to be 3%.

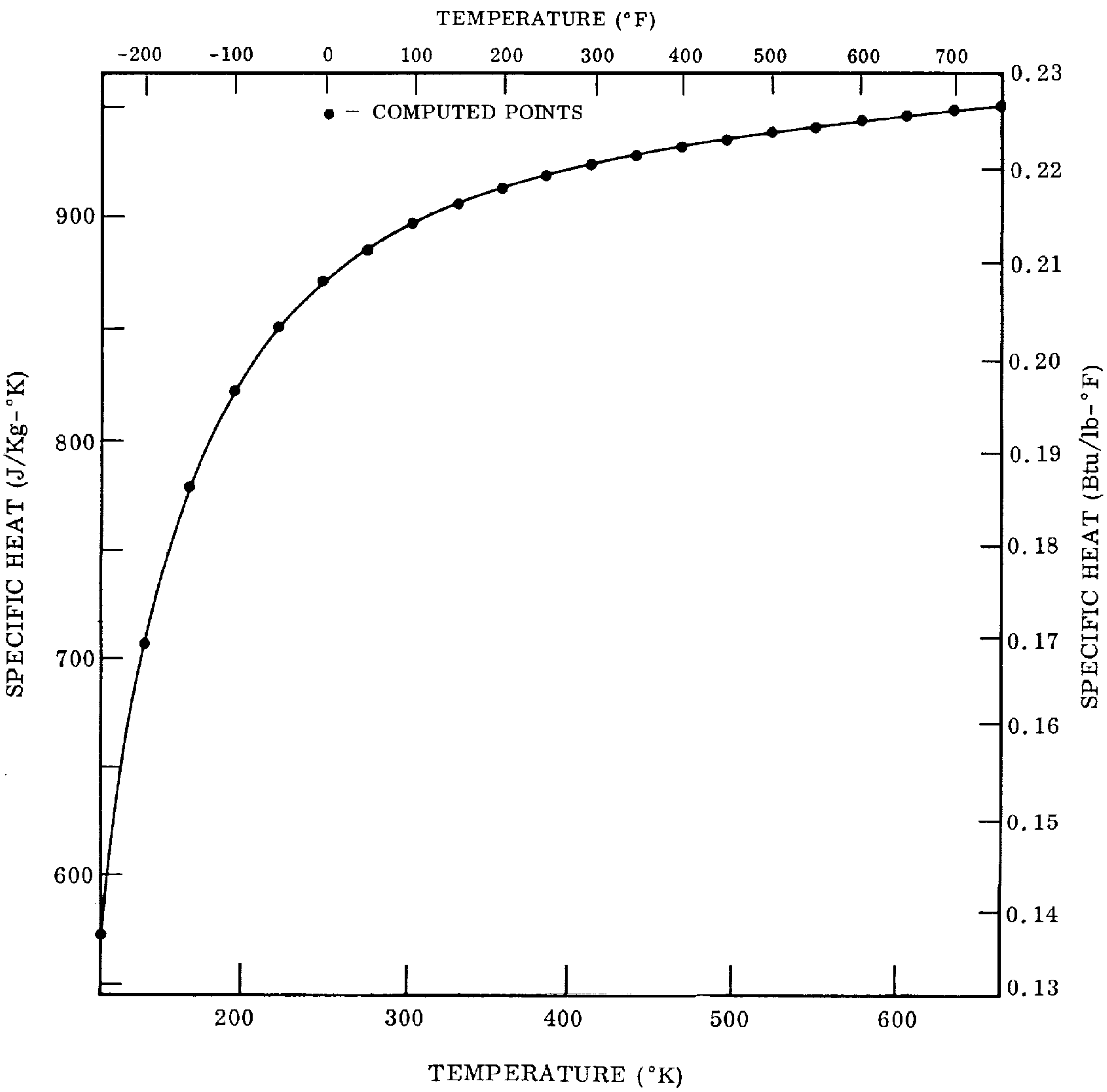

Fig. 3-1 Specific Heat Data of 6061-T6 Aluminum

Section 4
EXPERIMENTAL APPARATUS

4.1 THERMAL CYCLING

The ability of the coating systems to withstand thermal stresses was evaluated by cycling two samples of each coating-substrate combination four times between their maximum intended operating temperature and 83°K (-310°F).

Samples of the coatings were tested in the thermal cycling apparatus shown by Fig. 4-1. The apparatus consisted essentially of a sample holder, vacuum system, temperature control systems for the sample holder, and recorder for continuously monitoring coating substrate temperature. The sample holder was supported on the stainless steel base plate of the vacuum chamber within a glass bell jar. The system was pumped through a liquid nitrogen trap with a 4-in. oil diffusion pump and 5-cfm mechanical pump.

The sample holder, Fig. 4-2, was a machined copper block having six flat surfaces for mounting of the specimens. A 500-W cartridge heater was incorporated into the upper portion of the block, and a copper cooling coil, for passage of liquid nitrogen, was brazed to the lower end of the block. Heater power was controlled with a variable transformer. The cooling rate was controlled using two solenoid valves which regulated the flow of liquid nitrogen to the block by a bypass arrangement. This permitted maximum flow of liquid at the start of the cycle in order to achieve the required initial rapid cooling rate and then a reduction in flow to decrease the rate as a function of time.

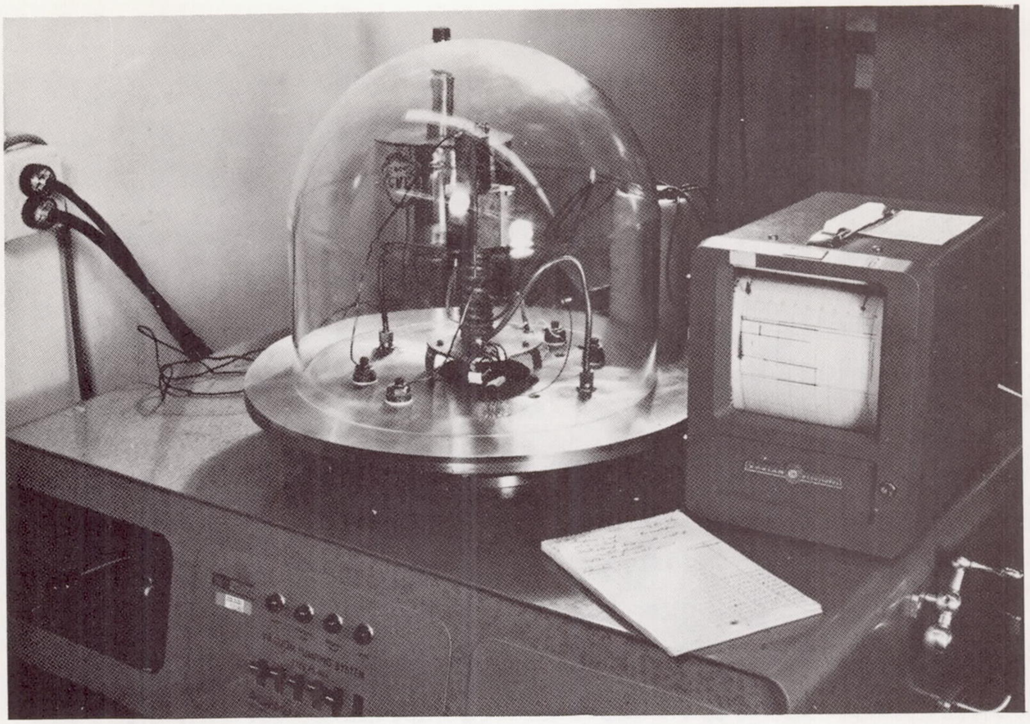

Fig. 4-1 Temperature Cycling Apparatus

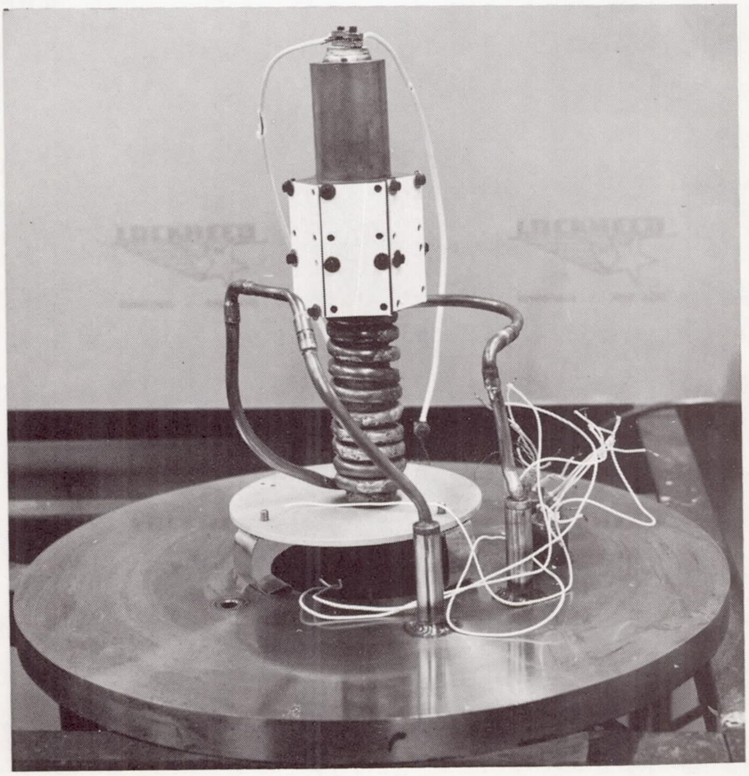

Fig. 4-2 Sample Holder

4.2 SPECTRAL REFLECTANCE MEASUREMENT APPARATUS

Pre- and post-test values of solar absorptance for each coating system were determined from room temperature near normal spectral reflectance measurements over the wavelength region of 0.27 to 1.8 μm. Pre-test total hemispherical emittance was calculated from room temperature near normal spectral reflectance measurements from 2.0 to 25.0 μm. A Lion Research Corp. Optical Surface Comparator was also employed to obtain a room temperature emittance value for each specimen of a given coating system.

The solar absorptance of test samples was determined by two separate procedures. The first method was by measurement of the spectral reflectance, 0.27 to 1.8 μm, with a Cary Model 14 spectrophotometer with an integrating sphere attachment. The resulting spectral data are then integrated against the Johnson curve (Ref. 52) to obtain solar reflectance from which the solar absorptance is inferred from Kirchoff's law. The Cary sphere is small and has relatively large apertures for entrance and exit of sample, reference, and sphere illumination beams. The sphere is illuminated by external optics and the reflected sample energy is directed to the entrance slits of the monochromator. Because of large apertures, a bright spot from the illuminating beam, and the small sphere size, it is obvious that the instrument has significant sources of error. The absolute magnitude of error is considerably reduced by establishing operational procedures which circumvent the major difficulties. Normal operations in the laboratory call for calibration of the system against a known first surface aluminum mirror. This is done by setting reflectance values at each wavelength to correspond to the known mirror properties. Unknown samples are then run, and the reading is obtained in absolute reflectance units. This procedure minimizes but does not eliminate effects of the apertures and bright spot. The data obtained are relative in the sense that the instrument is initially calibrated against a known surface. Therefore, continuous checks must be made to assure the validity of the values used for the calibration. The instrument is used as a control for large numbers of samples since it is easily operated, is fast, and within limits has reasonable accuracy. Where changes in spectrum or comparisons among identical samples are desired, it is a highly useful laboratory tool.

In view of the relative nature of Cary results,it is also necessary to obtain a limited number of absolute measurements to verify the Cary spectrum. These measurements were performed on a single beam Gier-Dunkle Model SP210 integrating sphere attached to a Perkin-Elmer Model 98 monochromator. This sphere is much larger than the Cary (24-cm diameter), has only two small apertures (entrance port 2.54-cm diameter, detector area ~ 2.5-cm diameter), and does not suffer from direct sample illumination of the detector. The sample is centrally mounted in the sphere and may be rotated at angles from 0 to 90 deg relative to the entrance port. When the sample is normal to the port, its shape factor to the hole is approximately 0.011. This construction permits direct measurements of the absolute reflectance of test samples and also permits cross checks which verify the validity of data obtained.

In normal operation, a 2.54-cm disk sample is mounted on the sample holder and rotated 10 deg off axis from the entry port. Monochromatic energy is then directed alternately to the sphere wall and then to the sample. Detector response is ratioed for each beam position with the ratio of response being directly the absolute reflectance of the sample. Detector response is rated for each beam position with the ratio of response being directly the absolute reflectance of the sample. This procedure is repeated for each required wavelength throughout the spectral region of 0.275 to 2.75 μm. The data are then integrated against the Johnson curve to obtain the solar absorptance.

The Gier-Dunkle instrument has an inherent accuracy of 0.01% in determination of spectral reflectance. When initial measurements are made using the Gier-Dunkle sphere and the results used to calibrate Cary measurements on identical samples, the accuracy in reflectance for the latter instrument is 0.02.

Measurements of spectral reflectance between 2 and 25 μm, are made with a Gier-Dunkle Model HC-300 heated cavity reflectometer, which is used in conjunction with a Perkin-Elmer Model 98 monochrometer and a Brewer Model 129 chopper-amplifier system. The optical system is a single-beam, double-pass arrangement. Near-normal reflectance measurements are made point-by-point at each wavelength of interest. For

most sample surfaces, the limit of precision is on the order of ±0.002, and the maximum absolute error is no greater than ±0.010 of the value of the measured reflectance, depending on the surface characteristics and reflectance of the sample. The heated cavity reflectometer contains a cooled sample that is irradiated by a surrounding hot cavity. Radiant flux reflected from the sample, in a small solid angle about the polar and azimuthal angles to the surface, fills the entrance slit of the monochrometer. The major sources of measurement error are associated with nonuniformity of the cavity wall intensity and with sample emission. Principal contributors to nonuniform intensity are (1) the presence of the water-cooled sample and sample holder, (2) specularity of the cavity walls, (3) temperature gradients along the cavity walls, and (4) the presence of the viewing port. By careful design of the cavity and sample-holder geometry and of the cavity heater circuits, the effects of the first three factors are reduced to negligible proportions relative to the viewing-port error. For a perfectly diffuse sample, the shape factor from the sample to the viewing point is $0.035 \cos \theta$. Thus, at near-normal viewing angles, an error of 3.5% is introduced. For a perfectly specular sample, the measurement at $\theta = 0$ deg is invalid since the reflected flux viewed from the sample originates from the viewing port itself. At angles of θ greater than about 15 deg, however, there is no error for a specular sample since the reflected flux then originates entirely from the cavity wall. For an arbitrary sample that is neither perfectly diffuse nor perfectly specular, some knowledge of the reflectance distribution function or bidirectional reflectance is necessary to assess the viewing-port error.

For the low infrared reflectance radiator coating sample materials, the emission error is minimized because the coatings are relatively thin and they are mounted on good conducting substrates (6061 aluminum). Using a high coolant flow rate, the surface temperature of the sample is maintained near room temperature. Measurements on the samples were performed at several coolant flow rates, and no change in reflectance was observed. Thus, the sample emission error is negligible for these specimens.

The error introduced by stray energy scattered by the optical components of the monochrometer is minimized by the use of a scatter plate at long wavelengths (i.e., $\lambda > 11\ \mu m$) and by filters.

A Lion Research Corporation Model 25 emissometer was used for comparative measurement of the room temperature emittance of each coating specimen. This unit is a radiometric comparison instrument that functions in the following way: First, the detector views a 0.9-in.-diameter surface area. Energy emitted from the surface passes through a KRS-5 window and is detected with a cooled thermopile that is mounted in an evacuated chamber. Before each measurement, the detector output is calibrated using three standards. The temperatures of the standard and the specimen are kept the same for a measurement. The standards for the measurements have total hemispherical emittances of 0.59 and 0.98.

4.3 EXPOSURE APPARATUS

The experimental exposure apparatus, shown in Figs. 4-3 and 4-4, consists of a vacuum chamber with liquid nitrogen cooled walls, a xenon lamp for the ultraviolet radiation source, a tungsten lamp source for maintaining the desired sample temperature, and the necessary controls and instrumentation for measuring sample temperature and monitoring and controlling the xenon and tungsten lamps. The vacuum is maintained by an electronic pump.

4.3.1 Vacuum Chamber

The vacuum chamber is a cylinder 30.5 cm (12.5 in.) in diameter and 63.5 cm (25.0 in.) long mounted in its major axis in a horizontal plane. It is capped with removable end plates sealed with O rings. Two 5.1-cm (2.5-in.) diameter Suprasil windows are provided, one in each end on the centerline of the cylinder, to transmit the ultraviolet irradiation and the energy from a tungsten lamp source to maintain the sample at the required temperature. The Suprasil windows were selected for stability in the long-term ultraviolet environment. Exterior shutters are provided to allow the energy to

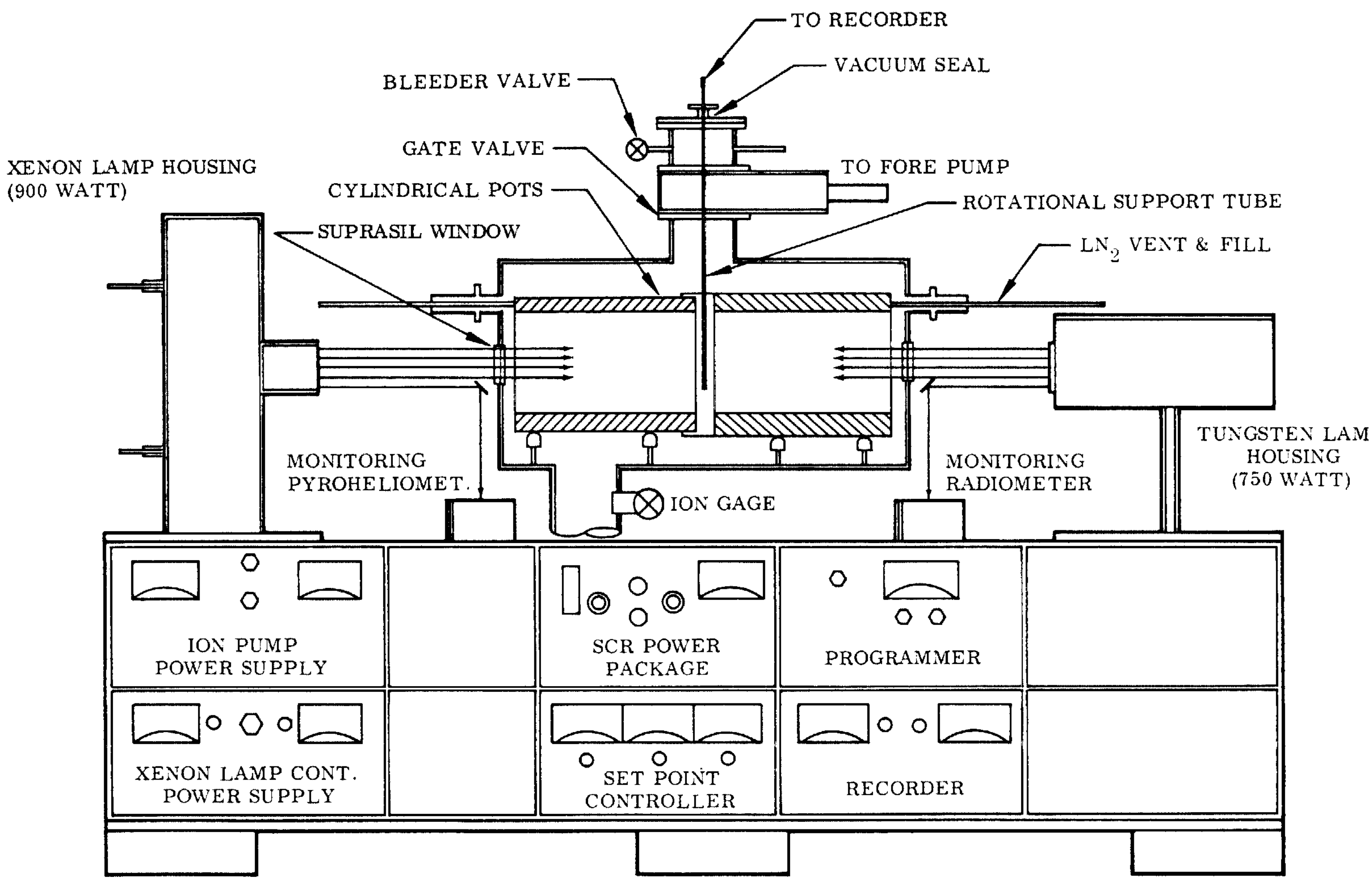

Fig. 4-3 Schematic of Exposure Device

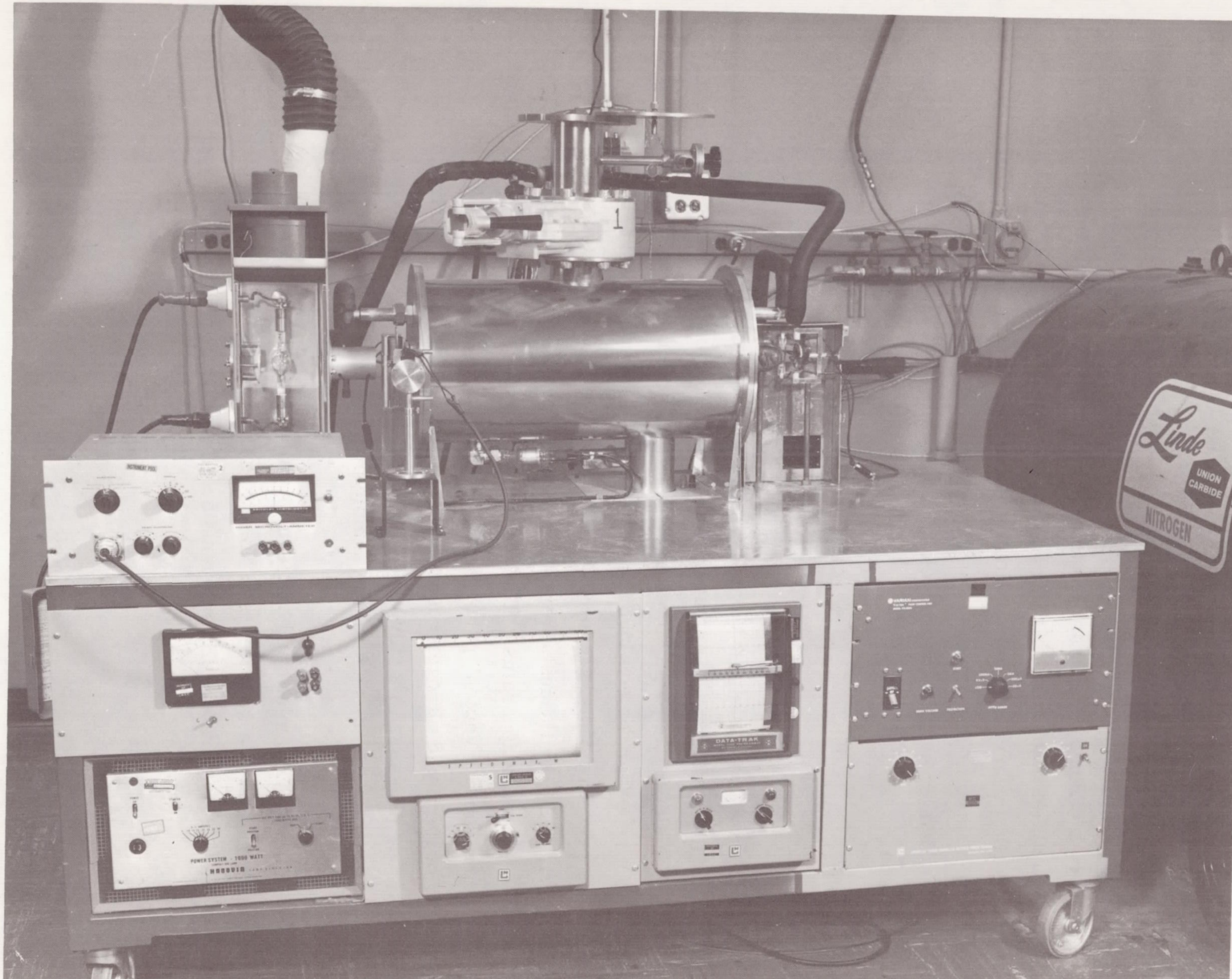

Fig. 4-4 Ultraviolet Exposure Apparatus.

be removed from the samples without disturbing the energy source. In addition, the chamber is equipped with 5.1-cm (2.5-in.)-diameter quartz inspection windows in the center of the cylinder and perpendicular to its centerline. Inside the vacuum chamber is a split copper liquid-nitrogen reservoir (Fig. 4-5), the halves of which may be separated to allow insertion of the test sample. The interior of the cold wall is painted black to ensure a diffusely absorbing heatsink. The paint is a Finch Paint and Chemical Co. "Cat-a-lac" flat black, Code 463-3-8, consisting of a carbon pigment in an epoxy binder. The LN_2 reservoir is automatically maintained nearly full by use of a timer-controlled fill system. The sample, suspended by the 0.003-in.-diameter thermocouple leads, is installed through a vacuum lock on the chamber with the cold wall in the separated position.

4.3.2 Vacuum System

The vacuum system consists of a Varian "VacSorb" forepump and a Varian 140 liter/second "VacIon" main pump. An ion gage is provided to measure chamber pressure. In addition, the electronic pump power control unit has a calibrated output which is connected to a recorder for continuous monitoring of pump pressure. The system operates at a pressure of not greater than 1×10^{-7} Torr. The vacuum system was modified during 1967 by the installation of a turbomolecular pump to increase the reliability of the exposure apparatus. The addition of this pump eliminated the possible loss of vacuum due to "VacIon" pump shutoff which occurs during gas burst loads or warming up of the liquid nitrogen reservoirs. It also is used when starting a test to reduce chamber pressure to a value such that ion pump starting time is less than 1 min, and, therefore, possible damage to the sample by pump starting discharge is eliminated.

The added pump is a complete turbomolecular pumping system, Welch Model 3102A. The system consists of a 260 liter/sec No. 3102 turbomolecular pump, a closed system mechanical refrigerator for continuous cooling of bearing housings, and a Welch "Duo-Seal" No. 1397 Fore Pump with connected valving to the turbomolecular pump.

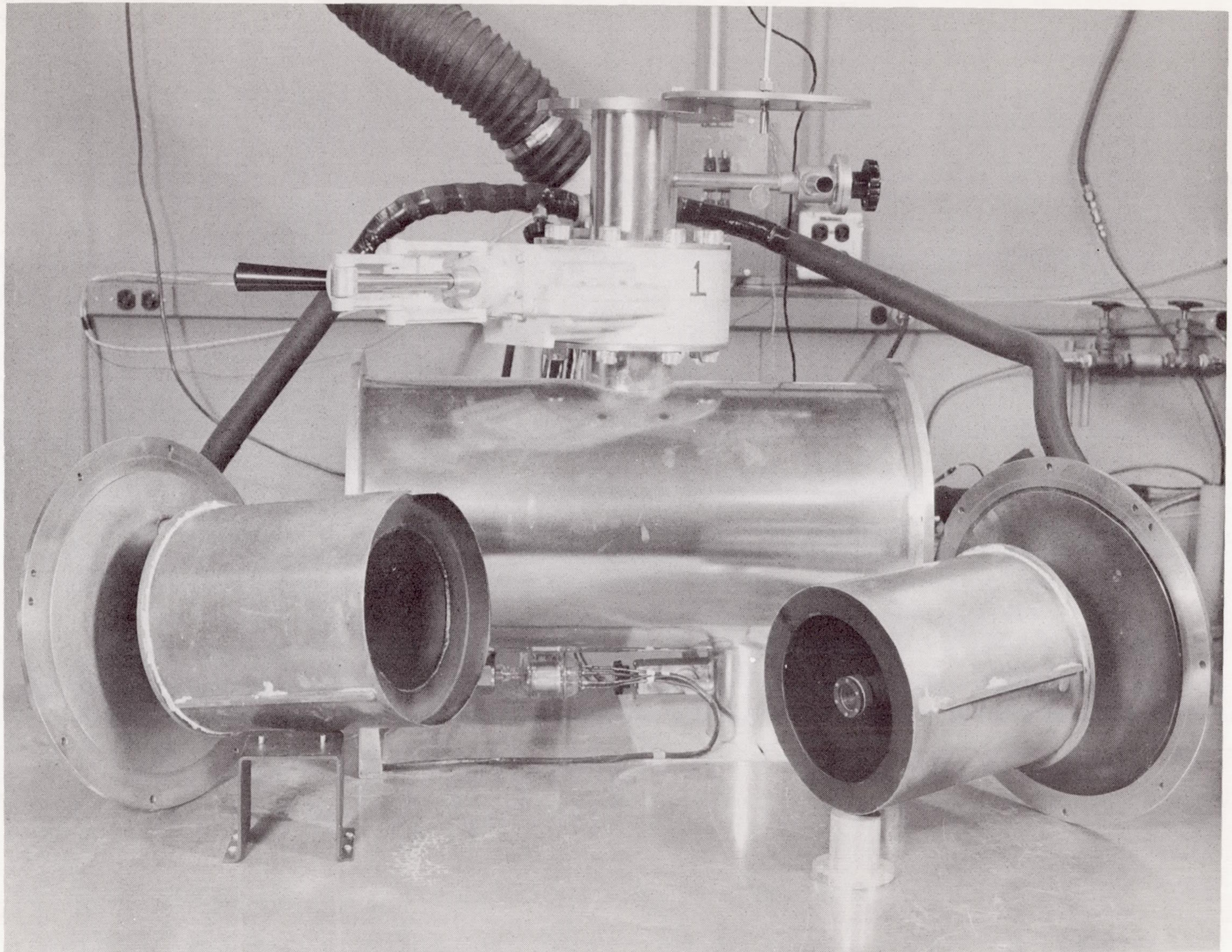

Fig. 4-5 Exposure Apparatus Inner Chambers

This turbomolecular system has a blank-off pressure of 2×10^{-9} Torr. The pumping speed is 260 liter/sec from 10^{-2} to 10^{-9} Torr. There is no detectable migration of forepump fluid vapors back into the system. The pump is connected to the two exposure chambers through pneumatically operated valves. The turbomolecular pump is used to rough down the chambers to 10^{-6} Torr and then used as a standby for the VacIon pumps. The pneumatically operated valves are controlled by a relay which is actuated by chamber pressure. A significant rise in pressure will connect the turbomolecular pump to the chamber until good vacuum conditions are reestablished.

4.3.3 Ultraviolet Source

The ultraviolet source is a 900-W Hanovia xenon lamp, Model 538-CL, mounted in an Orion Optics Corporation universal lamp housing, Model C-60-50-5-15. This lamp housing uses a 11.5-cm (4.5-in.) focal length, 3.8-cm (1.5-in.) diameter quartz condensing lens as a collector. The energy collected by the lens is augmented by the use of a spherical mirror placed behind the lamp to reimage the arc back on itself. The intensity of the lamp is controlled by an Engelhard Hanovia Model 27801, 1000-W, dc power system, including both a current regulating power supply and a high voltage RF starter.

The spectral energy distributions of the source were determined at the sample position in order to characterize specimen irradiation conditions. Measurements were performed with the lamp in its housing and the chamber window between the lamp and specimen position. Distances from lamp to window and window to specimen position were identical with those used for the exposure testing. In this manner, the effects of lamp optics and the window were included in the spectral irradiance data.

Xenon lamp calibration was accomplished using a Cary Model 14 spectrophotometer fitted with a Cary Part No. 50-601-020 radiometer accessory. This accessory utilizes a rotating integrating sphere to alternately collect the energy from the unknown source and a calibrated G. E. Type DXW-1000-W quartz-iodide reference lamp.

Light from the sphere is then passed through the entrance slit of the spectrophotometer. The reference lamp (Eppley No. EPI-1228) was previously calibrated against a NBS traceable standard lamp.

Spectral irradiance data at the sample position (39 cm from sphere entrance port) for the ultraviolet source are shown in Fig. 4-6. These are compared with the extra terrestrial solar spectral irradiance data of F. S. Johnson (Ref. 52). This lamp was aged 50 hr prior to measurement. Spectral irradiance measurements were also made on lamps which had been operated 1000 to 1500 hr. For these lamps, operated at power levels which gave the same total irradiance at the sample location as a new lamp, a 10 to 15% decrease in energy in the 0.20- to 0.40-μm spectral band was observed. Comparative band energy data are shown in Table 4-1.*

Table 4-1

COMPARISON OF XENON SOURCE ENERGIES AS A FUNCTION OF LAMP OPERATING TIME

Spectral Band (μm)	Irradiance (W/cm^2)		
	Solar (Ref. 52)	Xenon Lamp (50 hr)	Xenon Lamp (1500 hr)
0.20/0.40	0.0126	0.0127	0.0109
0.40/0.60	0.0392	0.0331	0.0315
0.60/0.85	0.0356	0.0522	0.0539

Uniformity of the source total irradiance at the sample position was determined by traversing across the beam using a thermopile detector. The radial variation in energy did not exceed 10% within 1 cm of the center of the sample position, Fig. 4-7. The irradiance as a function of distance along the optic axis was determined using a 1-cm aperture thermopile. A 1-cm variation in sample position resulted in less than 5% variation in irradiance, Fig. 4-8.

---

*As measured by an Eppley No. 9780 Thermopile located at sample position.

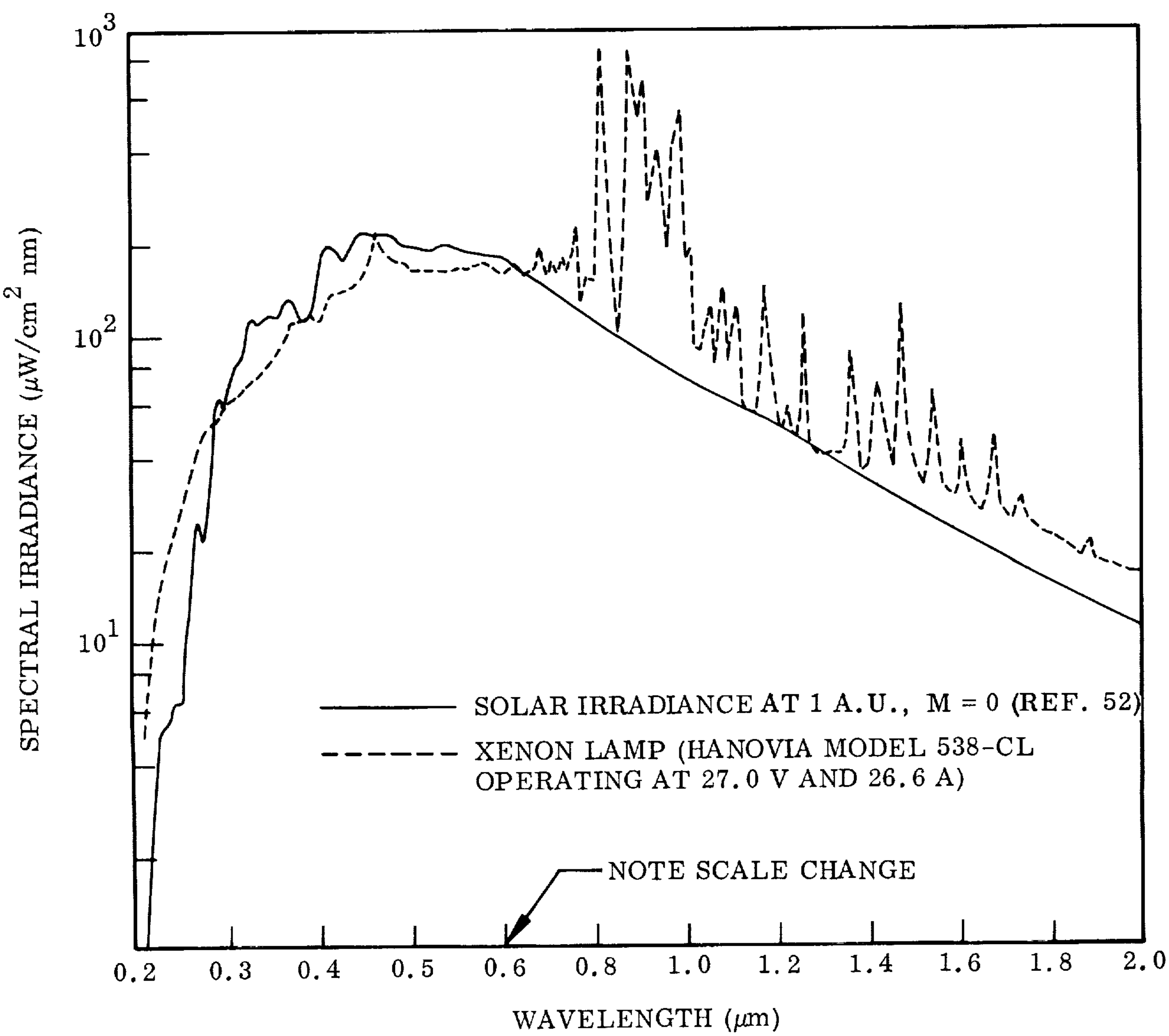

Fig. 4-6 Spectral Irradiance of Xenon Ultraviolet Source at Sample Position Compared to Extraterrestrial Solar Spectral Irradiance at 1 A. U.

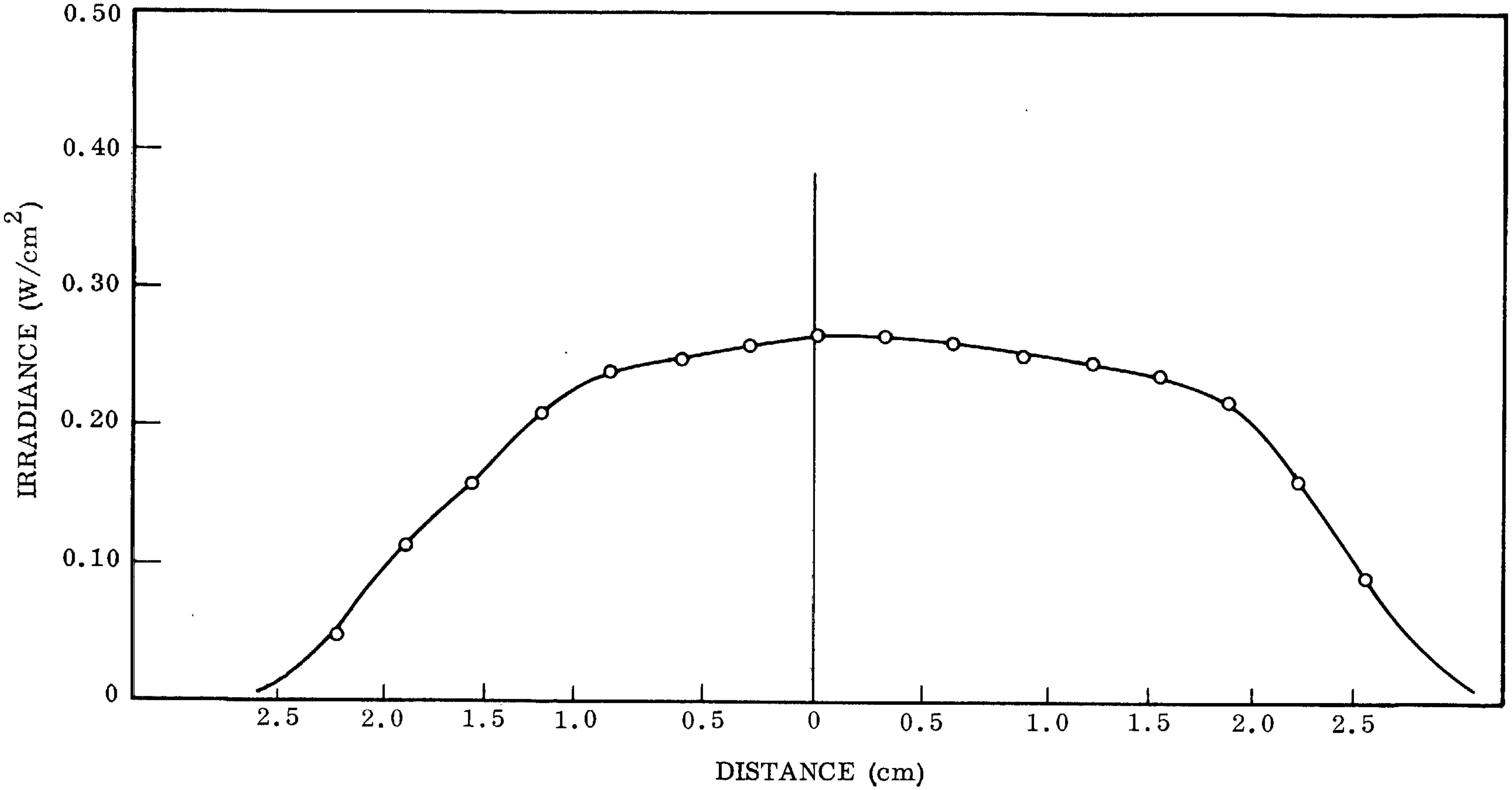

Fig. 4-7 Transverse Energy Distribution of Lamp Beam

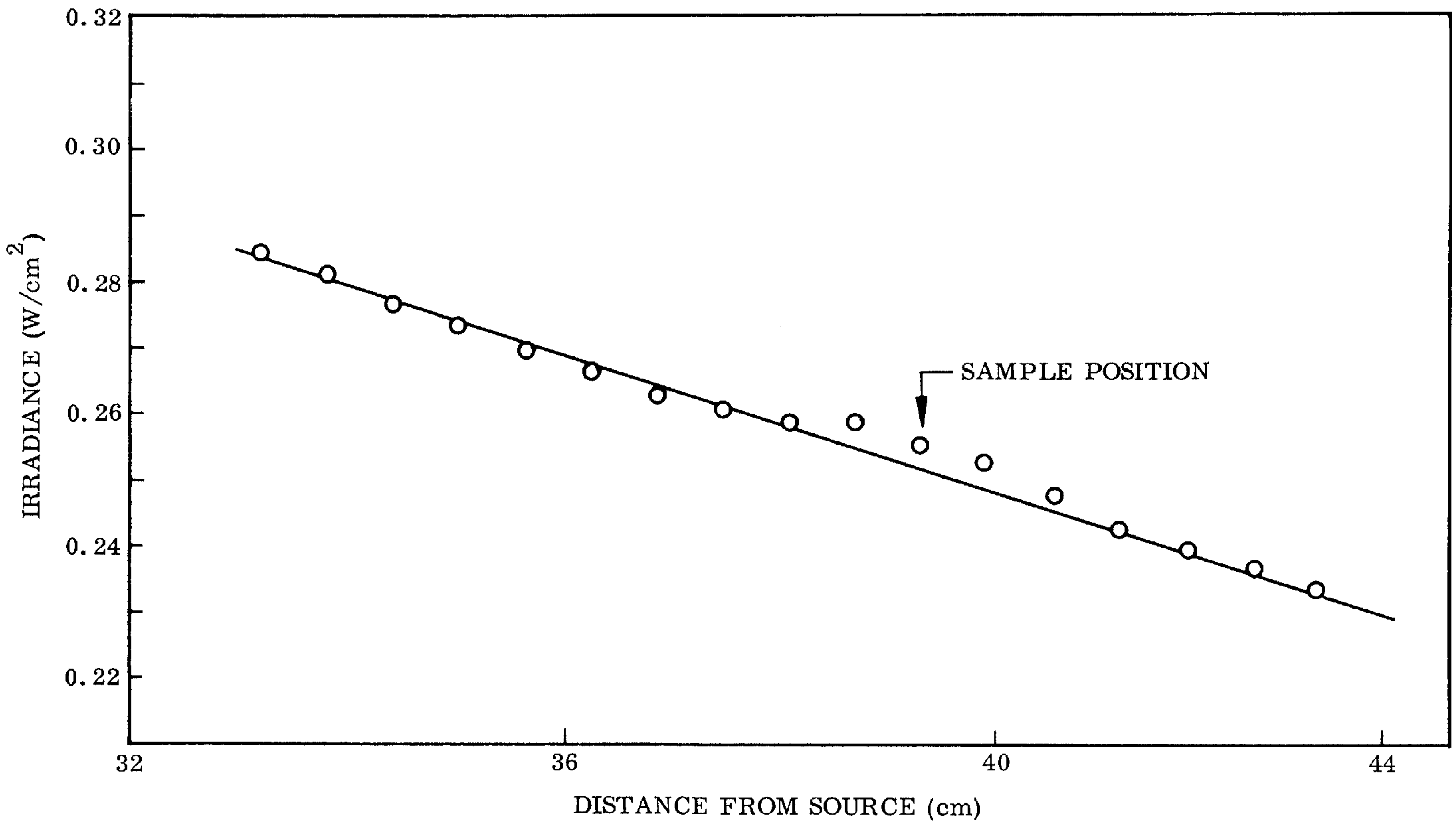

Fig. 4-8 Irradiance as a Function of Source Distance

Monitoring of the xenon source during a test was accomplished using an Eppley thermopile which was mounted exterior to the chamber and at the sample distance from the source as the test specimen. Energy was directed onto the thermopile by inserting a first surface mirror into the beam between the source housing and the exposure chamber. Both total irradiance and irradiance in the 0.23- to 0.42-μm band were monitored. A Corning No. 7-54 filter was used for the spectral monitoring. A Corning No. 2-63 filter was employed to correct for the 0.55- to 1.25-μm transmission band of the 7-54 filter.

4.3.4 Tungsten Lamp Radiant Heater

A tungsten lamp is used to provide the additional energy necessary to maintain the samples at the required temperature. A 1000-W tungsten iodide lamp, GE DXW, with a light pipe arrangement, is used to provide heating of the back surface of samples. The light pipe shown in Figs. 4-4 and 4-5 consists of a short external aluminum tube, polished on the inside, which extends from the lamp to the exterior of the chamber window. A spherical mirror mounted in back of the lamp augments the energy collected by the light pipe. The internal light pipe is a polished copper tube extending from the chamber window to the sample. The tube is attached to the liquid nitrogen cold wall, and its exterior surface is coated with a diffuse black paint. The end of the tube adjacent to the sample is fitted with a sapphire window. The optical and thermal properties of the window are such that it appears, to the sample, to be identical to the cold wall. This has been verified experimentally in the apparatus by measuring the slope of the temperature decay of the sample with the sample in normal position and then rotating the sample 90 deg and remeasuring temperature decay. Comparison of results indicates no errors are introduced by the tungsten source light pipe.

The tungsten source is controllable and programmable, thus the sample can be maintained at a given temperature or thermally cycled automatically. The control system and power supply consists of four major interconnected components. A Leeds and Northrup Speedomax W AZAR recorder provides a continuous record of sample

temperature. A slide wire output from the recorder is fed into a Leeds & Northrup current adjusting type set point controller. The controller regulates the power output from a Leeds & Northrup SCR, which in turn controls the intensity of the tungsten lamp. When the sample is to be temperature cycled, an RI Controls, "Data-Track" card programmer is used to provide the desired reference signal for control of the cycle.

Section 5
EXPERIMENTAL PROCEDURES

5.1 THERMAL CYCLING TEST

All coatings were thermally cycled, in duplicate, four times from their maximum intended operating temperature to near liquid nitrogen temperature. Chamber pressure was maintained at 5×10^{-6} Torr or lower during testing. The rate of temperature change during cooling was selected to simulate the cooling of a gas radiator in space, with the heat source removed, when the radiator is in the earth's shadow. Calculations of the cooling curves were based upon a 0.159 cm (1/16 in.) thick 6061-T6 aluminum flat plate radiator having a coating with a 0.85 total hemispherical emittance on both faces. Figures 5-1 and 5-2 show the calculated cooling curves for the 395°K (250°F) and 533°K (500°F) operating temperatures and the actual cooling curves as measured during the testing. Each cycle consisted of holding the sample at test temperature (395° or 533°K) for 1/2 hr, a cooling period for 6 hr, and a 17.5-hr period during which time the sample temperature slowly increased to 300°K (80°F). The specimen was then brought to test temperature within 10 min and the cycle repeated. Specimens were attached to the holder at the edge of the disk at two points 180 deg apart, using No. 8-32 stainless steel screws and washers. As heating and cooling were by conduction between the copper block and substrate, a silicone heat-transfer grease (Dow-Corning DC-340) was placed at this interface to minimize thermal contact resistance. Sample temperatures were measured using chromel-constantan thermocouples affixed to the coating substrate. Temperatures were measured using a Minneapolis-Honeywell (SX153X-67) multipoint strip chart recorder.

The test criterion was based upon visual observation of the coatings during and following testing with no cracking or spalling evident to the unaided eye. Also pre- and post-test photographs were made of each sample 1× and 100× magnification.

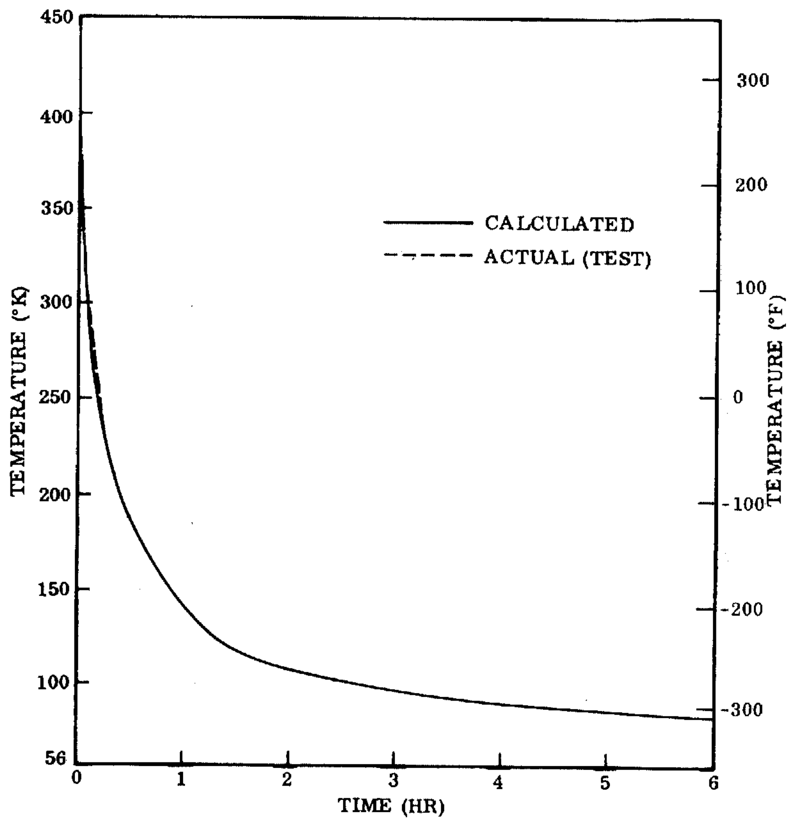

Fig. 5-1 Calculated and Actual Cooling Curve for 395°K (250°F) Coatings

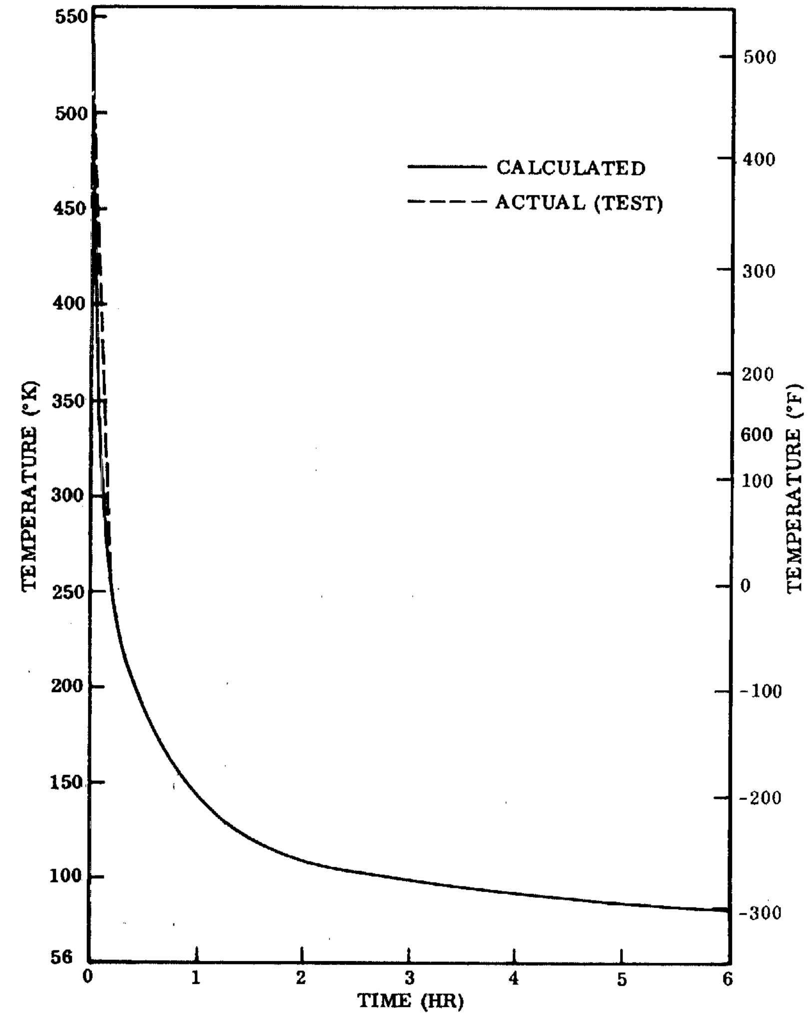

Fig. 5-2 Calculated and Actual Cooling Curve for 533°K (500°F) Coatings

5.2 EXPOSURE TEST

5.2.1 Total Source Absorptance

Absorptance measurements are made by alternately heating and cooling the specimen which is an aluminum disk coated on one surface with the material undergoing exposure. This specimen is suspended in a vacuum chamber having liquid nitrogen cooled walls, and the coated surface is exposed to a nearly collimated beam of energy from the xenon lamp. Energy from the tungsten filament lamp is focused onto the polished rear surface of the disk for maintaining the specimen at a desired temperature level.

For a disk sample having one side painted, while the edges and other sides are polished aluminum surfaces, the thermal behavior is described by the following equation:

$$mc_p \frac{dT}{d\theta} = G_H A_H \alpha_H - \epsilon_H A_H \sigma T^4 - (A_e + A_t)\,\epsilon_t \sigma T^4 - CA_w T + G_t A_t \alpha_t \qquad (5.1)$$

where

mc_p = sensible heat of specimen

$dT/d\theta$ = rate of change of absolute temperature with time

$G_H A_H \alpha_H$ = energy absorbed from a source of irradiance G_H by the painted surface A_H having an absorptance for the source spectral distribution of α_H

$\epsilon_H A_H \sigma T^4$ = energy emitted by painted surface area A_H at temperature T with surface emittance ϵ_H

$(A_e + A_t)\,\epsilon_t \sigma T^4$ = energy emitted by the back surface area A_t and the edge surface A_e at temperature T with surface emittance ϵ_t

$CA_w T$ = energy transferred from the sample by thermocouple lead wires

$G_t A_t \alpha_t$ = energy absorbed from tungsten lamp source of irradiance G_t by the sample back surface A_t with absorptance α_t for the lamp spectrum

If the sample is held at a constant temperature by the tungsten lamp and then exposed to irradiation at the front surface by a solar simulation source at a constant energy level, the heating response is:

$$mc_p\left(\frac{dT}{d\theta}\right)_h = G_H A_H \alpha_H - \epsilon_H A_H \sigma T_h^4 - (A_e + A_t)\epsilon_t \sigma T_h^4 - CA_w T_h + G_t A_t \alpha_t \quad (5.2)$$

By blanking off the solar simulation source with a shutter, and maintaining the tungsten source constant, the cooling response is:

$$mc_p\left(\frac{dT}{d\theta}\right)_c = - \epsilon_H A_H \sigma T_c^4 - (A_c + A_t)\epsilon_t \sigma T^4 - CA_w T_c + G_t A_t \alpha_t \quad (5.3)$$

Subtraction of the cooling response from the heating response yields:

$$mc_p\left[\left(\frac{dT}{d\theta}\right)_h - \left(\frac{dT}{d\theta}\right)_c\right] = G_H A_H \alpha_H \qquad \text{for} \qquad T_c = T_h \quad (5.4)$$

Let

$$\left(\frac{dT}{d\theta}\right)_h = R_h \quad \text{and} \quad \left(\frac{dT}{d\theta}\right) = R_c \quad (5.5)$$

Then

$$mc_p(R_h - R_c) = G_H A_H \alpha_H \quad (5.6)$$

and

$$\alpha_H = \frac{mc_p(R_h - R_c)}{G_H A_H} \quad (5.7)$$

Total source irradiance, G_H, is measured for each data point using a thermopile detector located exterior to the chamber. Measured irradiance is corrected for window transmission and mirror reflectance to yield sample irradiance.

5.2.2 Conversion From Source to Solar Absorptance

From the spectral irradiance H_λ incident on the sample and the spectral absorptance of the sample, the source absorptance α_H may be converted into a solar absorptance α_s. The value of α_H obtained in the preceding manner may be written as

$$\alpha_H = \frac{1}{H} \int_0^\infty \alpha_\lambda H_\lambda d\lambda$$

The solar absorptance may be written as

$$\alpha_s = \frac{1}{S} \int_0^\infty \alpha_\lambda S_\lambda d\lambda \quad (5.8)$$

Thus,

$$\alpha_s = \alpha_H \frac{H}{S} \frac{\int_0^\infty \alpha_\lambda S_\lambda d\lambda}{\int_0^\infty \alpha_\lambda H_\lambda d\lambda} \quad (5.9)$$

A knowledge of the spectral absorptance of the sample is required to convert from a source absorptance to a solar absorptance. Absorptances obtained from pre- and post-test reflectance measurements may be used, but these are valid only for coating systems which do not exhibit partial recovery of the ultraviolet damage upon reexposure to air (Ref. 53). Also, if absorptance data are desired as a function of time during continuous exposure, some spectral data are required at each time interval. Broad-band spectral measurements are made to form a basis for shifting the original spectral absorptance curve as the surface degrades. This permits an increased accuracy in the conversion from source absorptance to solar absorptance both during testing and for the final value at the completion of the exposure.

5.2.3 Broadband Spectral Absorptance

Broadband spectral absorptances are determined by the use of sharp cut-off filters, Corning filters Nos. 7-57, 2-63, and 3-75. Transmissions of these are shown plotted in Fig. 5-3 with the relative spectral distribution of a xenon lamp. This choice divides the absorptances into four regions; 0.2 to 0.41, 0.41 to 0.60, 0.60 to 0.85, and 0.85 to 2 μm. The absorptances are determined from the filter transmissions and the spectral distribution of the source. From the relation

$$\alpha_H = \frac{m\,C_p}{A_H G_H}(R_h - R_c)$$

Let

$$\frac{m\,C_p}{A_H G_H} = K_H$$

$$\alpha_H = K_H(R_n - R_c) \qquad (5.10)$$

then

Placing the 3-75 filter, f_1, in front of the xenon lamp then

$$\alpha_{f_1} = \frac{A}{\tau_{f_1}}(R_n - R_c)_{f_1} \qquad (5.11)$$

where τ_{f_1} is the transmission of the 3-75 filter for the xenon source, and R_h and R_c are the measured heating and cooling slopes for the sample with the filter interposed between the sample and source. Likewise for the other two filters, filter 2-63 = f_2 and filter 7-57 = f_3, we have

$$\alpha_{f_2} = \frac{K_H}{\tau_{f_2}}(R_n - R_c)_{f_2} \qquad (5.12)$$

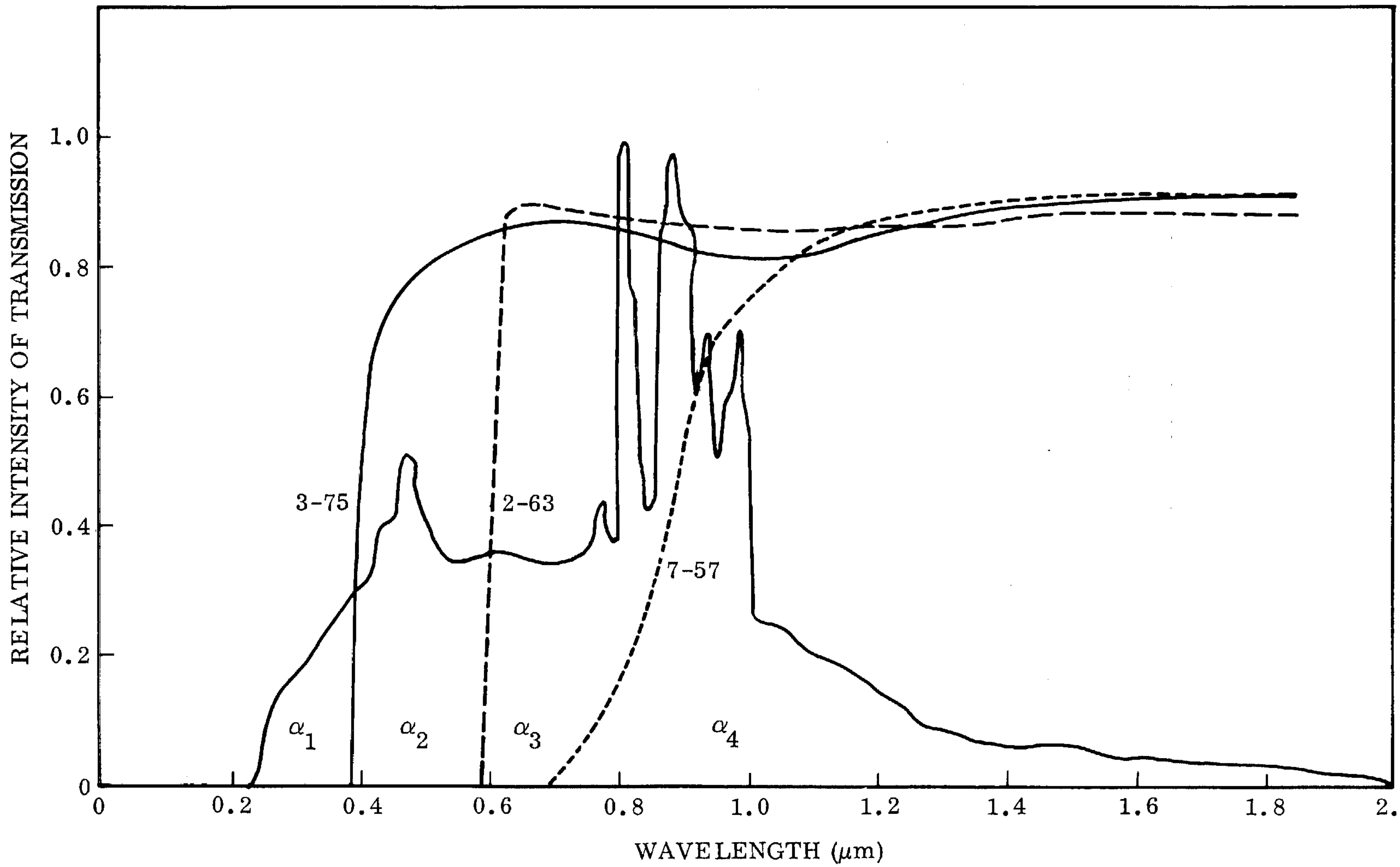

Fig. 5-3 Spectral Radiant Intensity of Xenon Lamp and Transmission of Filters

and

$$\alpha_{f_3} = \frac{K_H}{\tau_{f_3}} (R_n - R_n)f_3 \tag{5.13}$$

The transmissions τ_{f_1}, τ_{f_2}, and τ_{f_3} are measured using the xenon source and an Epply thermopile. Thus, the total transmission of the filters weighted for the spectral distribution of the xenon source is determined directly.

The relative distribution of the xenon source in the four spectral bands is determined using two identical sets of the filters. By measuring the transmission for one filter and then for both filters, the transmission of the filter in its transmission band is determined. Dividing the transmitted signal by this transmission band transmission and the total signal we have the percentage energy of the xenon lamp source in the transmission band of the filter. Subtracting this from 100 gives the percentage energy in the cut-off region of the filter. In this manner the percentage energies of the source E_1, E_2, E_3, and E_4 in the four spectral regions shown in Fig. 5-3 are determined. The band absorptances may now be calculated. For the total absorptance and filter f_1 the following relationship applies

$$\alpha_H = E_1\alpha_1 + (1 - E_1)\alpha_{f_1}, \qquad \text{total} \tag{5.14}$$

where $\alpha_1 = \alpha_{0.2 \text{ to } 0.41\,\mu\text{m}}$

$$\alpha_1 = \frac{\alpha_H - (1 - E_1)\alpha_{f_1}}{E_1} \tag{5.15}$$

For filters f_1 and f_2 we have

$$(1 - E_1)\alpha_{f_1} = E_2\alpha_2 + [1 - (E_1 + E_2)]\,\alpha_{f_2} \tag{5.16}$$

$$\alpha_2 = (1 - E_1)\alpha_{f_1} - \frac{[1 - E_1 + E_2]\,\alpha_{f_2}}{E_2} \quad \text{for} \quad 0.41 \text{ to } 0.6\,\mu \tag{5.17}$$

For filters f_2 and f_3 we have

$$(1 - E_1 - E_2)\alpha_{f_2} = E_3\alpha_3 + (1 - E_1 - E_2 - E_3)\alpha_{f_3} \tag{5.18}$$

$$\alpha_3 = \frac{(1 - E_1 - E_2)\alpha_{f_2} - (1 - E_1 - E_2 - E_3)\alpha_{f_3}}{E_3} \quad \text{for } 0.6 \text{ to } 0.85\,\mu\text{m} \tag{5.19}$$

For the wavelength region α_4 from $\lambda > 0.85\,\mu m$ the absorptance of this region is given by the 7-57 filter or α_{f_3} thus

$$\alpha_4 = \alpha_{f_3} \tag{5.20}$$

5.2.4 Uncertainty Analysis

The total source absorptance is determined from Eq. (5.7)

$$\alpha_H = \frac{mc_p(R_h - R_c)}{G_H A_H}$$

The maximum probable error of a variable $M = f(w, y, z)$ is given by the relation

$$\Delta M = \left[\left(\frac{\partial M}{\partial x}\right)^2 + \left(\frac{\partial M}{\partial y}\right)^2 + \left(\frac{\partial M}{\partial z}\right)^2\right]^{1/2} \tag{5.21}$$

Thus, for the above equation we have the maximum probable error in α_H given by

$$\frac{\Delta\alpha_H}{\alpha_H} = \left[\left(\frac{\Delta m}{m}\right)^2 + \left(\frac{\Delta c_p}{c_p}\right)^2 + \left(\frac{\Delta G}{G}\right)^2 + \left(\frac{\Delta A}{A}\right)^2 + 2\left(\frac{\Delta R}{R_h - R_c}\right)^2\right]^{1/2} \tag{5.22}$$

Data typical for the samples measured result in the following uncertainty:

$$m = 1.70 \text{ g} \qquad \frac{\Delta c_p}{c_p} = 0.05^*$$

$$c_p = 900 \frac{J}{Kg} \text{ °K} \qquad \frac{\Delta G}{G} = 0.03$$

$$\alpha_H = 0.20 \qquad \frac{\Delta R}{R_h - R_c} = 0.006$$

$$G_h A_H = 1.0 \text{ W} \qquad \frac{\Delta m}{m} = 0.003$$

$$R_h - R_c = 7 \times 10^{-1} \text{ °K/sec} \qquad \frac{\Delta A}{A} = 0.0020$$

$$\frac{\Delta m}{m} = 0.003$$

Thus, the maximum uncertainty in source absorptance, α_H, is 5.9%. The total solar absorptance is determined from Eq. (5.9)

$$\alpha_s = \frac{H\alpha_H \int_0^\infty \alpha_\lambda S_\lambda d\lambda}{S \int_0^\infty \alpha_\lambda H_\lambda d\lambda} \tag{5.23}$$

A parameter N is established which relates the spectral absorptance and the solar and source spectrums. It is defined as:

$$\frac{\int_0^\infty \alpha_\lambda S_\lambda d\lambda}{\int_0^\infty \alpha_\lambda H_\lambda d\lambda}$$

---

*Includes effect of uncertainty in coating heat capacity on total heat capacity of coating plus aluminum substrate.

Therefore:

$$\Delta\alpha_s = \left[\left(\frac{\Delta H}{H}\right)^2 + \left(\frac{\Delta S}{S}\right)^2 + \left(\frac{\Delta\,\alpha_H}{\alpha_H}\right)^2 + \left(\frac{\Delta N}{N}\right)^2\right]^{1/2} \qquad (5.24)$$

For a material having an absorptance of 0.2, the calculated uncertainty, based upon spectral absorptance data, is 9.3%.

For the broadband absorptance measurements, consider a filter which transmits all the source radiant energy above 0.4 μm. The probable error given as

$$m = 1.7 \text{ g} \qquad \frac{\Delta A}{A} = 0.002$$

$$c_p = 900 \frac{J}{Kg} \,{}^\circ K \qquad \frac{\Delta G}{G} = 0.03$$

$$\alpha_H = 0.20 \qquad \frac{\Delta c_p}{c_p} = 0.05$$

$$G_H A_H = 0.83 \text{ W}$$

$$(R_h - R_c) = 1.2 \times 10^{-1} \,{}^\circ K/sec \qquad \frac{\Delta R}{(R_h - R_c)} = 0.0035$$

$$\frac{\Delta m}{m} = 0.003 \qquad \frac{\Delta T'}{T'} = 0.02$$

$$\frac{\Delta\alpha_{H_1}}{\alpha_{H_1}} = \left[\left(\frac{\Delta m}{m}\right)^2 + \left(\frac{\Delta c_p}{c_p}\right)^2 + \left(\frac{\Delta G}{G}\right)^2 + \left(\frac{\Delta A}{A}\right)^2 + \left(\frac{\Delta T'}{T}\right)^2 + 2\left(\frac{\Delta R}{R_h - R_c}\right)^2\right]^{1/2} \qquad (5.25)$$

Where T is the transmission of filter and ΔT its uncertainty.

$$\frac{\Delta\alpha_{H_1}}{\alpha_{H_1}} = 7.9\%$$

For a filter which transmits all the source radiant energy above 0.6 μm, the probable error is 8.7%, and for a filter which transmits all the source radiant energy above 0.8 μm, the probable error is 12.0%.

In summary, the maximum uncertainty for the xenon source absorptance value is 5.9%. The maximum uncertainty in the solar absorptance value computed from the broad-band spectral absorptance data is determined by the uncertainty for each of the broad-band spectral absorptances weighted against the energy in each spectral band. This is calculated to be 12% for the data reported here.

5.2.5 Total Hemispherical Emittance

The total hemispherical emittance of the coating is determined by blanking off both incident beams from the xenon and tungsten lamps, and recording the temperature response of the sample.

With $G_T = G_h = 0$, Eq. (5.2) becomes

$$m\, c_p \frac{dT}{d\theta} = - \epsilon_{TH} A_H \sigma T^4 - (A_e + A_t)\epsilon_t \sigma T^4 - C A_w T \tag{5.26}$$

$$\epsilon_{TH} = - \left[\frac{m\, c_p \frac{dT}{d\theta} + (A_e + A_t)\epsilon_t \sigma T^4 + C A_w T}{A_H \sigma T^4} \right] \tag{5.27}$$

This relationship permits computation of ϵ_{TH} from the temperature history recorded during cooling and a knowledge of $m \cdot c_p$. The measured emittance of the aluminum edges and backface of the disk provides a very low value of ϵ_t making the second term small in comparison to the first. Also, the sample is suspended in the chamber by 3 mil thermocouple wires which makes the third term in Eq. (5.27) negligible. The specific heat is that of the coating-aluminum disk combination. Substrate

specific heat is known to 3%. For some of the coatings, actual specific heat measurements had been made earlier on the coating material under a separate program. For those which had not been measured, specific heat was calculated using the law of mixtures from data in the literature on the various constituents of the system. For these specimens, the mass of the coating was less than 10% of the total. Thus, a 20% error in calculated coating specific heat results in a 2% error in specific heat of the composite. The calculated maximum uncertainty in ϵ_{TH} is 0.04 for the specimens tested in this program (i.e., for an ϵ_{TH} of 0.86, the uncertainty results in $\epsilon_{TH} = 0.90/0.82$).

Section 6
EXPERIMENTAL RESULTS

6.1 THERMAL CYCLING TEST

No evidence of cracking or spallation of any of the coatings was observed by the unaided eye or at 100× magnification. The areas directly adjacent to the mounting screws were disregarded during the examination as clamping pressures could have introduced stresses at these points which are not relevant to the purpose of this test. Both samples of the aluminum silicate/potassium silicate coating had several areas of a slightly brown appearance during and after testing. One sample had a greater number of discolored brown spots than the other. Room temperature spectral reflectance measurements were performed on these samples after the test. The sample solar absorptances calculated from these data showed an increase of 0.04 for one specimen and 0.07 for the other. No attempt was made to determine the cause of this discoloration. However, it was extremely improbable this could be attributed to contamination by the test system. Four other specimens were tested in the chamber at the same time and they showed no evidence of discoloration.

6.2 EXPOSURE TEST

Test samples of seven thermal control coatings were exposed to uv irradiation at a 1-sun level. The exposure conditions and a summary of the results are presented in Table 6-1. During the screening tests, the samples were cycled to room temperature every 4.7 hr. Cycle time was 10 min.

Table 6-1

SUMMARY OF ULTRAVIOLET EXPOSURE TESTS

Coating	Spec. No.	Time (hr)	Temperature	ϵ_{TH}		α_s				$\Delta\alpha_s$	
						Initial		Final			
			°K °F	Initial	Final	Cary	Cal.	Cary	Cal.	Cary	Cal.
Titanium Dioxide/ Methyl Silicone (Thermatrol 2A-100)	1	550	395/250	0.87	0.85	0.15	0.18	0.26	0.32	0.11	0.14
Zinc Oxide/Methyl Silicone (S-13)	27	500	395/250	0.86	0.86	0.18	0.21	0.28	0.28	0.10	0.07
	28	636[a]	395/250	0.85	0.87	0.19	0.20	0.31	0.30	0.12	0.10
Zinc Oxide/Methyl Silicone (S-13G)	43	500	395/250	0.90	0.91	0.19	0.20	0.31	0.28	0.12	0.08
	44	520	395/250	0.91	0.91	0.20	0.19	0.27	0.25	0.07	0.06
Zirconium Silicate/ Potassium Silicate	9	100	534/500	0.80	0.71	0.12	0.13	0.36	0.36	0.24	0.23
	14	500	534/500	0.71	0.71	0.12	0.12	0.51	0.42	0.39	0.30
Aluminum Silicate/ Potassium Silicate	19	122	534/500	0.72	0.72	0.14	0.20	0.41	0.46	0.27	0.26
	21	530	534/500	0.82	0.81	0.14	0.16	0.45	0.50	0.29	0.34
Zinc Oxide/ Potassium Silicate (Z-93)	35	502	534/500	0.81	0.81	0.14	0.12	0.26	0.25	0.12	0.13
	36	331[a]	534/500	0.81	0.81	0.14	0.11	0.42[a]	0.30	(b)	0.19[a]
	40	1004	450/350	0.87	0.87	0.14	0.12	0.23	0.26	0.12	0.14
	38	500	422/300	0.88	0.88	0.14	0.14	0.20	0.19	0.06	0.05
	39	4574[a]	422/300	0.91	0.88	0.14	0.11	0.34[a]	0.16	(b)	0.05[a]
	59	10,014	422/300	0.88	0.88	0.15	0.14	0.21	0.20	0.06	0.06
	56	2024	366/200	0.89	0.89	0.15	0.14	0.21	0.20	0.06	0.06
	42	2001	300/80	0.90	0.88	0.14	0.14	0.17	0.18	0.03	0.04
OSR	60	2024	339/150	0.80	0.79	0.06	0.06	0.06	0.06	0.00	0.00

(a) Vacuum system or instrumentation failure during test.
(b) Post-test Cary taken after vacuum failure; substantial change in absorptance observed due to test failure.
(c) Test in progress.

6.2.1 Titanium Dioxide/Methyl Silicone (Thermatrol 2A-100)

Specimen 1 was exposed at the 1-sun level for 500 hr at 395°K (250°F). At 245 hr the electronic pump shut off and chamber pressure rose to 20−50 μ. The pump was restarted and data taken as soon as chamber pressure was decreased to the operating level of 6×10^{-8} Torr. These data showed that α_s had decreased from the last value computed before vacuum failure. The solar absorptance slowly increased after vacuum was reestablished and the final value of α_s was 0.32 after 550 hr of uv exposure. The absorptance and total hemispherical emittance data as a function of time are shown graphically by Fig. 6-1. Total hemispherical emittance at 395°K (250°F) was measured to be $0.87\,^{+0.01}_{-0.02}$ over the entire test period. The absorptance and emittance data are contained in Table B-1.

The decrease in solar absorptance observed after the vacuum failure is in agreement with the data reported by McMillan et al. (Ref. 53) and is believed to be associated with recovery in the near infrared region due to the presence of oxygen. Room temperature normal spectral reflectance data taken at 5 min and 30 min intervals after exposure of the specimen to air show the recovery phenomena (Fig. 6-2).

Solar absorptance appeared to reach a saturation level of 0.32, $\Delta\alpha_s = 0.14$, after 400 hr under these exposure conditions. If the vacuum failures had not occurred, it is estimated the solar absorptance would have been essentially constant after approximately 200 hr. The change in α_s during this test is greater than that reported in Ref. 53 for room temperature exposure to an AH-6 lamp (mercury) at a 1-sun level for the same time period. The room temperature data, however, reached approximately the same saturation value. The initial α_s value based upon Cary data was 0.15, whereas the calorimetric value was 0.18. This latter value is in good agreement with the integrated absolute reflectance data from the Gier-Dunkle apparatus, 0.17. The specularity of the coating is felt to account for the lower values measured using the Cary which has a small integrating sphere. Considering the uncertainty limits for each measurement, the three values of α_s all fall within the uncertainty ban ($\alpha_{Cary} = 0.15 \pm 0.02$, $\alpha_{GD} = 0.17 \pm 0.01$, $\alpha_{Cal} = 0.18 \pm 0.02$).

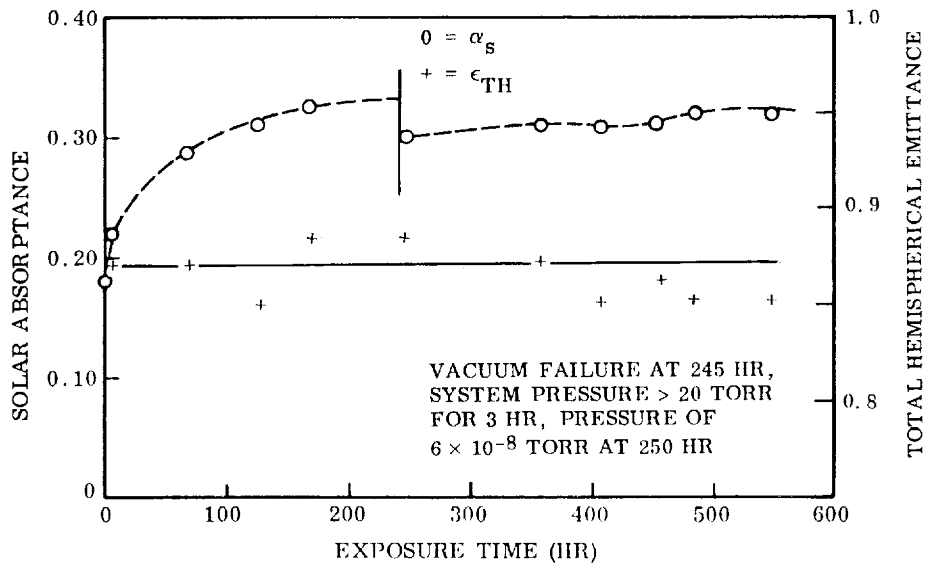

Fig. 6-1 Solar Absorptance and Total Hemispherical Emittance of Titanium Dioxide/Methyl Silicone Coating (Thermatrol 2A-100), Sample 1, as a Function of Exposure Time at a 1-Sun Level (0.2 to 0.4 μm, Xenon Source), Sample Temperature 395°K (250°F)

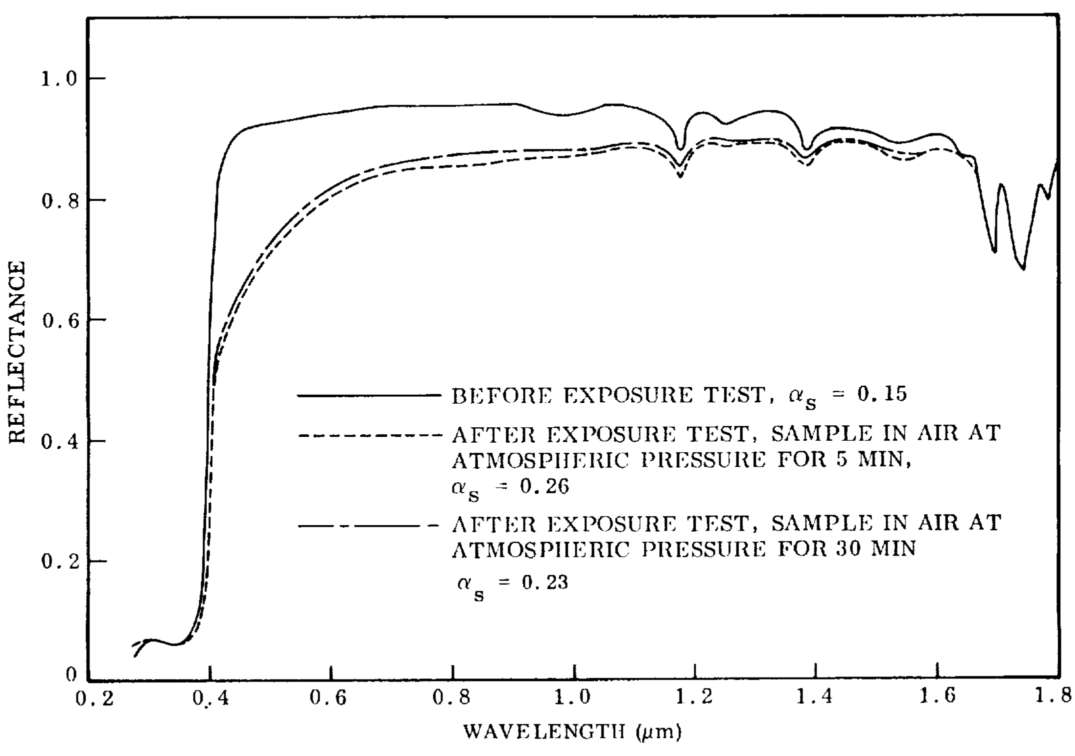

Fig. 6-2 Room Temperature Normal Spectral Reflectance of Titanium Dioxide/Methyl Silicone (Thermatrol 2A-100), Sample 1, Before and After 550-hr Exposure Test

6.2.2 Zinc Oxide/Methyl Silicone (S-13)

The results of the calorimetric in situ measurements made during the exposure tests on the duplicate Samples 27 and 28 are tabulated in Tables B-2 and B-3. The solar absorptance and total hemispherical emittance of the two samples as a function of exposure time are shown graphically by Fig. 6-3. The solar absorptance of Sample 27 increased from 0.21 to 0.28 under uv irradiation at a 1-sun level. This increase occurred during the first 250 hours of exposure time with the absorptance remaining essentially constant after that time. Solar absorptance of Sample 28 increased from 0.20 to 0.30 under these conditions. The loss of vacuum for Sample 28 at 325 hr is marked by a partial recovery as is shown by the data presented in Fig. 6-3. This is believed to be due to the oxygen recovery phenomena discussed by Greenberg et al. (Ref. 14) for the zinc oxide. After reexposure under high vacuum, the absorptance of

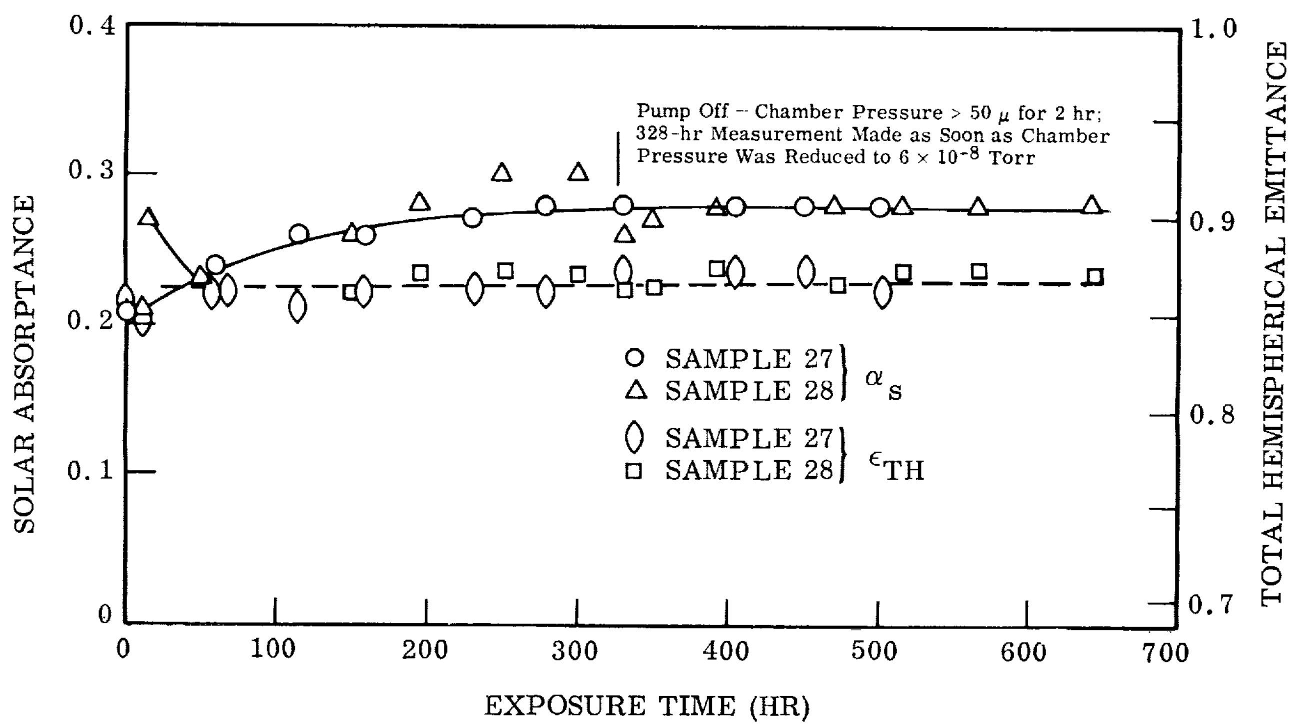

Fig. 6-3 Solar Absorptance and Total Hemispherical Emittance of Zinc Oxide/Methyl Silicone (S-13) Coating Samples as a Function of Exposure Time at a 1-Sun Level and 395°K (250°F)

the sample increased to near its previous level and remained constant for the duration of the test. Sample 28 was exposed for a total of 636 hr. The change in solar absorptance, α_s, measured during these tests agrees well with that determined by S. Greenberg et al. at LMSC using the in situ bidirectional reflectance exposure apparatus. They report a limiting value of $\Delta\alpha_s$ of 0.09 for the S-13 coating when exposed at approximately 300°K (80°F). Data from the OSO-II flight experiment show a change in solar absorptance of 0.06 for 500-hr exposure (equivalent sunhours in space flight). As no specimen temperatures are reported for these flight experiment data, a direct comparison cannot be made with the laboratory data of this program. After exposure, the sample coatings had turned to a light tan color. The color was not quite uniform, varying from light tan to almost white for a small portion on one side of the sample.

Pre- and post-test room spectral reflectance data for the two samples are shown in Figs. 6-4 and 6-5. The spectral band absorptances are determined from these reflectance curves and presented in the data tables for the two samples. Comparison of the > 0.85-μm spectral band absorptances from the in situ data show the near infrared recovery of this system when exposed to air.

The total hemispherical emittance measured calorimetrically during the exposure test was $0.86 \begin{smallmatrix} +0.02 \\ -0.01 \end{smallmatrix}$ for both samples, and was essentially constant for the test duration. Pre-test solar absorptances calculated from spectral reflectance data using the Gier-Dunkle apparatus were 0.20 for both samples which agrees well with the calorimetric values of 0.20 and 0.21.

6.2.3 Zinc Oxide/Methyl Silicone (S-13G)

The S-13G coating developed by IITRI was formulated from a zinc oxide pigment treated* to improve the resistance to degradation in the near-infrared region. The results of the calorimetric in situ measurements made during the exposure tests of the duplicate Samples 43 and 44 are tabulated in Tables B-4 and B-5. The solar absorptance and

*See Appendix A.

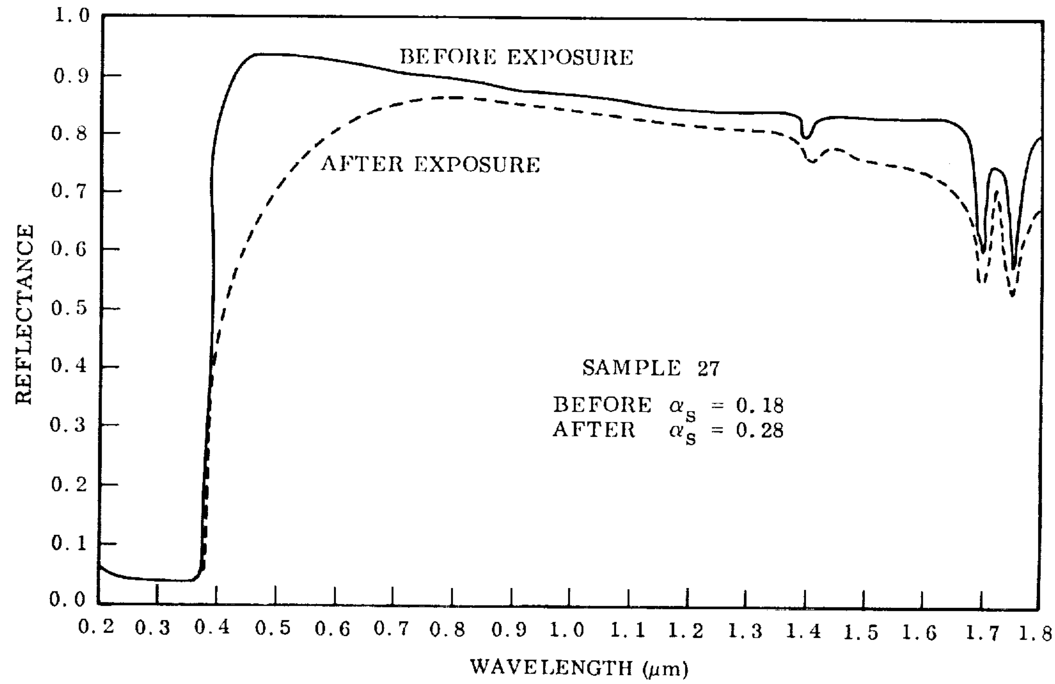

Fig. 6-4 Room Temperature Spectral Reflectance of Zinc Oxide/ Methyl Silicone (S-13) Coating, Sample 27, Before and After 500-hr Exposure Test

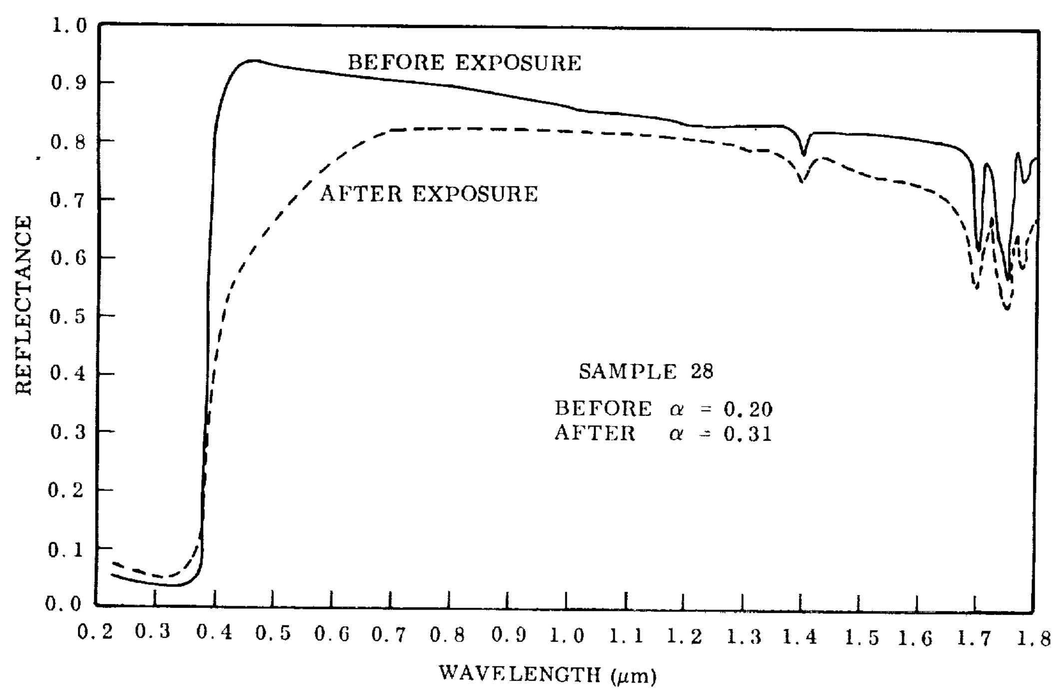

Fig. 6-5 Room Temperature Spectral Reflectance of Zinc Oxide/Methyl Silicone (S-13) Coating, Sample 28, Before and After 636-hr Exposure Test

total hemispherical emittance of the two samples as a function of exposure time are shown graphically by Fig. 6-6. Solar absorptance of S-13G Sample 43 increased from 0.20 to 0.28 under uv irradiation at a 1-sun level. The change in solar absorptance for Sample 44 was not as great as that observed for Sample 43; the corresponding change was from 0.19 to 0.25. Visual inspection of the sample showed an area on the side of the sample (approximately 20% of the exposed area) to be considerably lighter in color than the remainder of the surface. A slight shift in the beam position occurred which resulted in this portion of the sample being exposed to a somewhat lower uv intensity. Therefore, it is felt that the change in α_s of 0.08 is the relevant figure. Coating color was a light tan for both samples at the completion of the exposure tests.

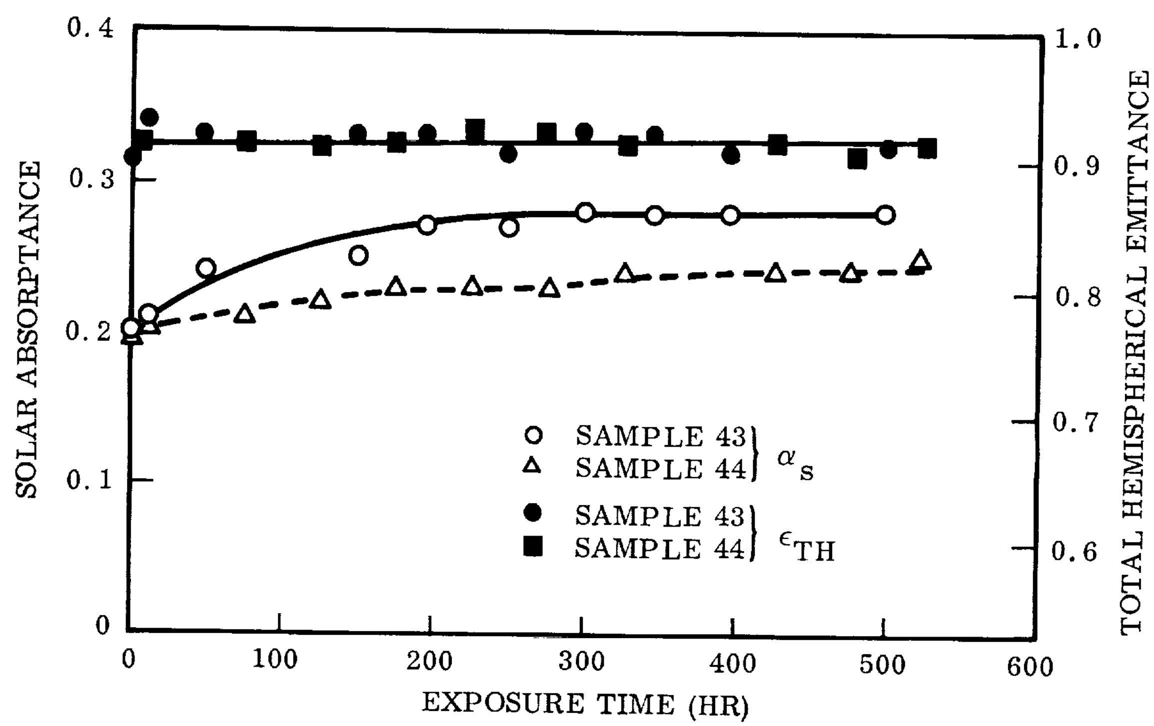

Fig. 6-6 Solar Absorptance and Total Hemispherical Emittance of Zinc Oxide/Methyl Silicone (S-13G) Coatings as a Function of Exposure Time at a 1-Sun Level and 395°K (250°F)

The broadband spectral data show the improvement in the near infrared region for this coating as reported by IITRI. In the >0.85- m region the final absorptance was 0.18 for the S-13G coating and 0.28 and 0.30 for the S-13 coatings. However, the change in absorptance from 0.2 to 0.8 μm is as great or greater than that for S-13, as is seen in the tabulated data in Appendix B.

Pre- and post-test room temperature spectral reflectance data are plotted in Figs. 6-7 and 6-8 for Samples 43 and 44. These data show a greater degradation in the 0.4- to 0.85-μm spectral region for Sample 43.

The total hemispherical emittance, measured calorimetrically during the exposure test, was $0.91^{+0.02}_{-0.01}$ at 395°K (250°F) for both samples and was essentially constant for the test duration. Initial measurements of ϵ_{TH} as a function of temperature showed essentially no change for Sample 44 over the temperature range of 295°K (70°F) to 395°K (250°F) (0.90 to 0.91). For Sample 43, the measured values of ϵ_{TH} versus temperature were 0.86 at 295°K (70°F), 0.89 at 339°K (150°F), and 0.92 at 395°K (250°F). No obvious reason is apparent for the small emittance temperature dependence of this sample. No temperature dependence was evident for either of the S-13 coatings or the other S-13G coating.

6.2.4 Zirconium Silicate/Potassium Silicate (LMSC)

The results of the calorimetric in situ measurements made during the exposure test on these samples at 534°K (500°F) are tabulated in Tables B-6 and B-7. The solar absorptance and total hemispherical emittance as a function of exposure time are shown graphically by Fig. 6-9. Sample 9 was exposed for a period of 100 hr. The test was terminated at this time due to a vacuum chamber failure. The second duplicate sample, 14, was exposed for the full 500-hr period. The solar absorptance of this coating increased from 0.12 to 0.42. Almost all this increase occurred in the first 150 hr of exposure time. This agrees very well with data reported by Streed (Ref. 27). Absorptance increased from 0.13 to a final value of 0.42 for 700-sun hr at 10-sun intensity and at a temperature of 527°K (490°F). Since this coating showed

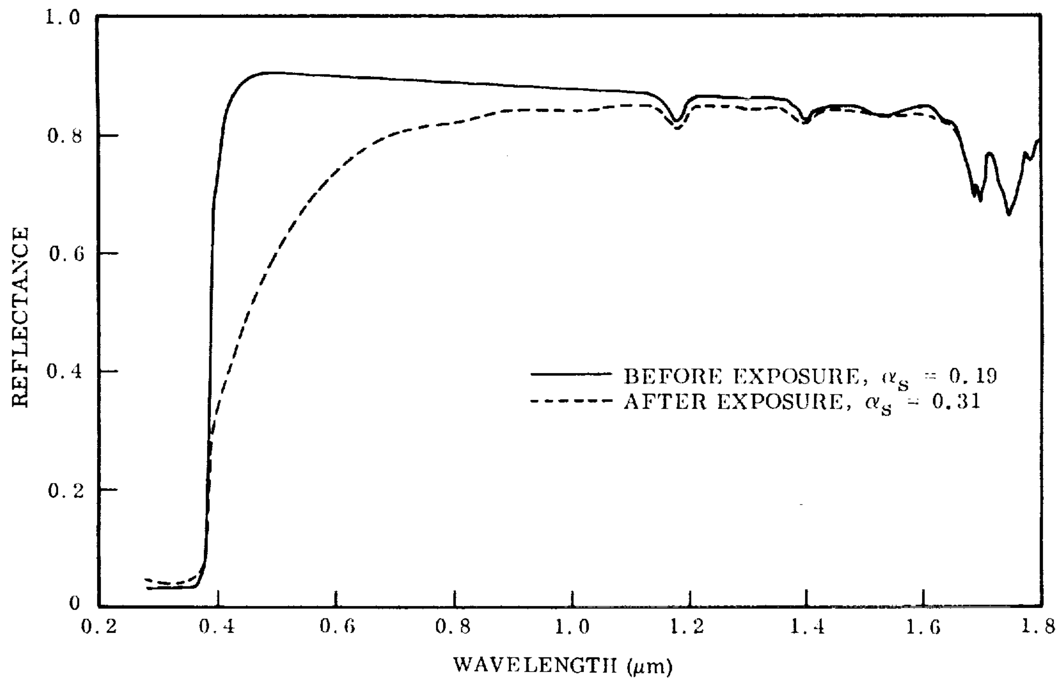

Fig. 6-7 Room Temperature Spectral Reflectance of Zinc Oxide/ Methyl Silicone (S-13G) Coating, Sample 43, Before and After 500-hr Exposure Test

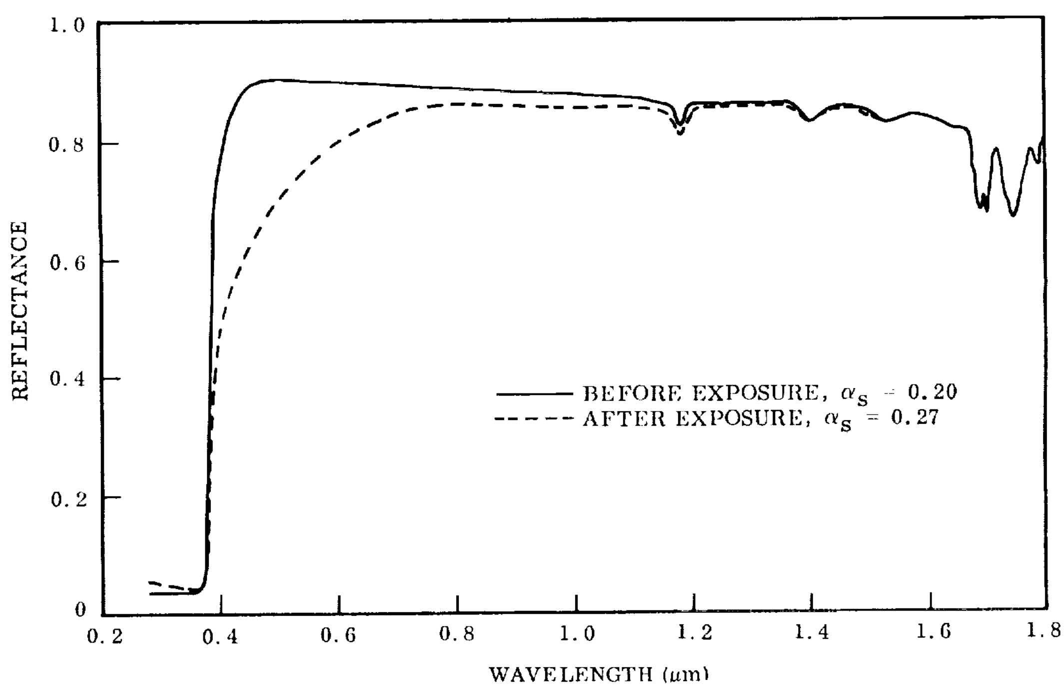

Fig. 6-8 Room Temperature Spectral Reflectance of Zinc Oxide/Methyl Silicone (S-13G) Coating, Sample 44, Before and After 520-hr Exposure Test

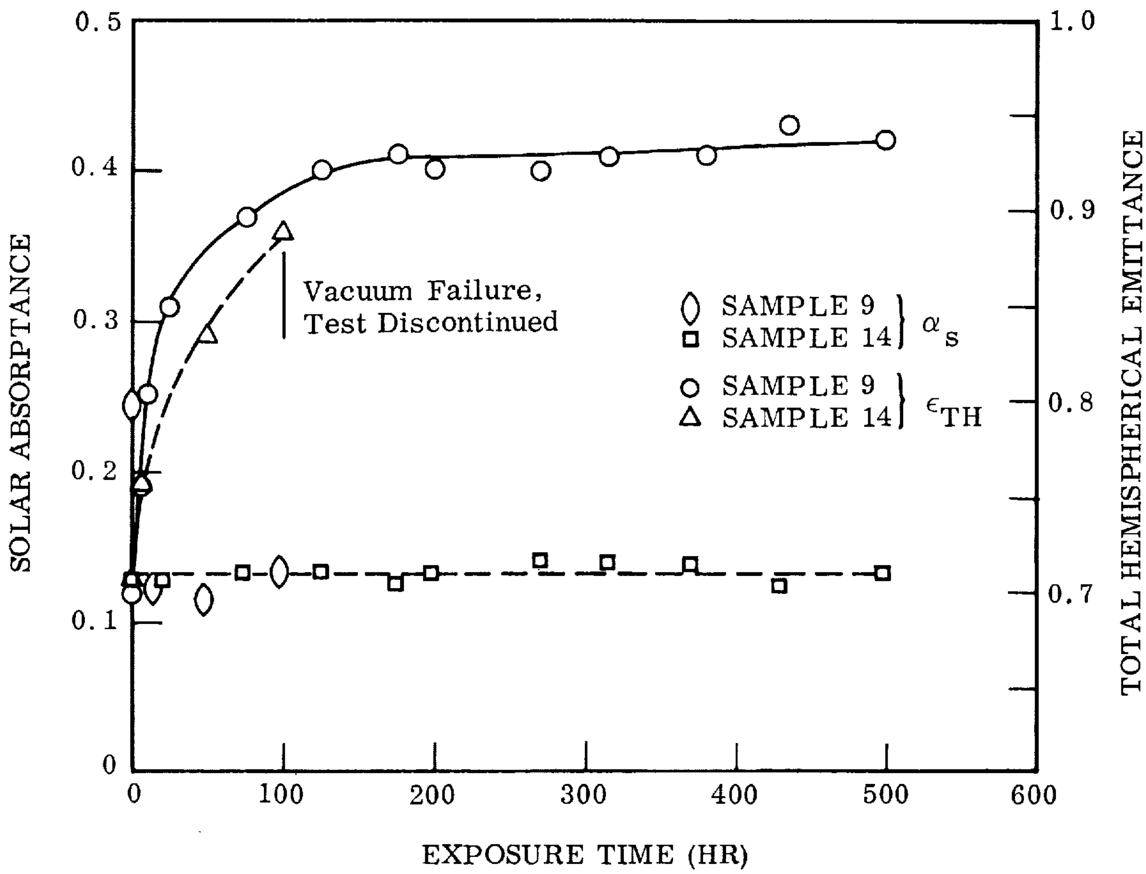

Fig. 6-9 Solar Absorptance and Total Hemispherical Emittance of Zirconium Silicate/Potassium Silicate Coatings as a Function of Exposure Time at 1-Sun Level and 534°K (500°F)

a very high degree of degradation upon exposure to uv at a temperature of 534°K (500°F), and since the data for Sample 9 showed the same trend of a large increase in absorptance, it was felt unnecessary to run a third sample. Although the coating has a low initial α_s, 0.12, it is severely and rapidly degraded by 1-sun level uv exposure at 534°K (500°F).

Sample 14 turned a dark grey with a visible narrow ring around the edge of the sample. Inside of the ring the surface was slightly darker in color. This appears to be due to variations in surface texture and thickness. Sample 9 was lighter in color than Sample 14, with a slightly tan hue. A large portion of surface had a mottled appearance. Pre- and post-test room temperature reflectance data for the samples are shown in Figs. 6-10 and 6-11.

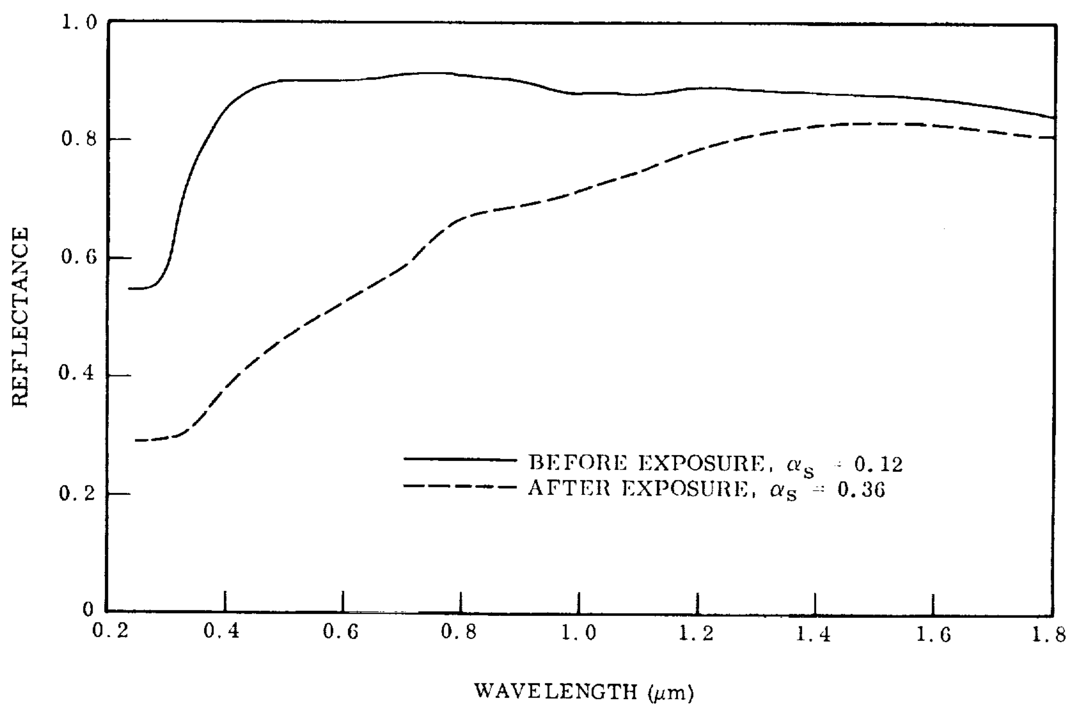

Fig. 6-10 Room Temperature Spectral Reflectance of Zirconium Silicate/Potassium Silicate, Sample 9, Before and After 100-hr Exposure Test

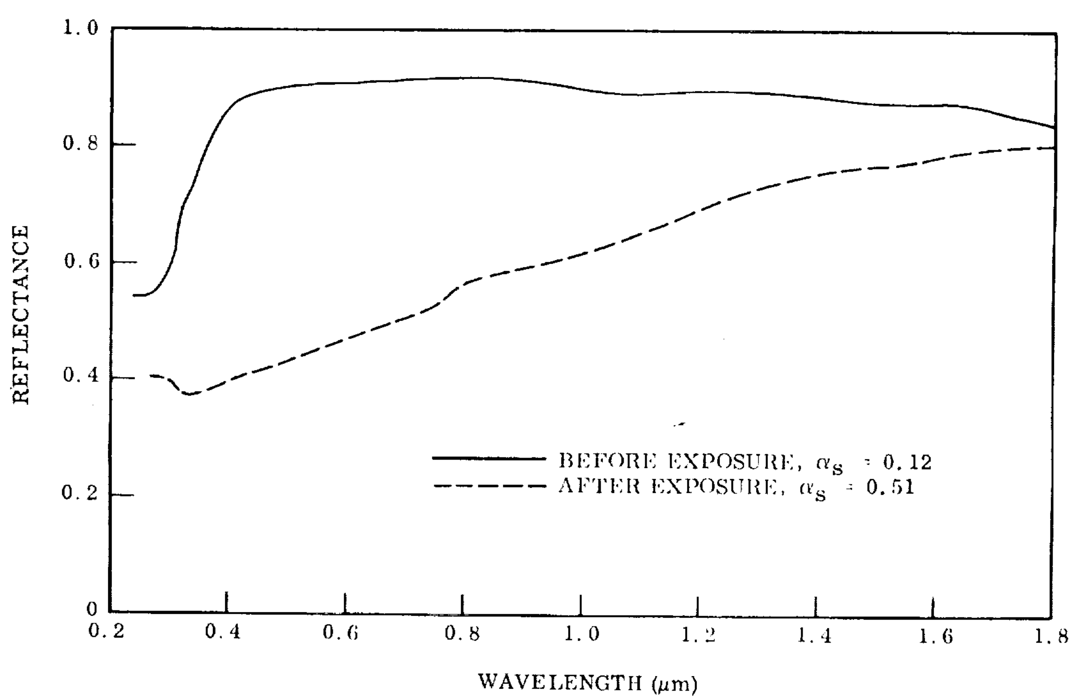

Fig. 6-11 Room Temperature Spectral Reflectance of Zirconium Silicate/Potassium Silicate Coating, Sample 14, Before and After 500-hr Exposure Test

The total hemispherical emittance measured calorimetrically for this coating decreased from 0.87 at 294°K (70°F) to 0.71 at 534°K (500°F). The emittance of both samples remained relatively constant at $0.70^{+0.02}_{-0.01}$ for the duration of the tests. For Sample 9 emittance initially at 534°K was 0.80 but dropped to 0.70 at 1 hr. A value of 0.71 was measured after 1 hr for Sample 14.

6.2.5 Aluminum Silicate/Potassium Silicate (Hughes)

The results of the calorimetric in situ measurements made during the exposure tests at 534°K (500°F) on the duplicate samples, 19 and 21, are tabulated in Tables B-8 and B-9. The solar absorptance and total hemispherical emittance of the two samples as a function of exposure time are shown graphically by Fig. 6-12. The test on Sample 19 was terminated at 122 hr because of a broken thermocouple support wire. It is seen that the solar absorptance of both samples degraded very rapidly in the first 100 hr of exposure, with the absorptance increasing from 0.15 to over 0.40. The solar absorptance of Sample 21 increased from an initial value of 0.16 to 0.50 after 530 hr of exposure. Severe damage occurred in the 0.41 to > 0.85-μm spectral bands. Because of the large degradation in solar absorptance at 534°K, a third test was not conducted to 500 hr.

After exposure both samples showed a definite ring-like discoloration around the outer periphery of the sample. It was postulated that this might be due to the contact with the strippable protective coating on the edge of the sample during application and curing of coating. The strippable coatings were also baked on and were extremely hard to remove. They were finally removed by scraping with a knife blade. The sample color after exposure was a medium grey with a slightly darker border around the outer edge of the sample. A microprobe analysis of the coating was made to determine if any contamination was present which could have caused the ring-like discolorations.

An electron microprobe x-ray analyzer with an electron beam scanning system was used to test the two sample surfaces for carbon and titanium contamination. The field-of-view of the instrument is 500 μ, the resolution is 1 μ, and the detection range is atomic number 5 and up. Both specimens were tested only for carbon and titanium since it was

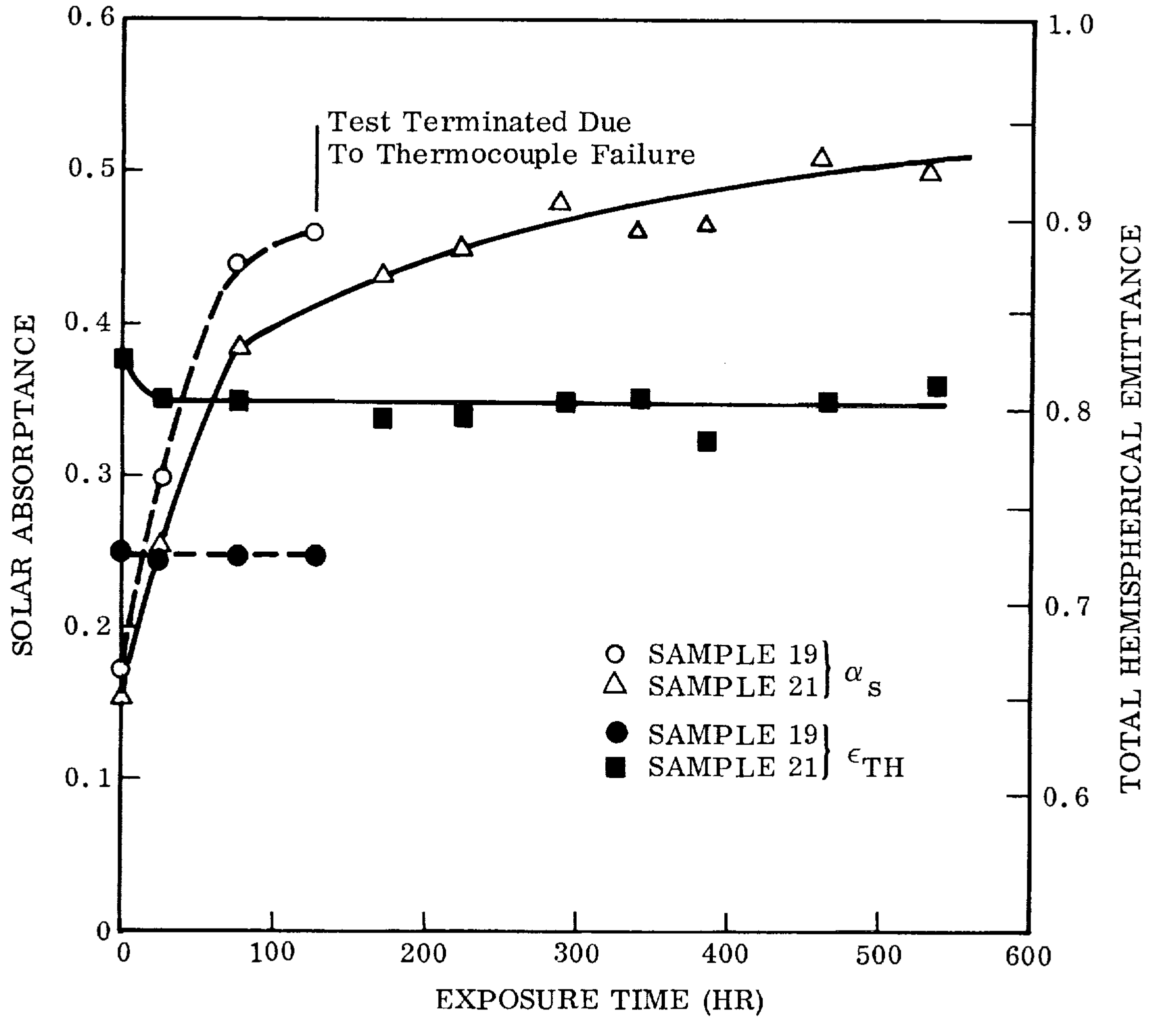

Fig. 6-12 Solar Absorptance and Total Hemispherical Emittance of Aluminum Silicate/Potassium Silicate Coatings as a Function of Exposure Time at 534°K (500°F)

believed that these were the most likely contaminants – carbon from the strippable coating and the inner chamber black coating, and titanium from the ion pumps. There was no evidence of carbon on either of the samples. There was no evidence of titanium on Sample 21. Sample 19 showed a very minor trace of titanium at a single location on the surface. If pump contamination had occurred, one would expect a uniform deposition of this element. It is most probable this element was present in a trace amount in the coating ingredients.

Pre- and post-test room temperature reflectance data for the two samples are shown in Figs. 6-13 and 6-14. The spectral band absorptances were determined from these reflectance curves and are presented in the data tables for comparison.

The total hemispherical emittance of Sample 19 decreased from 0.90 at room temperature to 0.72 at 535°K (500°F). Sample 21 decreased from 0.94 at room temperature to 0.80 at 535°K (500°F). There is no evident indication of why this large difference occurred between the two samples.

6.2.6 Zinc Oxide/Potassium Silicate (Z-93) (IITRI)

Initially two specimens of this coating were exposed to a 1-sun level at 534°K (500°F). The results of these tests showed an increase in solar absorptance of 0.13 which was far less than that shown by the other candidate coatings tested for this temperature level. Considering these data and those for the material from the OSO-II flight experiment which showed no degradation in 1000 hr, it was decided to conduct additional tests at various temperatures in order to evaluate degradation as a function of exposure temperature for this material. This coating has a lower initial solar absorptance than the zinc oxide/methyl silicone system and a higher total hemispherical emittance at 395°K (250°F). Thus, if its change in α_s is of the same order of the S-13 or S-13G systems, it would be a better choice for a radiator coating at this temperature level. For clarity, the results of the various tests are reported in order of temperature rather than chronologically.

534°K (500°F) Exposure Tests

The results of the calorimetric in situ measurements made during the exposure tests on duplicate samples, 35 and 36, are tabulated in Tables B-10 and B-11. The solar absorptance and total hemispherical emittance of the two samples as a function of exposure time are shown graphically by Fig. 6-15. The solar absorptance of Sample 35 increased from 0.12 to 0.25 during 502 hr of exposure. The absorptance reached 0.24 at 256 hr and was essentially constant thereafter. The absorptance of Sample 36 increased more rapidly and reached a value of 0.24 at 87 hr and remained constant to

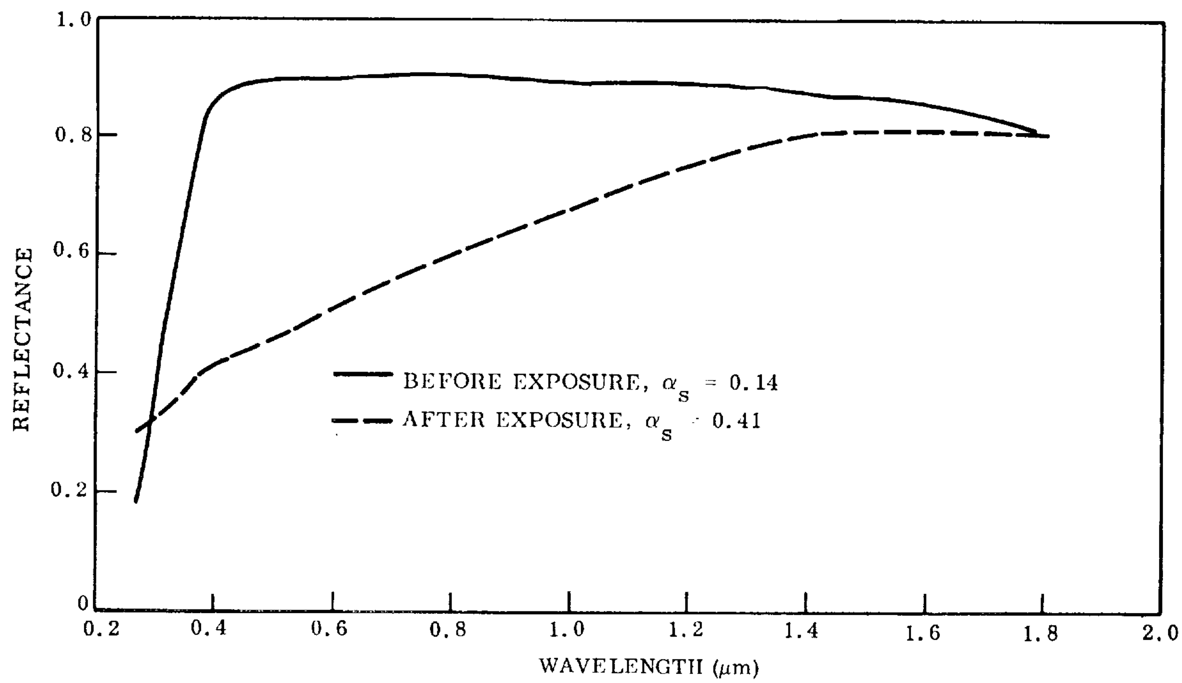

Fig. 6-13 Room Temperature Spectral Reflectance of Aluminum Silicate/Potassium Silicate Coating, Sample 19, Before and After 122-hr Exposure Test

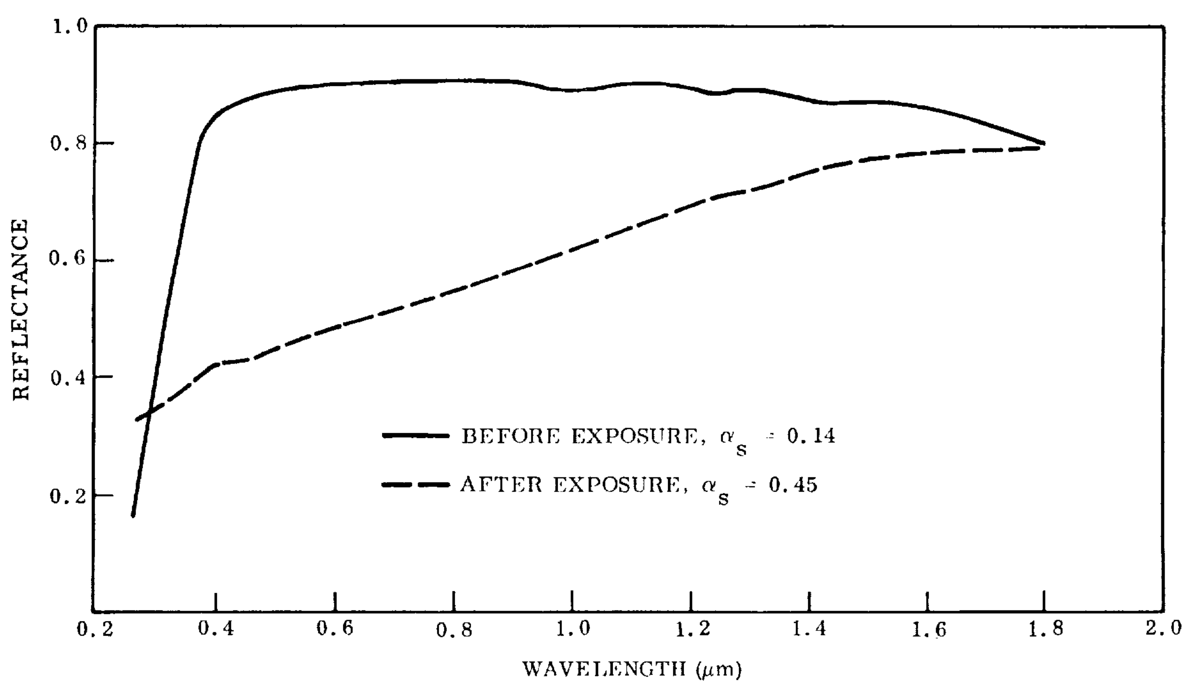

Fig. 6-14 Room Temperature Spectral Reflectance of Aluminum Silicate/Potassium Silicate Coating, Sample 21, Before and After 530-hr Exposure Test

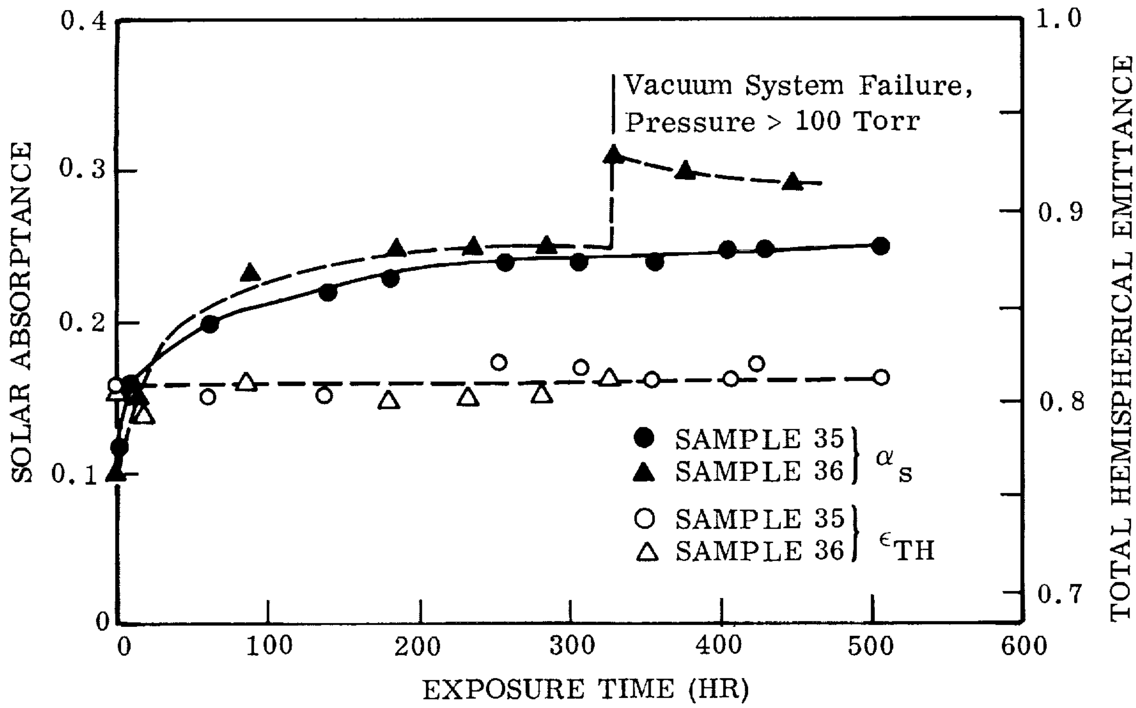

Fig. 6-15 Solar Absorptance and Total Hemispherical Emittance of Zinc Oxide/ Potassium Silicate Coating (Z-93) as a Function of Exposure Time at 535°K (500°F)

300 hr. A chamber vacuum failure occurred at 331 hr of exposure, and a very noticeable rise in the solar absorptance of the sample was found. The post-test visual appearance of Sample 35 showed a slight greying of the surface with a small speckled area slightly darker in color. Sample 36 appeared more uniform and without the grey cast. The test of Sample 36 was continued to 450 hr and a slight decrease in α_s was observed. However, as such severe damage occurred at 331 hr, the data after this time could not be used for comparison with that of Sample 35.

Pre- and post-test room temperature spectral reflectance data for the sample are shown in Figs. 6-16 and 6-17. Sample 36 shows a much greater degradation in the 0.4- to 1.4-μm range which is attributed to the vacuum failure. The reason for this increase in damage is not known, but it was also observed on a sample of this material tested at a later date.

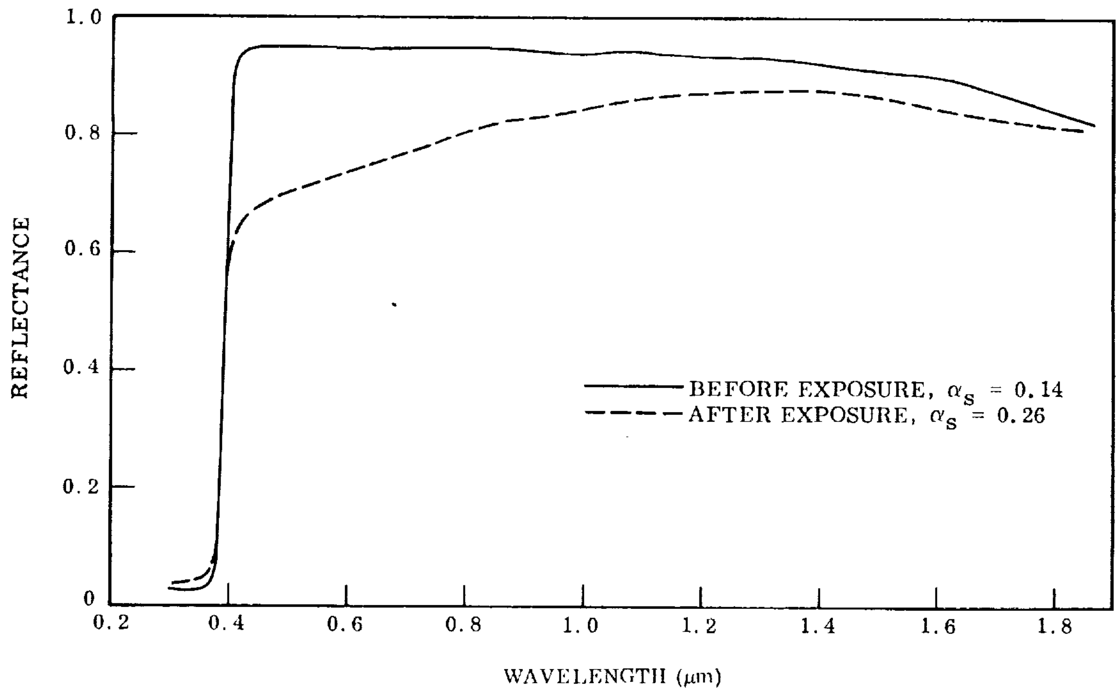

Fig. 6-16 Room Temperature Spectral Reflectance of Zinc Oxide/Potassium Silicate (Z-93), Sample 35, Before and After 502-hr Exposure Test

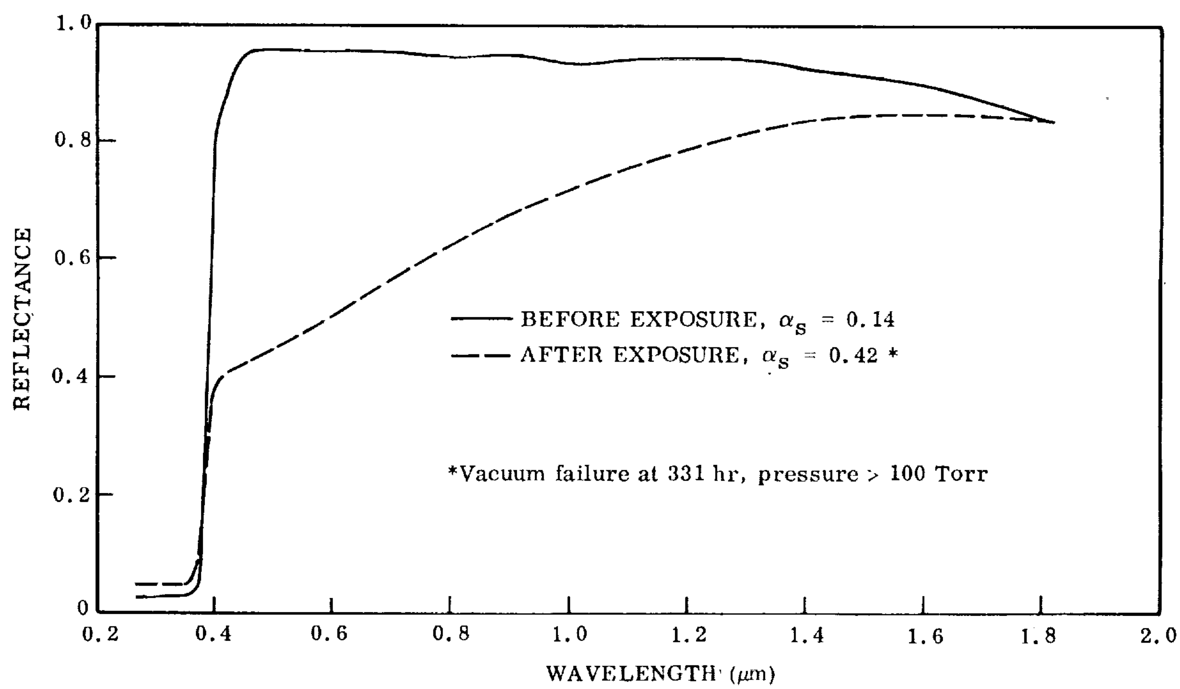

Fig. 6-17 Room Temperature Spectral Reflectance of Zinc Oxide/Potassium Silicate (Z-93), Sample 36, Before and After 450-hr Exposure Test

The total hemispherical emittance of both samples shows a temperature dependence decreasing from approximately 0.93 at room temperature to 0.81 at 534°K. The emittance remained relatively constant at 534°K during both tests.

450°K (350°F) Exposure Tests

The results of the calorimetric in situ measurements made during the exposure test on Sample 40 are tabulated in Table B-12, and the solar absorptance and total hemispherical emittance of the sample as a function of exposure time for 1004 hr are shown graphically in Fig. 6-18. Absorptance increased from an initial value of 0.12 to 0.26 at the end of the 1004-hr test. The change observed in solar absorptance at 450°K (350°F) is very similar to that at 534°K (500°F), but the rate of degradation was slightly less.

Pre- and post-test room temperature spectral reflectance data for the sample are shown in Fig. 6-19. The spectral band absorptances were determined from the reflectance curve and are presented in the data tabulation for comparison.

422°K (300°F) Exposure Tests

Three samples of the coating were exposed for varying periods of time at 422°K and a chamber pressure at less than 1×10^{-7} Torr. Sample 38 was the 500-hr screening test. Based upon the small change in α_s (0.05) observed during this test, it was decided to conduct a 10,000-hr exposure test on this coating (Sample 39). After 4574 hr, the chamber pressure rose to >100 μ due to failure of the LN_2 cold wall. A third test (Sample 59) was conducted for 10,014-hr of exposure. Prior to this last test, a turbomolecular pump was connected to the system to preclude any future vacuum failures.

The results of the calorimetric in situ measurements made during the exposure test on Sample 38 are tabulated in Table B-13. The solar absorptance and total hemispherical emittance of the sample as a function of exposure time are shown graphically in Fig. 6-20. The solar absorptance of Sample 38 increased to 0.19 at 265 hr and remained at this level to 500 hr. The total hemispherical emittance of the sample was

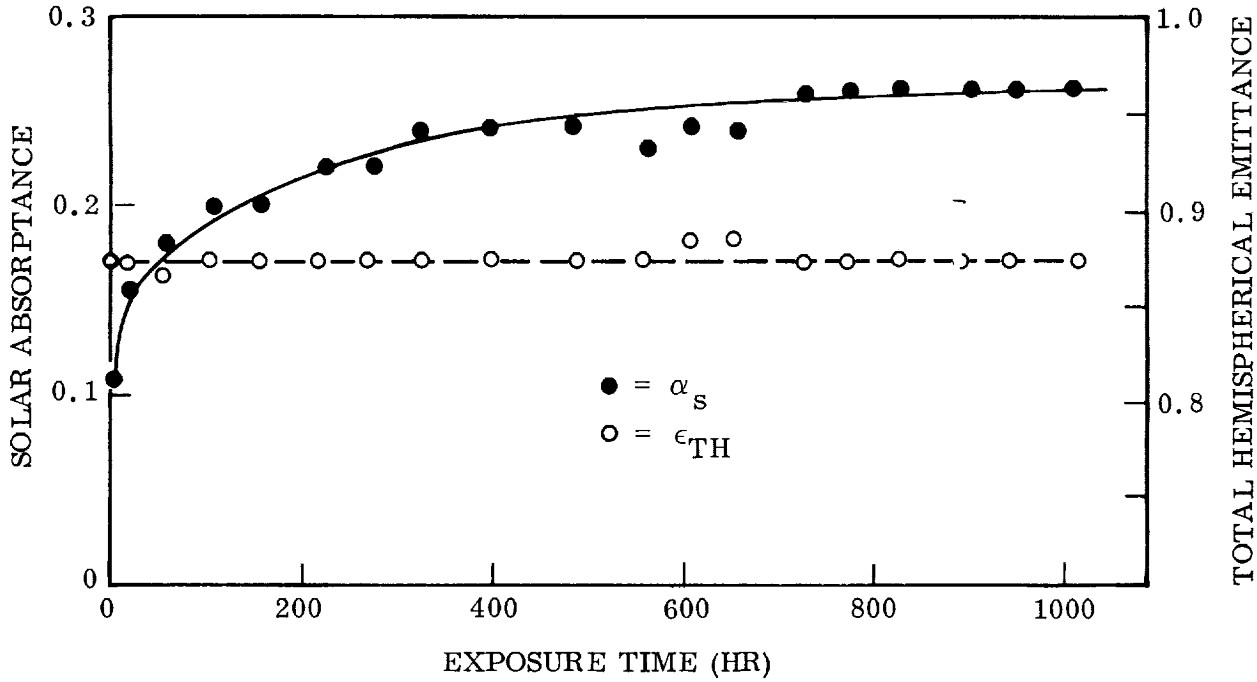

Fig. 6-18 Solar Absorptance and Total Hemispherical Emittance of Zinc Oxide/ Potassium Silicate (Z-93), Sample 40, as a Function of Exposure Time at 450°K (350°F)

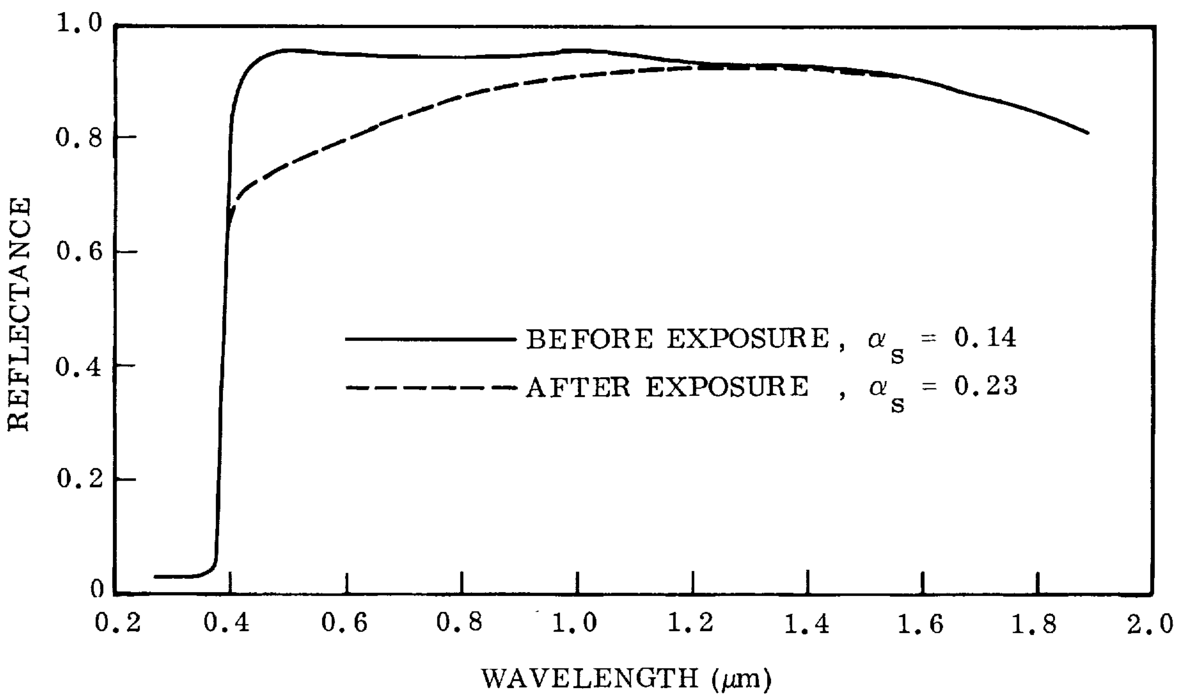

Fig. 6-19 Room Temperature Spectral Reflectance of Zinc Oxide/Potassium Silicate (Z-93), Sample 40, Before and After 1004-hr Exposure Test

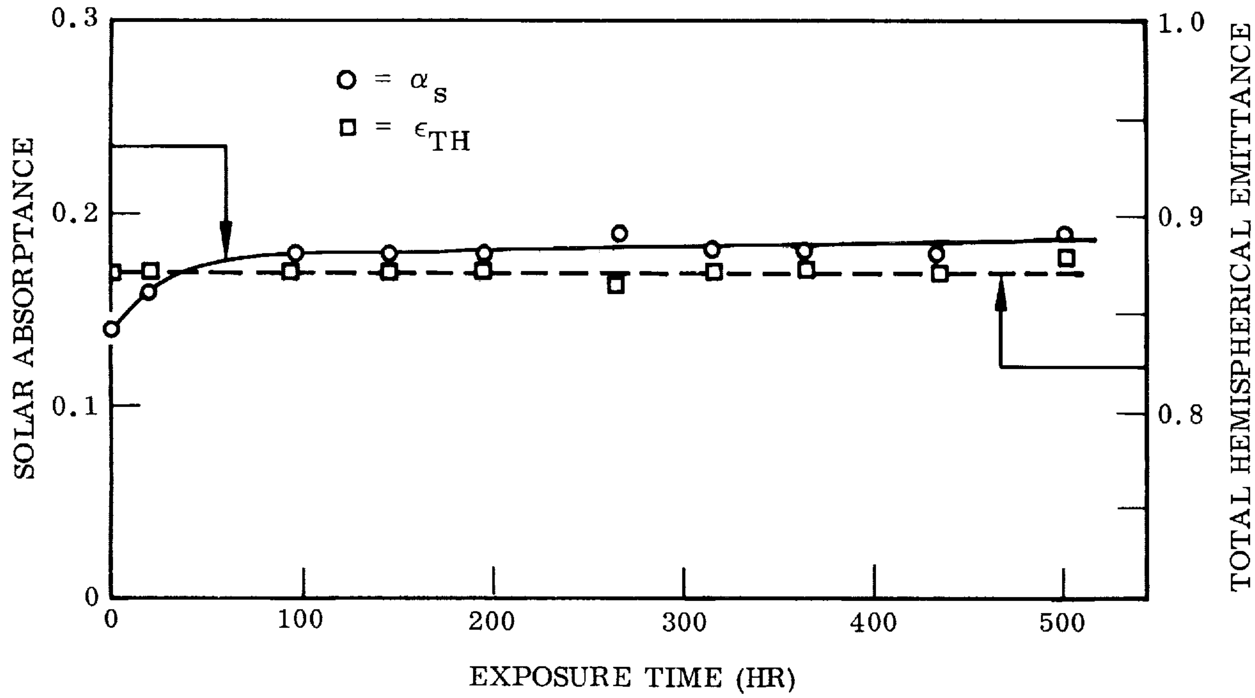

Fig. 6-20 Solar Absorptance and Total Hemispherical Emittance of Zinc Oxide/ Potassium Silicate Coating (Z-93), Sample 38, as a Function of Exposure Time at 422°K (300°F)

0.87 ± 0.01 through the test period. Pre- and post-test room temperature spectral reflectance data are shown in Fig. 6-21.

The results of the calorimetric in situ measurements made during the exposure test on Sample 39 are tabulated in Table B-14, and α_s and ϵ_{TH} as a function of time are shown in Fig. 6-22. The uv exposure test on this sample was terminated after 4574 hr. The decision to terminate the test was based upon a large increase in absorptance which occurred during a vacuum system failure. This failure is attributed to an intermittent fault in the solenoid valve controlling the liquid nitrogen fill system. The subsequent warming of the liquid nitrogen reservoirs released a volume of adsorbed gases which overloaded the VacIon pump and caused it to shut down. This overloading of the VacIon pumps and subsequent loss of vacuum has also been the cause of termination of previous tests. No explanation has been substantiated for the increase in absorptance caused by this failure. The specimen temperature did not exceed 422°K at any time during the period. A similar increase in absorptance upon pressure rise was observed for Sample 36. The sample appearance after removal from the chamber

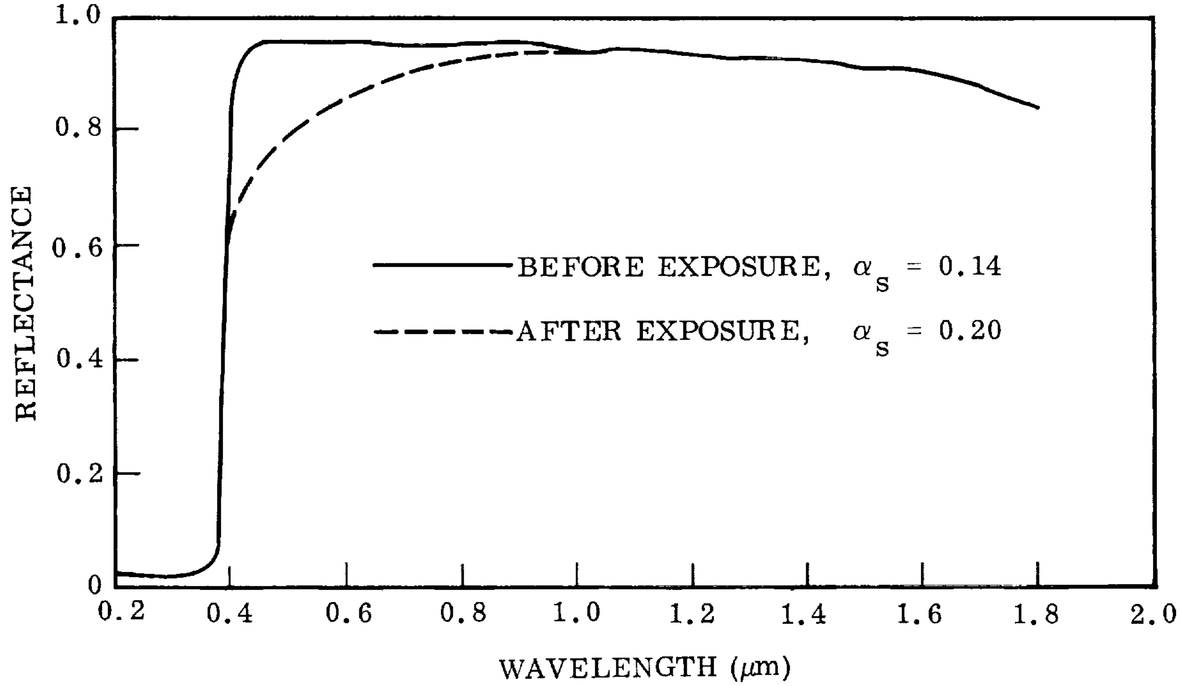

Fig. 6-21 Room Temperature Spectral Reflectance of Zinc Oxide/Potassium Silicate Coating (Z-93), Sample 38, Before and After 500-hr Exposure Test

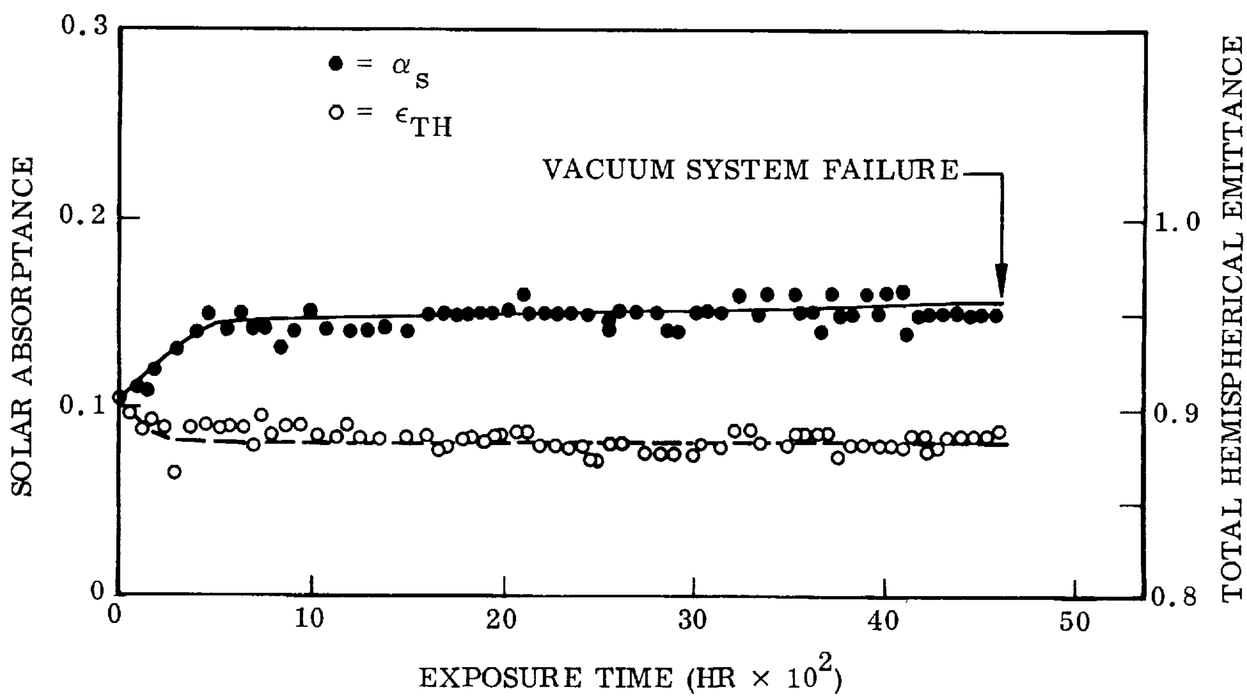

Fig. 6-22 Solar Absorptance and Total Hemispherical Emittance of Zinc Oxide/ Potassium Silicate Coating (Z-93), Sample 39, as a Function of Exposure Time at 422°K (300°F)

was a light brown with small darker areas distributed over the sample surface. The appearance of these small areas had been noticed on previous exposed samples of this coating. This specimen as well as Sample 36 and an unexposed sample were examined with the electron microprobe. No evidence of carbon or titanium was found on any of the samples which does not substantiate chamber contamination as the cause of the increase in absorptance.

Pre- and post-test room temperature spectral reflectance data for Sample 39 are shown in Fig. 6-23. The severe degradation in the 0.4- to 1.0-μm spectral region was observed as was the case for Sample 36. The spectral band absorptances were determined from the reflectance curves and are presented in the data tables for comparison. The sample total hemispherical emittance was 0.87 ± 0.02 during this test period.

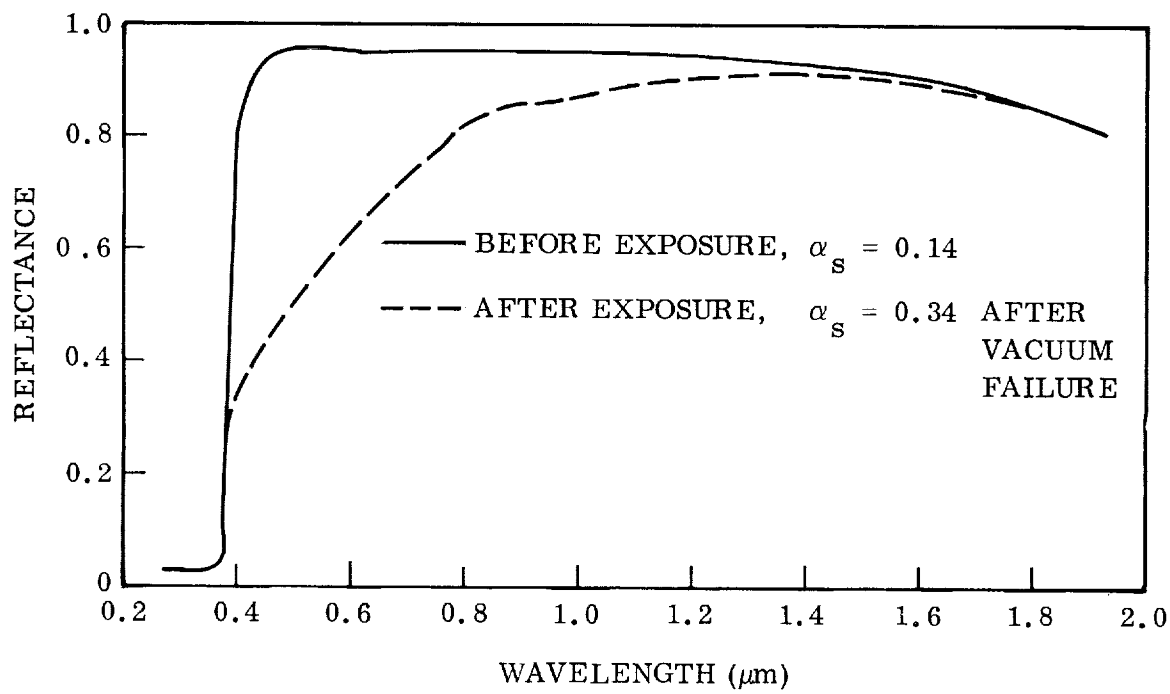

Fig. 6-23 Room Temperature Spectral Reflectance of Zinc Oxide/Potassium Silicate Coating (Z-93), Sample 39, Before and After 4574-hr Exposure Test

A third sample was exposed for 10,014 hr at a 1-sun level. The total time at temperature in vacuum was 10,517 hr. From 2832 to 3335 hr, the xenon source was inoperative as the lamp power supply unit was returned to the manufacturer for repair. No change in solar absorptance or total hemispherical emittance was observed due to vacuum or temperature without uv irradiation. The results of the in situ measurements are shown in Fig. 6-24, and the data are tabulated in Table B-15. Room temperature spectral reflectance data for Sample 59 are shown in Fig. 6-25.

Solar absorptance increased from an initial value of 0.14 to 0.18 at 500 hr and then remained essentially constant until approximately 8000 hr. After that time, the calorimetric absorptance values appeared to decrease slightly to the end of the test, $\alpha_s = 0.17$. Although this decrease in total absorptance is within the experimental uncertainty of the method, a definite decreasing trend became evident during the final 1000 hr. This decrease was most pronounced in the 0.20- to 0.41-μm broadband data. At the conclusion of the test the xenon source window in the vacuum chamber was examined, and a very thin film was observed to be present on the vacuum side of the window.

Spectral transmission measurements were made on the contaminated window, and they were compared with the transmission data for the window before the test and after cleaning, Fig. 6-26. Little difference was observed between the pre-test transmission values and those after cleaning indicating no significant degradation of the window material occurred during the prolonged ultraviolet exposure. However, the film resulted in an appreciable decrease in window transmission from 0.20 to 0.70 μm. Spectral transmission data for the contaminated window integrated over the four spectral bands are shown in Table 6-2.

The final calorimetric absorptance data were corrected by multiplying the band energies, based upon the initial transmission data, by the transmission factors shown in Table 6-2(c). The final corrected solar absorptance value becomes 0.19 which is in good agreement with the data to 7000 hr of ultraviolet exposure time and compares with a final value of 0.21 determined from post-test spectral reflectance measurements.

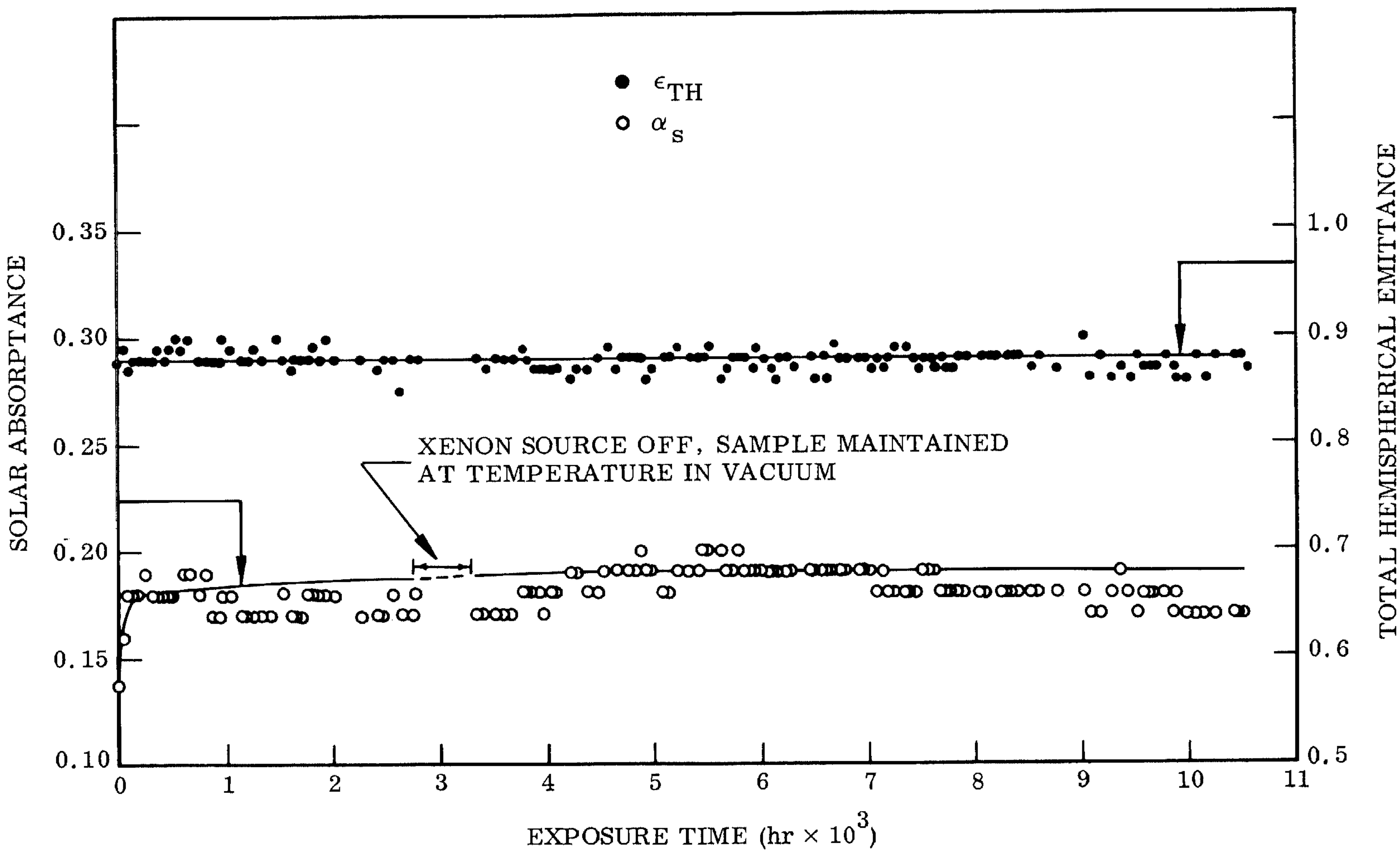

Fig. 6-24 Solar Absorptance and Total Hemispherical Emittance of Zinc Oxide/Potassium Silicate Coating (Z-93), Sample 59, as a Function of Exposure Time at 422°K (300°F)

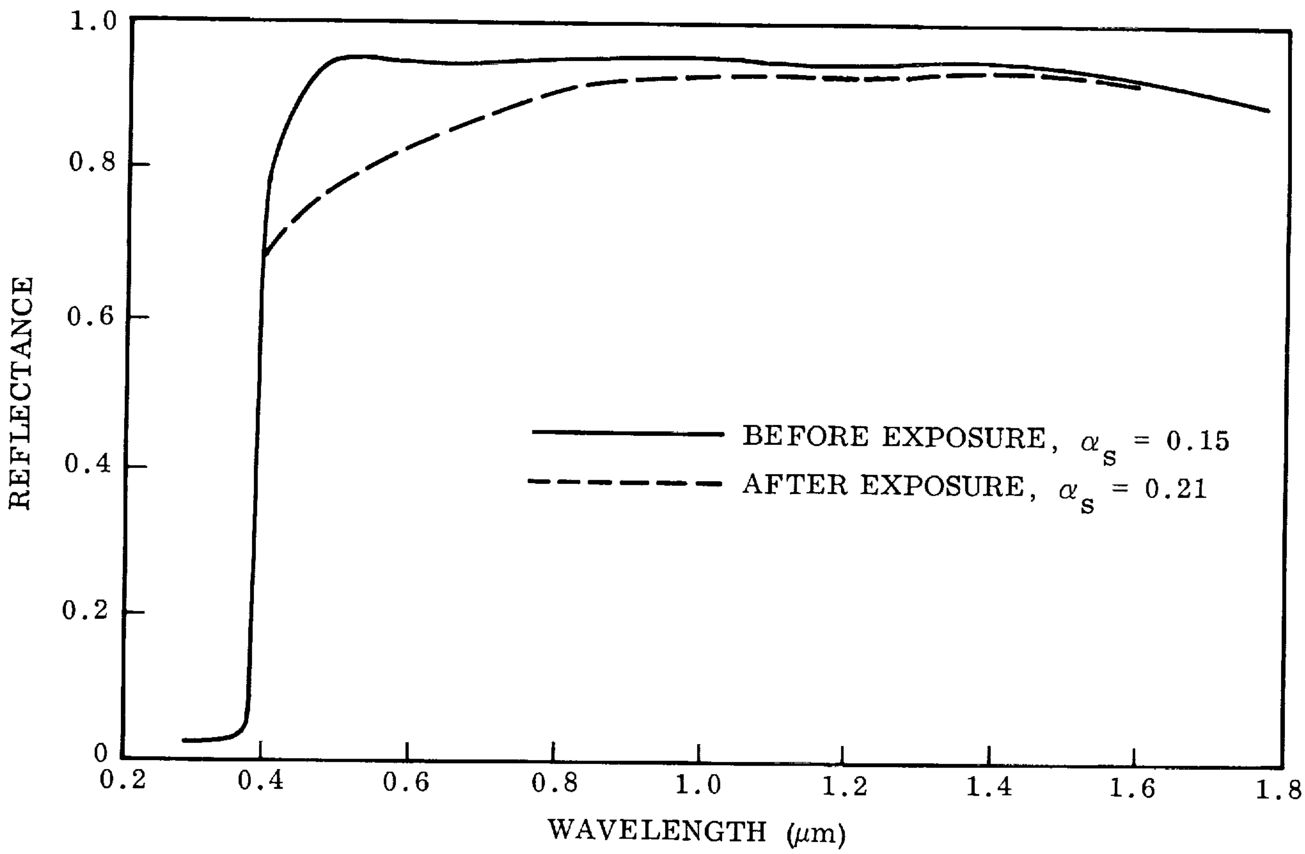

Fig. 6-25 Room Temperature Spectral Reflectance of Zinc Oxide/Potassium Silicate Coating, Sample 59, Before and After 10,014-hr Exposure Test

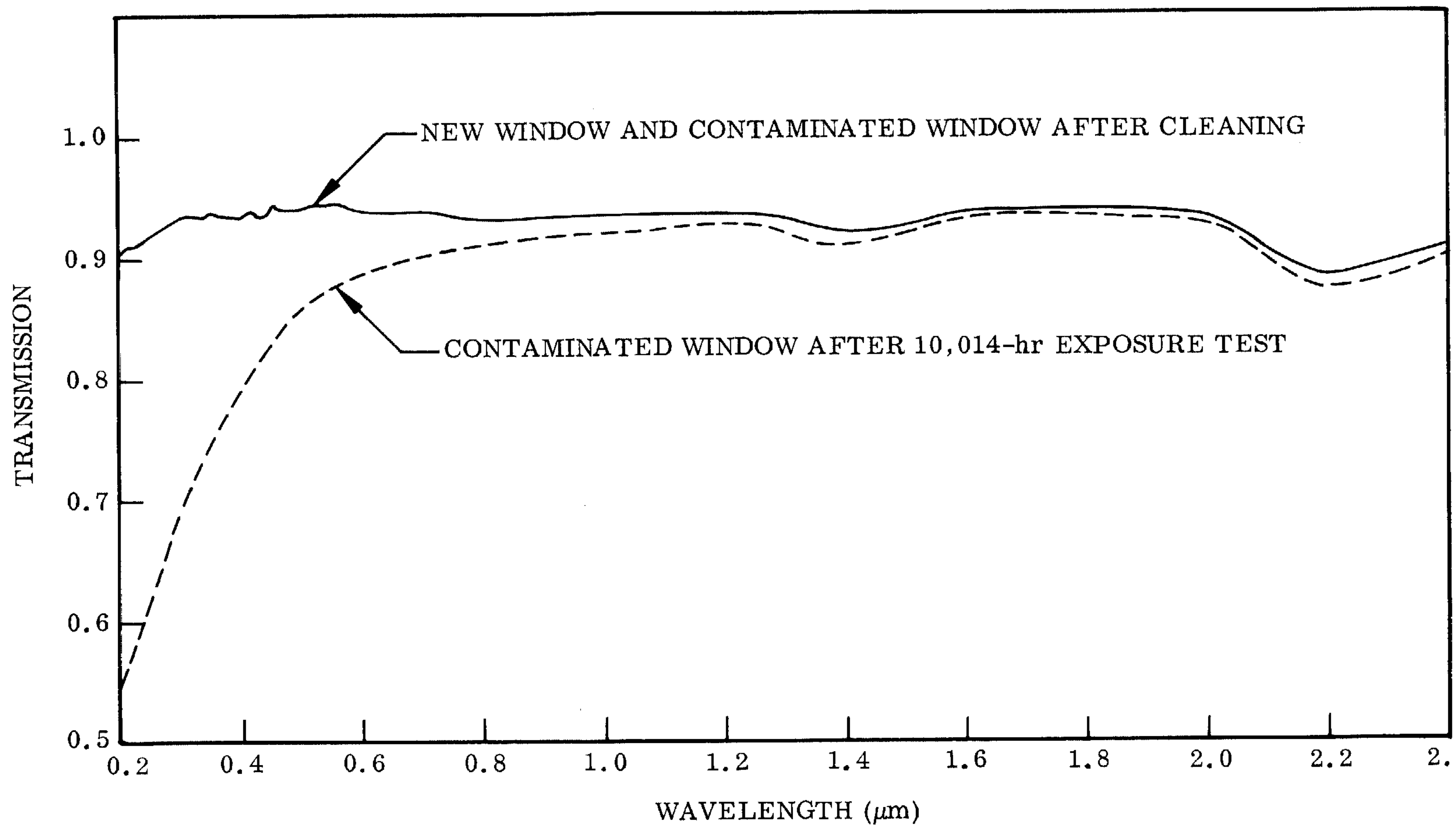

Fig. 6-26 Spectral Transmission of Window for Sample No. 59 Exposure Test. The difference in transmission for cleaned window and a new window did not exceed 1%

Table 6-2

SPECTRAL BAND TRANSMISSION FOR SOURCE WINDOW AT CONCLUSION OF 10,014 hr EXPOSURE TEST COMPARED TO PRE-TEST WINDOW TRANSMISSION

Transmission Degradation Factor[a]	Spectral Band (μm)			Total
	0.20/0.41	0.41/0.60	0.60/0.85	
F	1.26[b] 1.26[c]	1.11[b] 1.13[c]	1.08[b] 1.11[c]	1.10[b] 1.13[c]

(a) Ratio of spectral band energy before and after exposure test.
(b) From spectral transmission data (Fig. 6-26).
(c) From total band energy measurements using thermopile with filters.

As the transmission in the 0.20- to 0.40-μm wavelength region decreased with time, the specimen was exposed to less total ultraviolet energy than 1 sun for 10,014 hr. An approximation of the total exposure was made assuming that the film was deposited at a rate linearly proportional to time, i.e., thickness = a $\times$ time.

Using the relationship that transmission is inversely proportional to an exponential thickness term,

$$\tau = ae^{-bt}$$

transmission in the 0.20- to 0.40-μm region as a function of time was computed using the band transmission data at 10,000 hr. On this basis, the total uv exposure was equivalent to 9200 hr at a 1-sun level.

Electron microprobe (see subsection 6.4) and x-ray diffraction methods were employed in an attempt to determine the composition of the film, and from these data the probable source of the contamination. Neither procedure was successful in identifying the film. The material volatilized in the electron microprobe indicating it is probably an organic compound. Debye-Scherrer diffraction patterns showed some crystalline-type structure. The d spacings and intensities were not related to any zinc, titanium,

or copper compounds found in the ASTM Powder Data File. A diffraction pattern of material from the window "O" ring seal was found to be very similar to that of the film on the window. Although no identification was made of the film composition, the analysis eliminated the source as the specimen (zinc oxide/potassium silicate) or metals from the vacuum chamber or pumping system. The two suspected sources of contamination are the window "O" ring (Viton) and the epoxy-based black paint on the chamber walls. Based upon the comparison of diffraction patterns it is believed the "O" ring is the source of the film. For future very long-term exposure tests, it is recommended that chambers incorporate provisions for multiple windows so that transmission may be monitored during the test, and if a window becomes contaminated it may be replaced without disruption of vacuum.

The calorimetric data for Sample 59 are in good agreement with the data for Sample 39 for the length of the exposure test on the latter sample. Change in solar absorptance for the two specimens as a function of exposure time is shown in Table 6-3. The final data on change in solar absorptance and total hemispherical emittance for the three specimens of Z-93 tested at 422°K (300°F) are as follows:

Sample No.	Exposure Time (hr)	Final $\Delta\alpha_s$	Final ϵ_{TH}
38	500	0.05	0.88
39	4,452	0.05	0.88
59	10,014	0.05	0.88

Table 6-3

COMPARISON OF $\Delta\alpha_S$ FOR SAMPLES 39 AND 59 AS A FUNCTION OF EXPOSURE TIME AT 422°K (300°F)

Time (hr)	$\Delta\alpha_S$	
	Sample 39	Sample 59
1000	0.03	0.04
2000	0.04	0.04
3000	0.04	0.04
4000	0.05	0.04
4500	0.04	0.05

366°K (200°F) Exposure Test

Sample 56 was exposed for 2024 hr at a 1-sun uv level at a pressure of 2×10^{-8} Torr. The results of the calorimetric in situ measurements are given in Table B-16. Solar absorptance and total hemispherical emittance as a function of time are shown in Fig. 6-27. Starting with an initial solar absorptance of 0.14, $\Delta\alpha_s$ reached an equilibrium value of 0.06 at 600 hr and remained at 0.05 to 0.06 to the end of the test. Total hemispherical emittance of the sample was 0.89 ± 0.01 throughout the test period. Pre- and post-test room temperature spectral reflectance data are shown in Fig. 6-28.

300°K (80°F) Exposure Test

The zinc oxide/potassium silicate Sample 42 was exposed to uv irradiation at a 1-sun level for 2000 hr at 300°K (80°F). The chamber pressure was maintained at less than 2×10^{-8} Torr. The results of the calorimetric in situ measurements made during the exposure test on Sample 42 are tabulated in Table B-17. The solar absorptance and total hemispherical emittance of the sample as a function of exposure time are shown graphically in Fig. 6-29. These data show that the solar absorptance rises very slowly but constantly from an initial 0.14 at the start of the test to 0.18 after approximately 1400 hr and then was constant to the end of the test. Total hemispherical emittance was 0.88 ± 0.02 through the test period. Pre- and post-test room temperature spectral reflectance data for this sample are shown in Fig. 6-30. The spectral band absorptances were determined from the reflectance curves and are presented in the data for comparison.

6.2.7 Optical Solar Reflector

The calorimetric absorptance and total hemispherical emittance data for the LMSC OSR sample at 339°K (150°F) are tabulated in Table B-18 and are presented graphically in Fig. 6-31. No change in absorptance was observed during this exposure

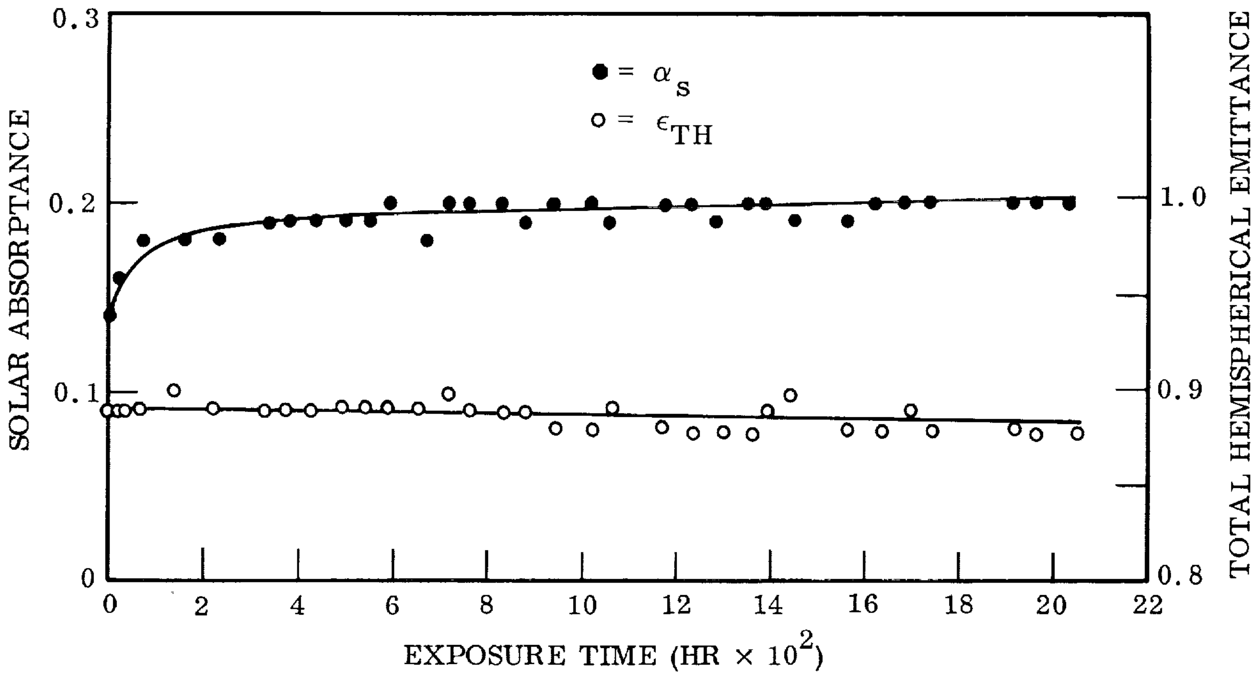

Fig. 6-27 Solar Absorptance and Total Hemispherical Emittance of Zinc Oxide/ Potassium Silicate Coating (Z-93), Sample 56, as a Function of Exposure Time at 366°K (200°F)

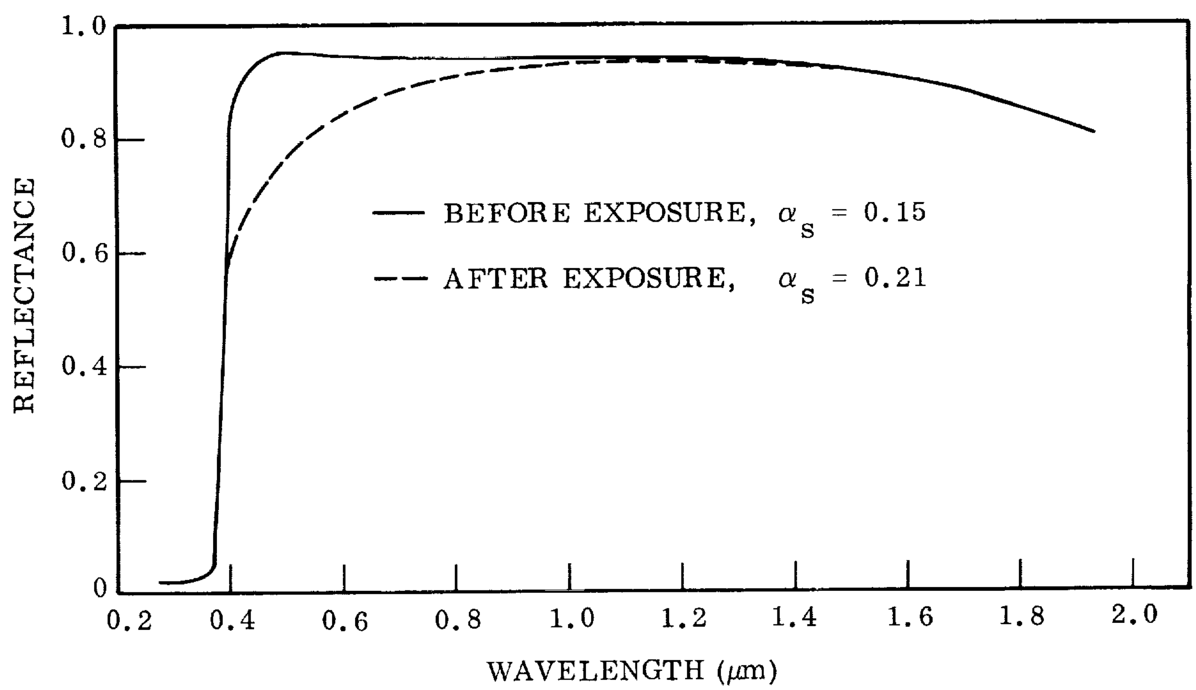

Fig. 6-28 Room Temperature Spectral Reflectance of Zinc Oxide/Potassium Silicate (Z-93), Sample 56, Before and After 2024-hr Exposure Test at 366°K (200°F)

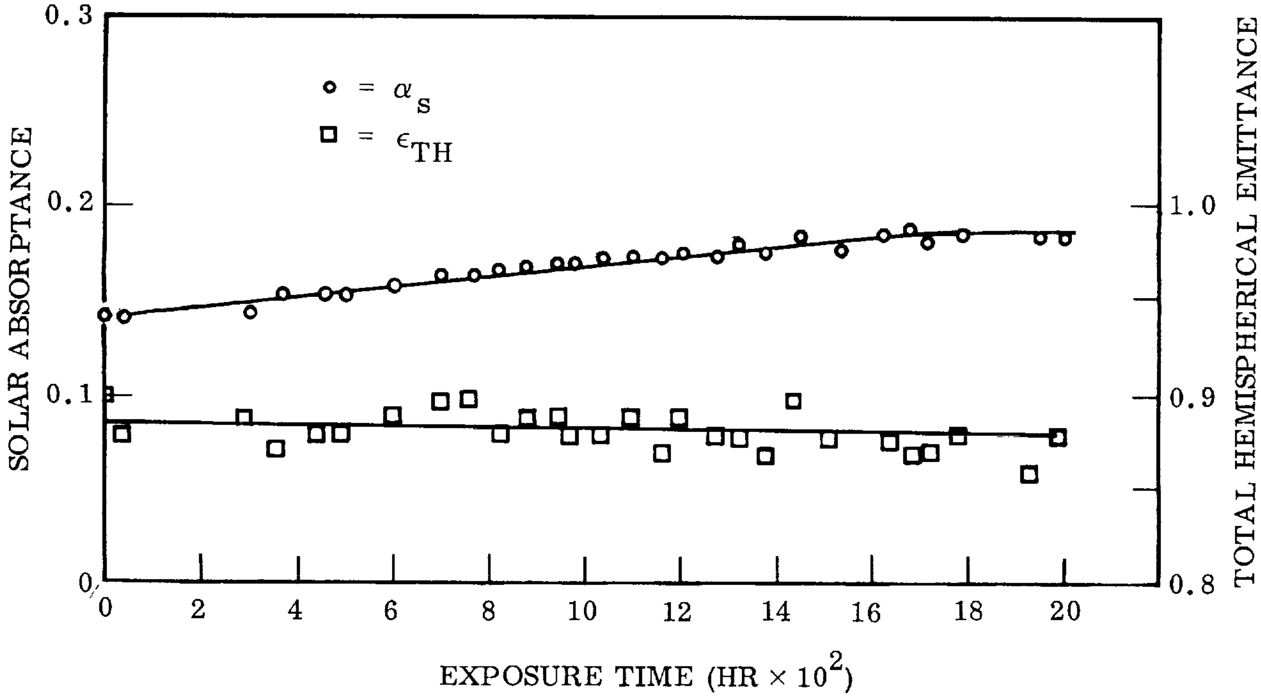

Fig. 6-29 Solar Absorptance and Total Hemispherical Emittance of Zinc Oxide/Potassium Silicate Coating (Z-93), Sample 42, as a Function of Exposure Time at 300°K (80°F)

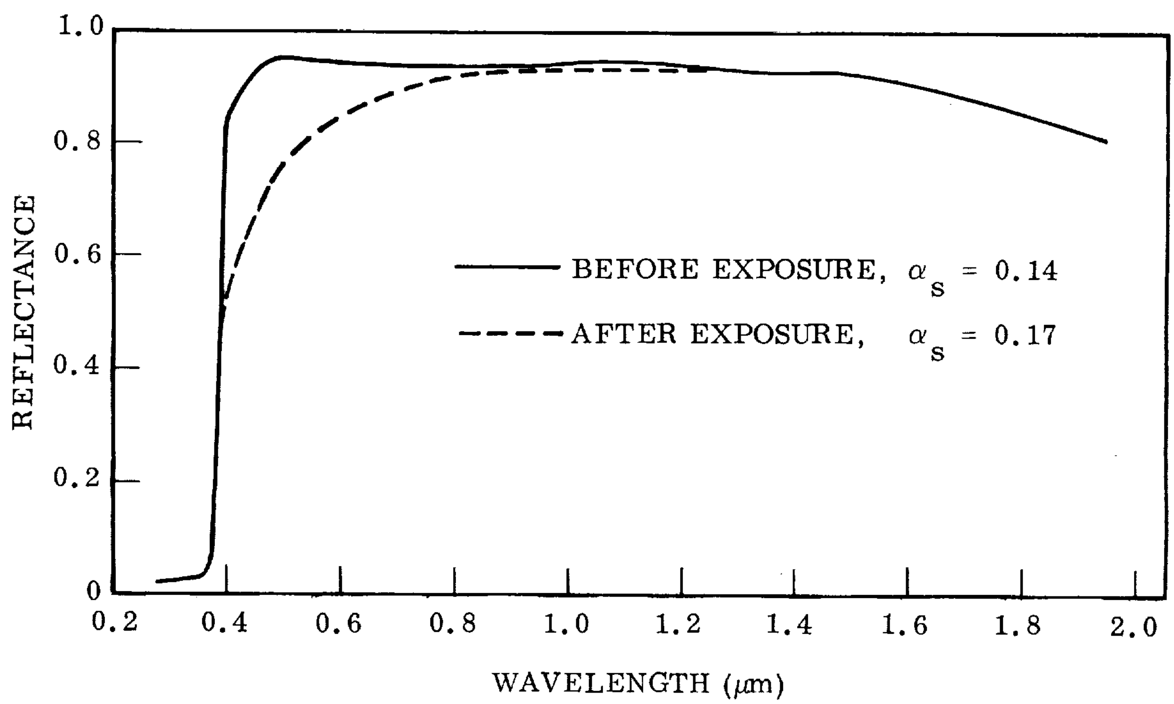

Fig. 6-30 Room Temperature Spectral Reflectance of Zinc Oxide/Potassium Silicate Coating (Z-93), Sample 42, Before and After 2001-hr Exposure Test

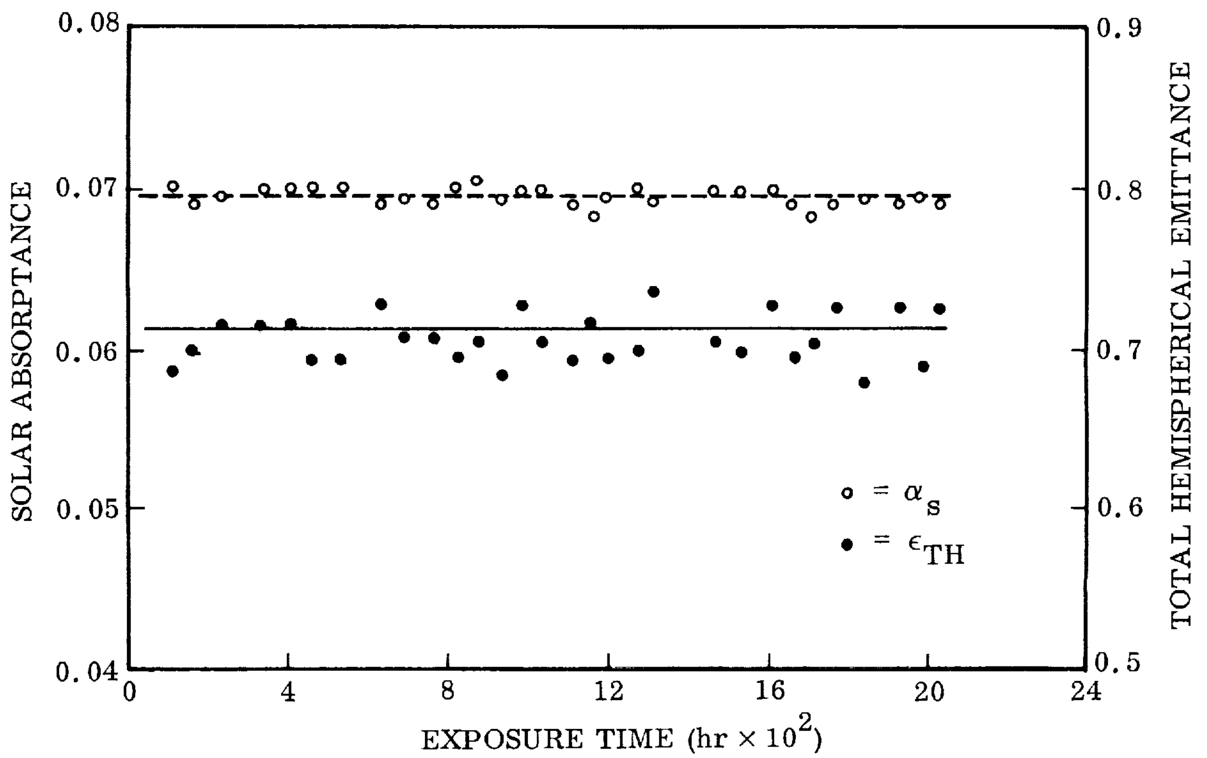

Fig. 6-31 Solar Absorptance and Total Hemispherical Emittance of Optical Solar Reflector, Sample 60, as a Function of Exposure Time at 339°K (150°F)

period, α_s = 0.061 ± 0.003. Total hemispherical emittance is $0.79^{+0.02}_{-0.02}$ at this temperature. Pre- and post-test room temperature spectral reflectance data for the sample are shown in Fig. 6-32. Pre- and post-test values of α_s from spectral reflectance measurements show a change in α_s of 0.006 which is less than the accuracy of this measurement. Total hemispherical emittance as a function of temperature is shown by Fig. 6-33.

6.3 INITIAL OPTICAL PROPERTIES FROM REFLECTANCE MEASUREMENTS

The solar absorptance values for all of the specimens are reported in Appendix A. The typical value of solar absorptance and total hemispherical emittance, calculated on the basis of reflectance measurements for each coating, are summarized in Table 6-4. Total hemispherical emittance values are based upon spectral reflectance data from 2.0 to 25.0 μm integrated over the blackbody distribution function for the temperatures shown in Table 6-4.

6.4 CRYSTALLOGRAPHIC STUDIES OF ZINC OXIDE/POTASSIUM SILICATE SAMPLE (Z-93)

The change in absorptance of the Z-93 system as a function of temperature appears to have a discontinuity in the region of 422 to 450°K (300 to 350°F). In order to determine if a gross change in structure was occurring or a zinc silicate compound was being formed, x-ray and electron diffraction studies were conducted on samples of the various specimens covering the test temperature range. The x-ray diffraction method was used initially to determine if any zinc silicate had formed during the prolonged temperature exposure. Samples from the 534°K (500°F) and 422°K (300°F) tests as well as a control specimen (unexposed to uv, elevated temperatures, or vacuum) were examined. In no case was any evidence of the silicate of zinc found. All of the lines and relative intensities corresponded to ZnO. Lattice parameters were measured for the specimens (Table 6-5) and within the resolution of the method no change was observed between tested and unexposed coatings.

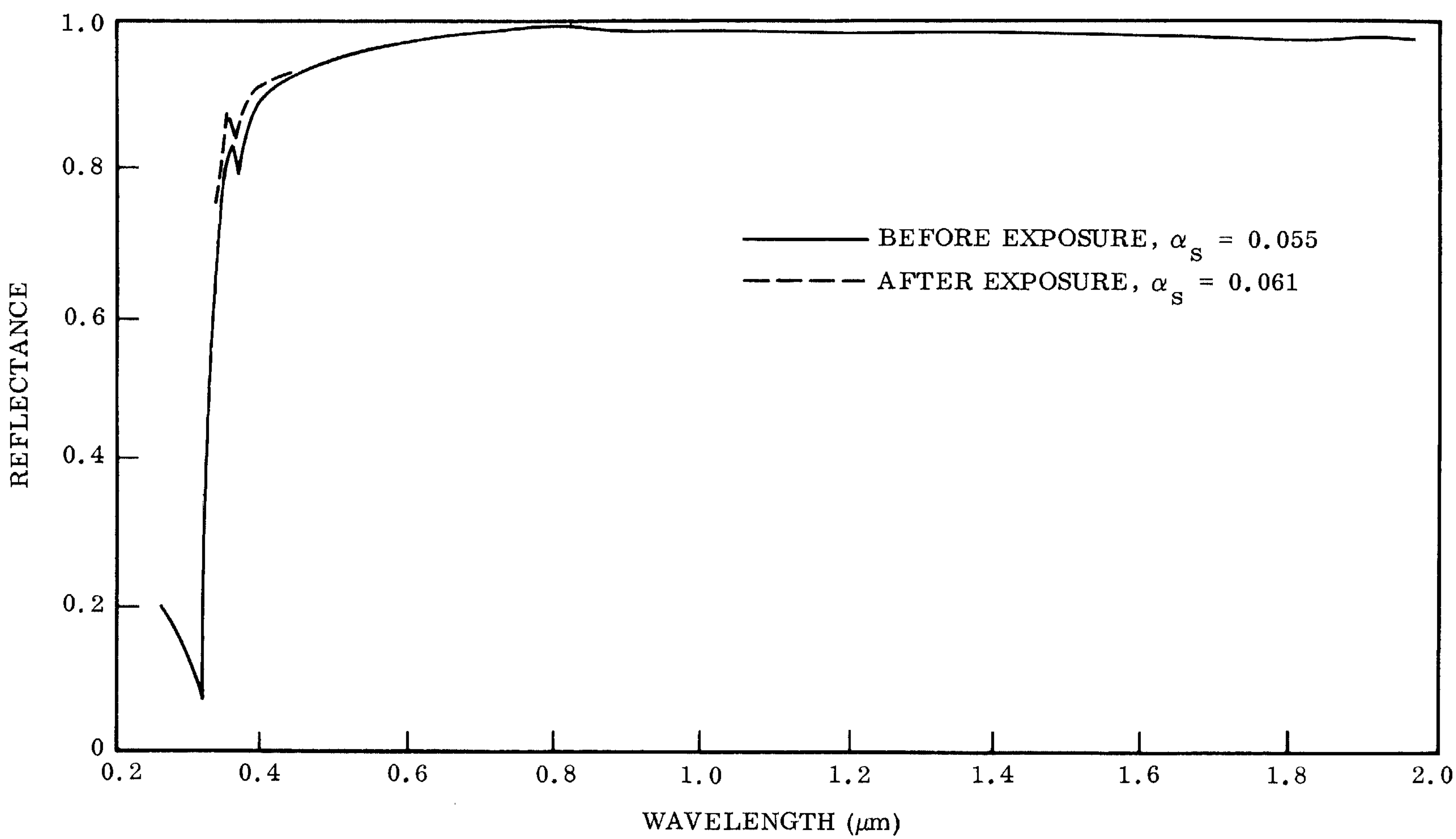

Fig. 6-32 Room Temperature Spectral Reflectance of Optical Solar Reflector Coating, Sample 60, Before and After 2040-hr Exposure Test

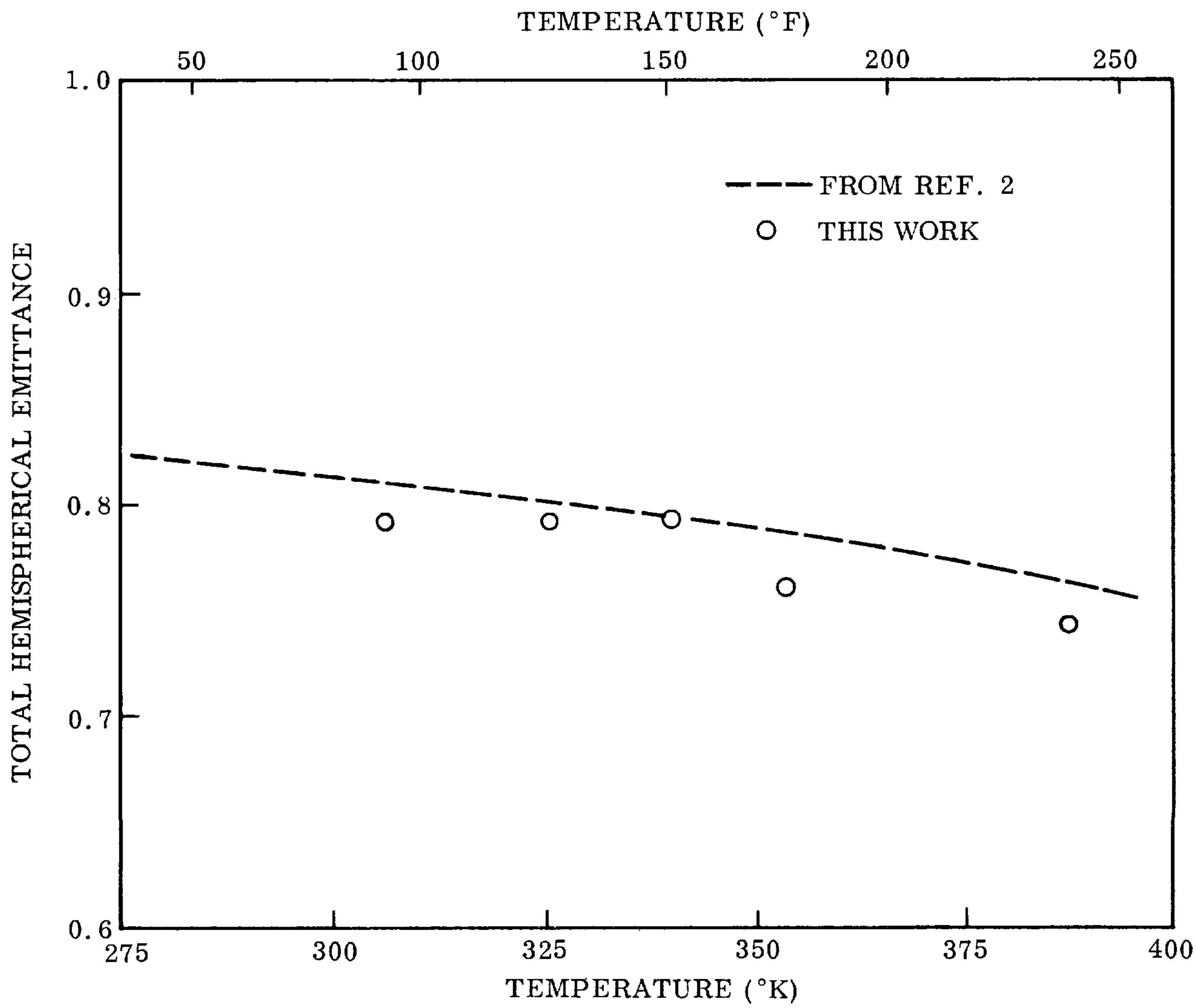

Fig. 6-33 Total Hemispherical Emittance of Optical Solar Reflector as a Function of Temperature

Table 6-4

INITIAL OPTICAL PROPERTIES SUMMARY

Coating	α_s	ϵ_{TH}
Titanium Dioxide/Methyl Silicone (Thermatrol 2A-100)	0.17	0.84 @ 70°F 0.84 @ 250°F
Zinc Oxide/Methyl Silicone (S-13)	0.20	0.87 @ 70°F 0.84 @ 250°F
Zinc Oxide/Methyl Silicone (S-13G)	0.20	0.84 @ 70°F 0.85 @ 250°F
Zirconium Silicate/Potassium Silicate	0.12	0.86 @ 70°F 0.87 @ 250°F 0.85 @ 500°F
Aluminum Silicate/Potassium Silicate	0.14	0.86 @ 70°F 0.86 @ 250°F 0.86 @ 500°F
Zinc Oxide/Potassium Silicate (Z-93)	0.15	0.87 @ 70°F 0.88 @ 250°F 0.86 @ 500°F
Optical Solar Reflector	0.05	0.80 @ 70°F 0.80 @ 150°F

Table 6-5

LATTICE PARAMETERS FOR SAMPLES 30, 36, 55

Sample	Exposure Temperature	a_o (Å)	c_o (Å)
36	534°K (500°F)	3.2495 ± 0.0005	5.2048 ± 0.001
30	422°K (300°F)	3.2499 ± 0.0005	5.2048 ± 0.001
55	Unexposed	3.2503 ± 0.0005	5.2046 ± 0.001

If any changes in structure or composition did occur, they were in quantities undetectable by this method. The slight shift in a_o with temperature falls within the uncertainty assigned to the measurement.

The exposure test specimens were also examined using an electron diffraction technique. These were Samples 35 (534°K—vacuum failure), 36 (534°K), 38 (422°K), and 55 (unexposed).

A small amount of the surface material was removed by a plastic stripping technique and the samples prepared for high resolution transmission electron diffraction at 75 kV. The camera constant was determined to be 18.841. It was determined that all samples were zinc oxide and that there were no detectable reaction products. The "d" spacings were as follows:

X-Ray	Electron Diffraction	X-Ray	Electron Diffraction
2.816	2.81	1.0422	1.03
2.602	2.62	1.0158	1.01
2.476	2.47	0.9848	0.982
1.911	1.90	0.9764	0.972
1.626	1.62	0.9555	0.952
1.477	1.47	0.9382	0.935
1.407	1.40	0.9069	0.904
1.379	1.37	0.8826	0.881
1.359	1.35	0.8675	0.868
1.301	1.30	0.8369	0.837
1.225	1.23	0.8290	0.827
1.1812	1.16	0.8237	0.822
1.0929	1.08	0.8125	0.812
1.0639	1.06		

Section 7
DISCUSSION AND CONCLUSIONS

The change in solar absorptance, $\Delta\alpha_s$, of the titanium dioxide/methyl silicone coating measured by the calorimetric method is in good agreement with that measured by MacMillan et al. (Ref. 53) using an in situ bidirectional reflectance technique. They reported a value of $\Delta\alpha_s$ of 0.11 at 500 equivalent sun hr (ESH) with the sample at approximately 320°K (115°F). This compares with a $\Delta\alpha_s$ of 0.14 at 395°K (250°F) as determined by the calorimetric method. The greater value at the higher temperature is believed to be due to a rate effect which is temperature dependent. After 1330 ESH, MacMillan's data showed a $\Delta\alpha_s$ of 0.15 which appears to have reached a saturation level. Data reported by Arvesen et al. (Ref. 62) for a titanium dioxide/methyl silicone coating show a large spread with temperature, source, and intensity. The reported changes in solar absorptance are considerably lower than those obtained from the in situ methods. This is attributed to the fact that they were computed on the basis of post-exposure reflectance measurements made in air, and the recovery of the TiO_2 in the near infrared upon reexposure to air resulted in a lower value of $\Delta\alpha_s$. This recovery has been demonstrated by both the in situ data (Fig. 6-1) after vacuum failure in the test chamber and the post-test reflectance measurement (Fig. 6-2) as a function of time after removal from the chamber. A summary of the properties of this coating system is as follows:

- Initial α_s, 0.18 ± 0.01 based upon Gier-Dunkle and calorimetric data
- $\Delta\alpha_s$ at 395°K (250°F), 0.14
- Total hemispherical emittance, 0.86 ± 0.02 at 395°K (250°F)

For both zinc oxide/silicone coatings, S-13 and S-13G, the change in solar absorptance was 0.06 to 0.10. This agrees with the data of MacMillan et al. (Ref. 53) and Greenberg (Ref. 63) using the bidirectional in situ method which resulted in a $\Delta\alpha_s$ for S-13 of 0.07 to 0.08 for 500 ESH. Data reported by Pearson (Ref. 54) on flight-test results for a zinc oxide/silicone system show a $\Delta\alpha_s$ of approximately 0.05 after 500-hr exposure to 1 extraterrestrial sun. However, the temperature of this flight sample was not reported.

No in situ data were found in the literature for comparison on the S-13G coating. Both the post-test spectral reflectance data and the broadband spectral data show the improvement of the S-13G in the near infrared region as reported by IITRI (Ref. 60). However, a greater degradation was observed in the 0.2- to 0.85-μm region for the S-13G system with the net result that the $\Delta\alpha_s$ of both systems was nearly equal. Millard (Ref. 61) reported the degradation of the S-13G coating to be approximately one-half that of S-13 from the OSO-III thermal control coating flight experiment. However, others (Ref. 64) have reported the degradation of the S-13G system to depend upon the exact method of coating preparation, so no direct comparison can be made between flight and laboratory test data. The radiative properties of these two systems are summarized as follows.

	S-13	S-13G
Initial α_s	0.20 ± 0.01	0.20 ± 0.01
$\Delta\alpha_s$ at 395°K (250°F)	0.08	0.07
Total Hemispherical Emittance	0.87 ± 0.02	0.89 ± 0.02

Of the three coatings tested at 534°K (500°F), the zinc oxide/potassium silicate system was by far the more stable in regard to solar absorptance. The $\Delta\alpha_s$ was 0.13 for this system (Z-93), whereas it was greater than 0.25 for the zirconium silicate/potassium silicate and aluminum silicate/potassium silicate (Hughes) coatings. The emittance at temperature was consistently higher for the Z-93 system and did not show the wide variation observed for the other two high-temperature systems. If this degradation of Z-93 did reach a saturation level before the 500 hr of exposure, the data are in reasonably good agreement with those reported by Streed et al. (Ref. 27). They exposed zinc oxide/potassium silicate and zirconium silicate/potassium silicate coatings to 7000 ESH at 530°K (495°F) with $\Delta\alpha_s$'s of 0.16 and 0.29, respectively. The radiative properties of these three coatings at 534°K (500°F) are summarized in the following tabulation.

	Zinc Oxide/ Potassium Silicate (Z-93)	Zirconium Silicate/ Potassium Silicate	Aluminum Silicate/ Potassium Silicate
Initial α_s	0.12	0.12	0.15
$\Delta\alpha_s$	0.13	0.30	0.35
ϵ_{TH}	0.81	0.71	0.80

The change in solar absorptance of Z-93 as a function of exposure temperature is shown in Fig. 7-1. Error bands assigned to the calorimetric data are shown by the bars on each point. Change in solar absorptance does not appear to be a linear function of temperature, but rather a discontinuity occurs between 422°K (300°F) and 450°K (350°F). If the degradation process is considered as following some rate function such as $\Delta\alpha_s = Ae^{-B/kT}$, the discontinuity becomes more pronounced (Fig. 7-2). If one considers interstitial zinc donors at 0.05 eV below the conduction band (Ref. 14), the data from 422°K (300°F) to 300°K (80°F) are reasonably approximated by a straight line as shown in Fig. 7-2. The data based upon the post-test spectral reflectance measurements, as shown by the square points of Fig. 7-2, are in good agreement in this range.

There is no obvious explanation for the large change in $\Delta\alpha_s$ at 450°K (350°F). The diffraction studies (subsection 6.4) of the specimen exposed at the various temperatures did not show any differences in composition or structure. No traces of carbon or titanium, which could indicate contamination in the apparatus, were observed from the electron microprobe examinations of the surfaces. One possible cause for this sudden increase in α_s might be that the zinc oxide is encapsulated with potassium silicate which may fail at the higher temperatures. If the silicate prevents loss of surface oxygen and depresses degradation in the near-infrared region, S-13G versus S-13, this protective coating or surface may be physically broken at the higher temperature with resultant degradation in the spectral region $>1.0\ \mu m$. Post-test spectral reflectance curves for the Z-93 as a function of exposure temperature are shown in Fig. 7-3. At 450 and 534°K (350 and 500°F) the reflectance at greater than 1.0 μm is affected significantly, whereas at 422°K (300°F) and below very little change in reflectance is observed past 1.0 μm.

The solar absorptance and total hemispherical emittance of the optical solar reflector (OSR) showed no change during the 2040-hr exposure test at 339°K (150°F). These results are in agreement with those of Marshall and Breuch (Ref. 2). Also, the absolute values of solar absorptance, 0.06, and total hemispherical emittance, 0.80 at 150°F, are identical with those given in this reference.

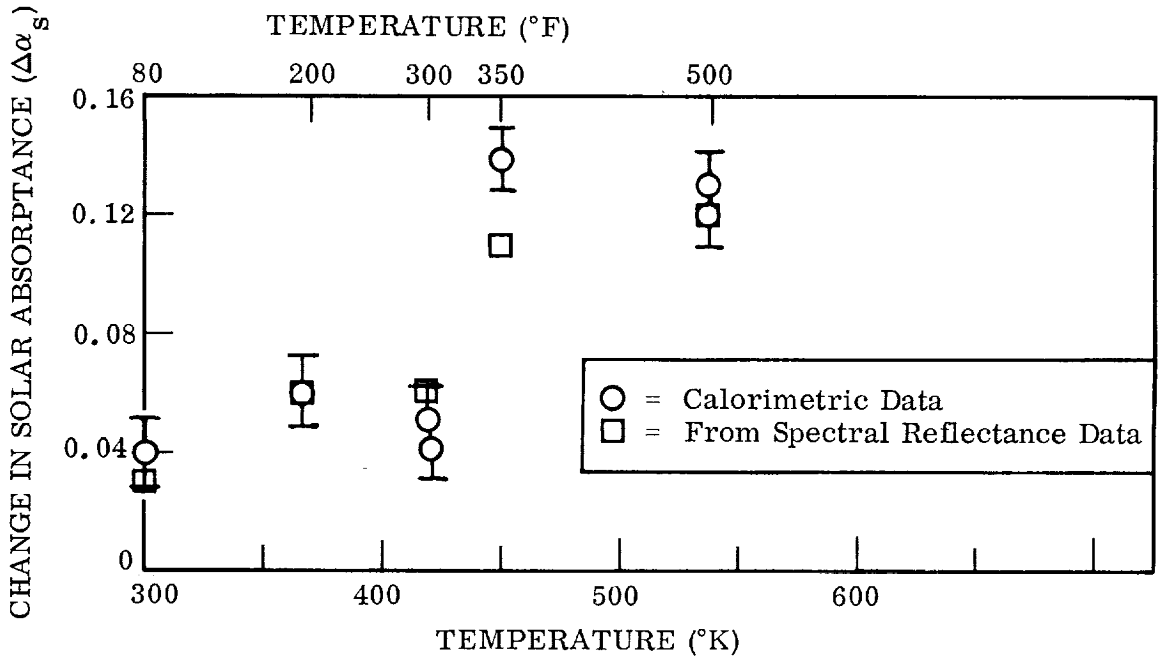

Fig. 7-1 Change in Solar Absorptance of Zinc Oxide/Potassium Silicate Coating (Z-93) as a Function of Exposure Temperature

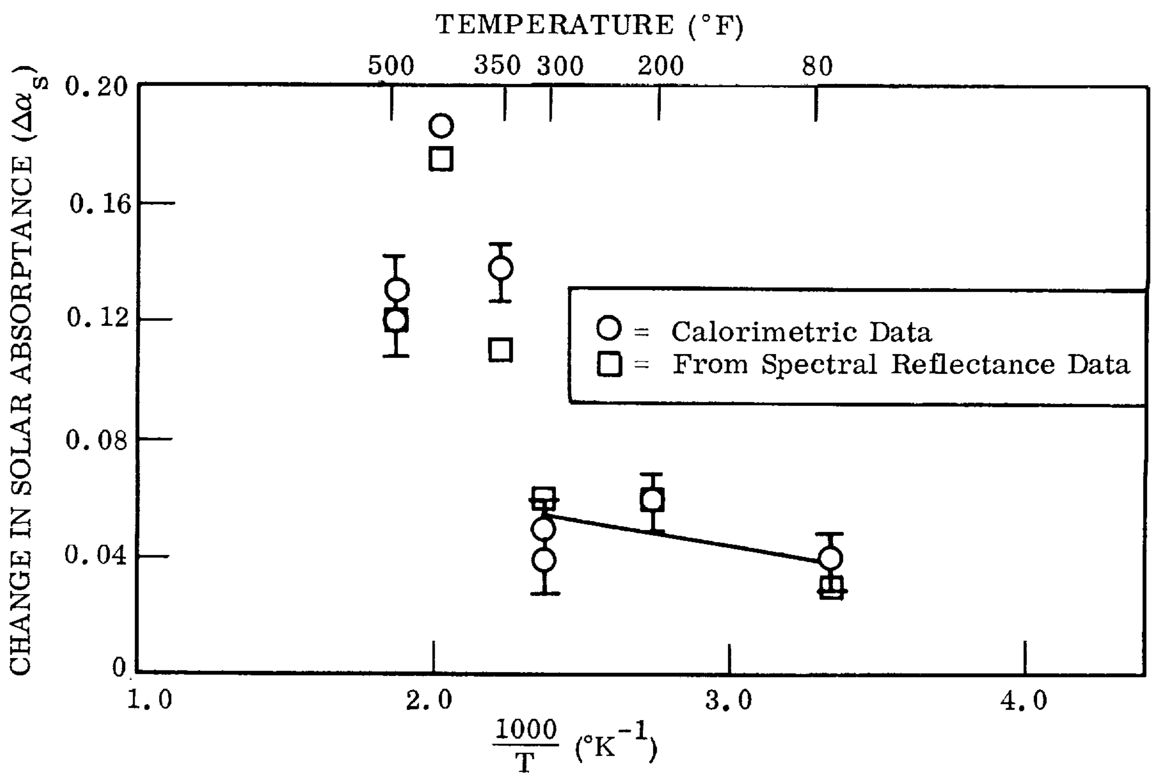

Fig. 7-2 Change in Solar Absorptance of Zinc Oxide/Potassium Silicate Coating (Z-93) as a Function of 1000/T

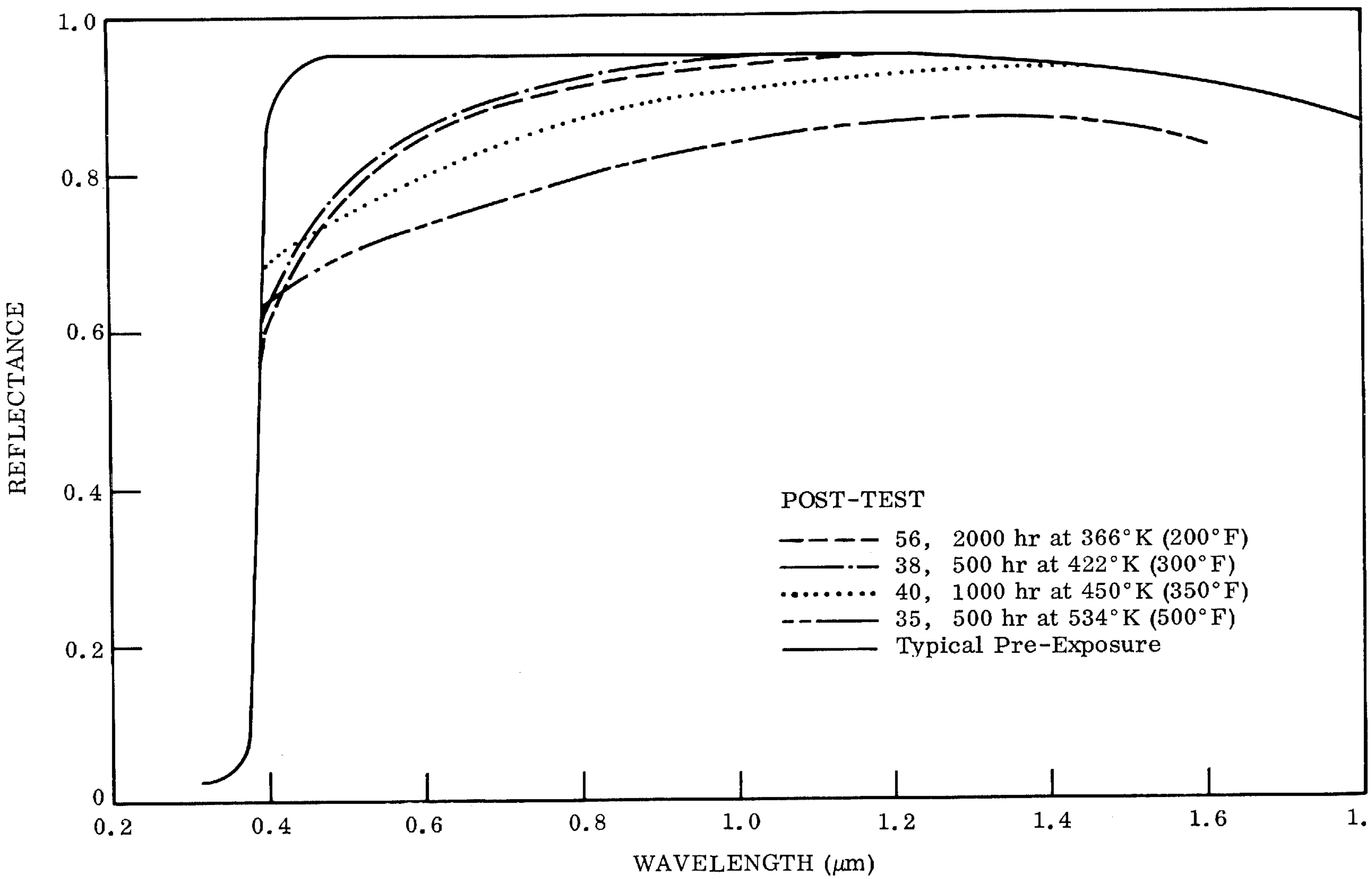

Fig. 7-3 Comparison of Post-Test Spectral Reflectance Curves for Zinc Oxide/Potassium Silicate Coating (Z-93) for the Various Exposure Temperatures

The zinc oxide/potassium silicate system (Z-93) is the best coating currently available for use as a moderate temperature space power system radiator surface treatment. Total hemispherical emittance is as high as any of the coatings tested, 0.90, and the solar absorptance is the lowest of the six paint systems investigated. The initial α_s is 0.14 (based upon absolute spectral reflectance measurements), and for applications to 422°K (300°F), the solar absorptance after prolonged exposure does not exceed 0.20. For low temperature space power system radiator applications, temperature < 365°K (200°F), absorbed solar energy becomes more significant, and a surface with a much lower α_s is required.

The influence of the optical properties of the surface, as exemplified by the Z-93 and OSR coatings, on radiator area is demonstrated by Fig. 7-4. The ratio of actual radiator surface area to that of a perfect radiator ($\epsilon_{TH} = 1.00$, $\alpha_s = 0$) are plotted as a function of surface temperature for a flat plate oriented normal to the solar vector at 1 A.U. from the sun (solar constant, $G_s = 0.139\ W/cm^2$) and radiating to a 0°K sink. For the computations of the OSR surface, α_s is 0.06 and ϵ_{TH} is taken from Fig. 6-33. For the Z-93 surface, α_s increases linearly from 0.18 at 300°K (80°F) to 0.20 at 422°K (300°F) and is constant at 0.26 from 450°K (350°F) to 534°K (500°F). Total hemispherical emittance as a function of temperature was taken from the calorimetric data, Fig. 7-5. From Fig. 7-4, the OSR coating provides a more efficient radiator surface at temperatures below 365°K (200°F). At 339°K (150°F) a radiator using the OSR has an area 20% less than one using the Z-93 coating with the degraded value of α_s. The reduction in area becomes larger with decreasing temperature, radiator area for the OSR surface is approximately one-half of that for one using the Z-93 coating at 300°K (80°F). A second advantage of the OSR surface for the low temperature region is that its α_s is stable, and no adjustments in operation are required to accommodate the increase in solar absorptance with exposure time that occurs for the Z-93 system. At 300°K (80°F), for example, the change in α_s of the Z-93 coating (0.14 to 0.18) represents a 45% increase in radiator area.

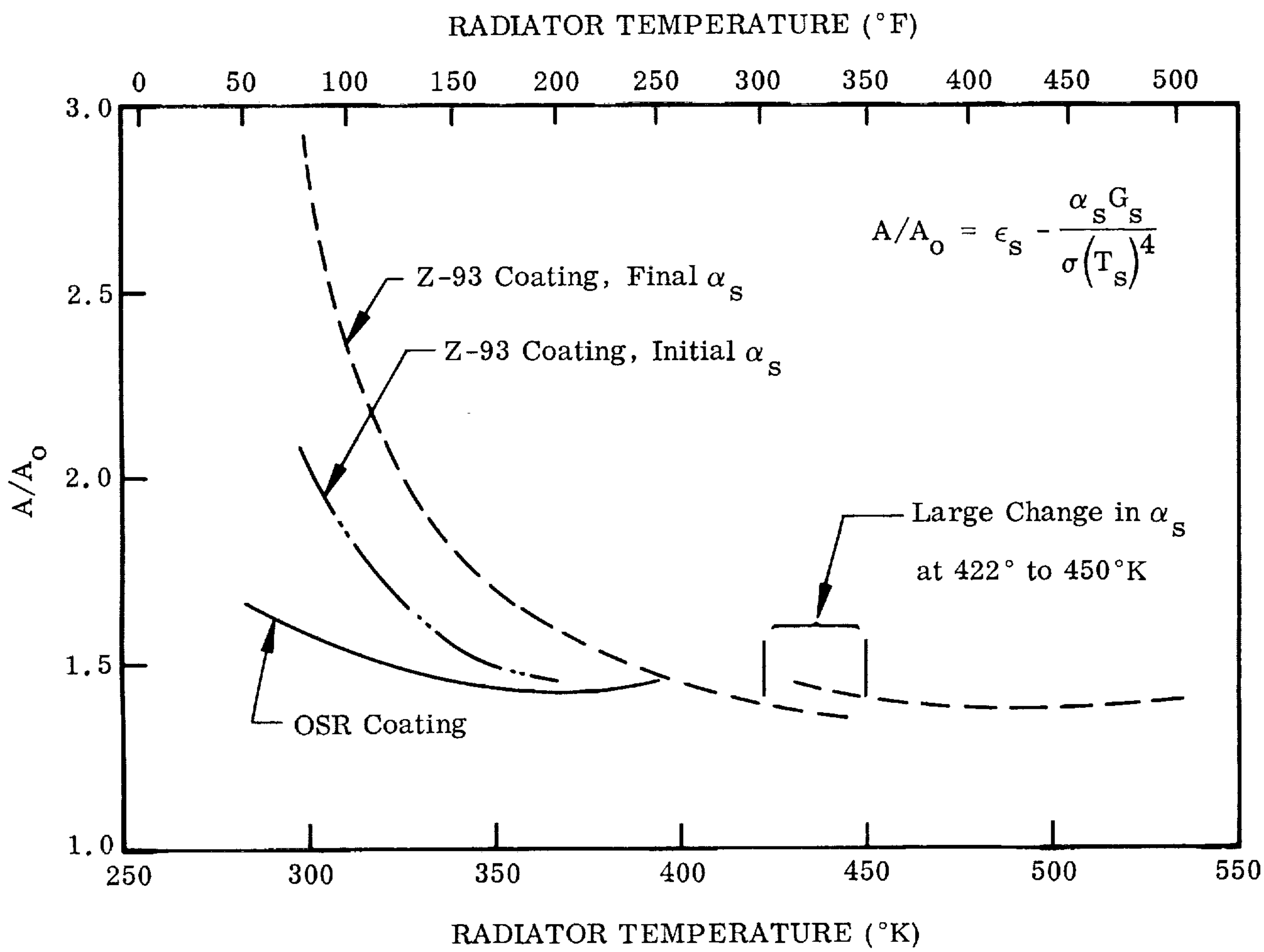

Fig. 7-4 Effect of Coating Optical Properties on Radiator Area as Compared to an Ideal Radiator as a Function of Temperature

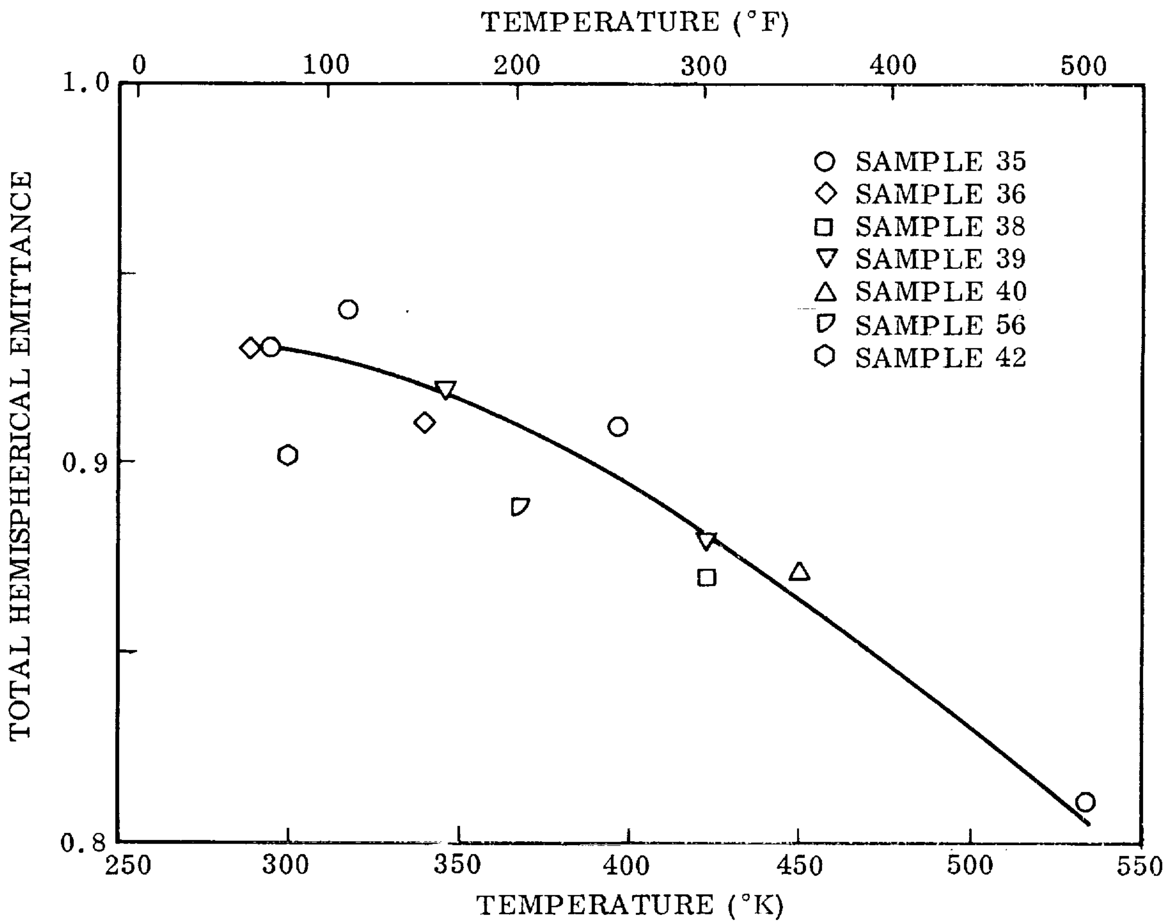

Fig. 7-5 Calorimetric Total Hemispherical Emittance of Zinc Oxide/Potassium Silicate (Z-93) as a Function of Temperature

Section 8
REFERENCES

1. E. R. Streed and J. Arvesen, "Survey of Status of Thermal Control Coatings," Pro. Soc. Aerospace Materials and Process Eng., Apr 1967

2. K. N. Marshall and R. Breuch, "Optical Solar Reflector: A Stable Low α_s/ϵ Spacecraft Thermal Control Surface," AIAA J. Spacecraft, Vol. 5, No. 9, Sep 1968

3. Lockheed Missiles & Space Co., Thermophysics Design Handbook, 8-55-63-3, Sunnyvale, Calif., Jul 1963

4. R.E. Gaumer, F.J. Clauss, M.E. Sibert, and C.C. Shaw, "Materials Effects in Spacecraft Thermal Control," Proceedings of WADD Conference on Coatings for Aerospace Environment, Dayton, Ohio, Nov 1960; WADD TR 60-773, pp. 117 – 136

5. Coatings for the Aerospace Environment, Symposium Sponsored by Wright-Patterson Air Development Center, Wright-Patterson Air Force Base, Ohio, Nov 1960; WADC TR 60-773

6. R.E. Gaumer and L.A. McKellar, Thermal Radiative Control Surfaces for Spacecraft, LMSC-704014, Lockheed Missiles & Space Co., Sunnyvale, Calif., Mar 1961

7. L.A. McKellar, "Effects of the Spacecraft Environment on Thermal Control Materials Characteristics," Spacecraft Thermodynamics Symposium, G.A. Etemad, ed., Holden-Day, 1962, pp. 99 – 128

8. W.F. Carroll, Development of Stable Temperature Control Surfaces for Spacecraft – Progress Report No. 1, JPL Technical Report No. 32-340, Jet Propulsion Laboratory, Pasadena, Calif., Nov 1962

9. "Putting Paints in Orbit," Chemical Week, 13 Feb 1965, pp. 61 – 64

10. Lockheed Missiles & Space Co., Final Report Program 461 Reliability Materials Research and Application Thermophysical Investigations, LMSC-A065463, Sunnyvale, Calif., Jul 1963

11. W.G. Camack and D.K. Edwards, "Effect of Surface Thermal Radiation Characteristics on the Temperature-Control Problem in Satellites," Surface Effects on Spacecraft Materials, F.J. Clauss, ed., New York, Wiley, 1960

12. C.G. Goetzel, J.B. Rittenhouse, and J.B. Singletary, eds., Space Materials Handbook, Lockheed Missiles & Space Co., Sunnyvale, Calif., Mar 1964

13. R.C. Gex and W.L. Hollister, Paints and Pigments for Spacecraft: A Selected Bibliography, LMSC SB-62-9, Mar 1962

14. Solar Radiation-Induced Damage to the Optical Properties of ZnO-Type Pigments, NAS 8-11266, M-50-65-2, Lockheed Missiles & Space Company, Sunnyvale, Calif., Sep 1965

15. W.F. Schmidt and L.A. Haslim, "Effects of the Ascent Environment on Spacecraft Thermal Control Surfaces," Symposium on Materials for Aircraft, Missiles, and Space Vehicles, ASTM Special Technical Publication No. 345, Oct 1962

16. R.E. Mauri, "Ultraviolet Radiation in Space and Its Interaction With Spacecraft Materials," I.E.S. 1963 Educational Seminar on the Space Environment, Moffett Field, Calif., Jan 1963

17. L.A. McKellar, R.L. Olson, and J.V. Stewart, "Laboratory Simulation of Ultraviolet Radiation," I.E.S. 1963 Educational Seminar on the Space Environment, Moffett Field, Calif., Jan 1963

18. N.E. Wahl and J.V. Robinson, "The Effects of High Vacuum and Radiation on Polymeric Materials," National Symposium on the Effects of the Space Environment on Materials, St. Louis, 7 – 9 May 1962, pp. 1 – 28

19. R.G. Schmidt and R.C. Hirt, Studies on the Protective Ultraviolet Absorbers in a High Vacuum Environment, WADC TR 59-354, Wright Air Development Center, Wright-Patterson Air Force Base, Ohio, Jan 1960

20. R. G. Schmidt and R. C. Hirt, Studies on the Protective Ultraviolet Absorbers in a High Vacuum Environment, WADC TR 59-354, Wright Air Development Center, Wright-Patterson Air Force Base, Ohio, Feb 1961

21. R. G. Schmidt and R. C. Hirt, Studies on the Protective Ultraviolet Absorbers in a High Vacuum Environment, Part II, WADC 60-704, Wright Air Development Center, Wright-Patterson Air Force Base, Ohio, Feb 1961

22. R. L. Olson, L. A. McKellar, R. A. Breuch, and J. V. Stewart, Thermal Control Surface Stability Studies, Final Report to Philco WDL, Lockheed Missiles & Space Co., Sunnyvale, Calif., 23 Aug 1963

23. J. V. Stewart, R. L. Olson, and L. A. McKellar, LMSC Results Round-Robin of Ultraviolet Stability Tests, Lockheed Missles & Space Co., Sunnyvale, Calif., Aug 1963

24. R. L. Olson, L. A. McKellar, and W. E. Spicer, The Energetics of Ultraviolet Radiation Damage to White Surface, 6-74-64-11, Lockheed Missiles & Space Co., Sunnyvale, Calif., Mar 1964

25. G. A. Zerlaut, Y. Harada, and E. H. Tompkins, "Ultraviolet Irradiation in Vacuum of White Spacecraft Coatings," Symposium on Thermal Radiation of Solids, San Francisco, Mar 1964

26. R. L. Olson, L. A. McKellar, and J. V. Stewart, "The Effects of Ultraviolet Radiation on Low α_s/ϵ Surfaces," Symposium on Thermal Radiation of Solids, San Francisco, Mar 1964

27. E. R. Streed and C. M. Beveridge, "The Study of Low Solar Absorptance Coatings for a Solar Probe Mission," Symposium on Thermal Radiation of Solids, San Francisco, Calif., Mar 1964

28. W. A. Weyl and Tormod Forland, "Photochemistry of Rutile," Industrial and Engineering Chemistry, Vol. 42, 1950

29. P. R. E. J. Croyley and H. W. Melville, F.R.S., "The Photo-Degradation of Polymethylmethacrylate, I. The Mechanisms of Degradation," Proc. Roy. Soc. (London), Vol. A210, 1952, p. 461; Vol. A211, 1952, p. 320

30. H. H. G. Jellinek, "Photo-Degradation and High Temperature Degradation of Polymers," Pure and Applied Chem., Vol. 4, No. 2-4, 1962

31. V. K. Miloslavskii and N. A. Kovalenko, Optika i Spektroskopiza, Vol. 5, No. 5, 1958, pp. 614 – 617

32. V. N. Filimonov, Optika i Spektroskopiza, Vol. 5, No. 6, 1958, pp. 709 – 711

33. F. M Noonan, A. L. Alexander, and J. E. Cowling, The Properties of Paints as Affected by Ultraviolet Radiation in a Vacuum – Part I, N.R.L. Report 5503, 13 Jul 1960

34. F. M. Noonan et al., The Ultraviolet Degradation of Organic Coatings – Part III, WADD TR-60-703, Pt. III, Dec 1960

35. M. E. Sibert, "Inorganic Coatings for Space Applications," Amer. Chem. Soc. Papers Presented at Annual Meetings 21, Vol. 2, 1961, pp. 349 – 381

36. J. Tsukamato, Inorganic Passive Thermal Control Surfaces, 3-77-61-15, Lockheed Missiles & Space Co., Oct 1961; presented at American Ceramic Society Meeting, San Francisco, Oct 1961

37. M. E. Sibert and F. J. Clauss, "Progress in Spacecraft Materials," Current Eng.-Practice (India), Vol. 5, No. 11, 1962, pp. 59 – 68

38. M. E. Sibert, "Inorganic Coating Systems of Variable Black to White Composition," Ind. Eng. Chem., Prod. Res. and Dev. Quart., Vol. 2, No. 3, 1963, pp. 240 – 244

39. G. A. Zerlaut and Y. Harada, Stable White Coatings Interim Report, ARF 3207-14, Armour Research Foundation, Apr – Oct 1962

40. G. A. Zerlaut, Y. Harada, and J. H. Baldrige, Stable White Coatings, Semi-Annual Report Jet Propulsion Laboratory, IITRI-C6027-7, IIT Research Institute, Chicago, Ill., 13 Aug 1964

41. N. Z. Searle, R. C. Hirt, and J. H. Daniels, Jr., Pigmented Surface Coatings for Use in the Space Environment, ASD-TDR-62-840, Part II, Feb 1964

42. F. M. Noonan, A. L. Alexander, and J. E. Cowling, The UV Degradation of Organic Coatings III – Effect on Physical Properties, WADD TR 60-703, Pt. III, Wright Air Development Center, Wright-Patterson Air Force Base, Ohio, Dec 1960

43. N. Z. Searle et al., Pigmented Surface Coatings for Use in the Space Environment, ML-TDR 64-319, Nov 1964

44. F. M. Noonan, A. L. Alexander, and J. E. Cowling, The Degradation of Polymers by UV Radiation, Part I – When Subjected to Radiation of the "Near" UV Region in Air, NRL 5257, Naval Research Laboratory, Feb 1959

45. H. H. Hormann, Improved Organic Coatings for Temperature Control in a Space Environment, ASD-TDR-62-917, USAF Aeronautical Systems Division, Feb 1963

46. L. A. Haslim, E. L. Riggs, W. F. Schmidt, and L. A. McKellar, "Room Temperature-Curing Surface Systems for Spacecraft Thermal Control," presented at Sixth National Society of Aerospace Materials and Process Engineers Symposium, Seattle, 18–20 Nov 1963

47. L. A. Haslim and E. L. Riggs, "Tailoring Silicones for Thermal Control," Astronautics and Aeronautics (in press)

48. WADC Technical Report 57-334 and Supplement I, Apr 1958

49. K. N. Marshall and R. L. Olson, Optical Solar Reflector Thermal Control Surface, 3-56-65-2, Lockheed Missiles & Space Co., Sunnyvale, Calif., 2 Feb 1965

50. R. E. Gaumer et al., "Calorimetric Determinations of Thermal Radiation Characteristics," Progress in International Research on Thermodynamic and Transport Properties, ASME, Academic Press, 1962, pp. 575–587

51. N. J. Douglas, "Directional Solar Absorptance Measurements," Symposium on Thermal Radiation of Solids, San Francisco, Mar 1964

52. F. S. Johnson, ed., Satellite Environment Handbook, Stanford, Calif., Stanford Univ. Press, 1961

53. H. F. MacMillan, Jr., A. F. Sklensky, and L. A. McKellar, "In Situ Bidirectional Reflectance Apparatus," Thermophysics and Temperature Control of Spacecraft and Entry Vehicles, Prog. in Astronautics and Aeronautics, Academic Press, Vol. 18, 1966

54. B. P. Pearson, Jr., "Preliminary Results From the Ames Emissivity Experiment on OSO-II," Thermophysics and Temperature Control of Spacecraft and Entry Vehicles, Prog. in Astronautics and Aeronautics, Academic Press, Vol. 18, 1966

55. J. R. Crosby and M. A. Perlow, "SNAP 10A Thermal Control Coatings," Thermophysics and Temperature Control of Spacecraft and Entry Vehicles, Prog. in Astronautics and Aeronautics, Academic Press, Vol. 18, 1966

56. L. A. McKellar, J. V. Stewart, and R. L. Olson, "Laboratory Technique for the Study of Ultraviolet Radiation Effects," J. Environ. Sciences, Vol. 8, No. 1, Feb 1965, pp. 22–26

57. Space Environmental Effects on Materials and Components, Vol. I, "Elastomeric and Plastic Materials," Appendix C, Coatings, RSIC-150, Redstone Scientific Info. Ctr., U. S. Army Missile Command, Redstone Arsenal, 1 Apr 1964

58. G. A. Zerlaut, Y. Harada, and L. U. Berman, Development of Space-Stable Thermal-Control Coatings (Paints With Low Solar Absorptance/Emittance Ratios), IITRI-C6014-13, IIT Research Institute, Chicago, Ill., 20 Jan 1964 to 20 Jun 1964

59. J. D. Plunkett, NASA Contributions to the Technology of Inorganic Coatings, NASA SP-5014, 1964

60. G. A. Zerlaut and B. H. Kaye, Development of Space-Stable Thermal-Control Coatings (Paints With Low Solar Absorptance/Emittance Ratios), IITRI-C6014-21, IIT Research Institute, Chicago, Ill., 23 Feb 1965

61. J. P. Millard, "Results From the Thermal Control Coatings Experiment on OSO-III," presented at the AIAA Thermophysics Specialists Conference, Los Angeles, Jun 1968

62. J. Arvensen, C. Neal, and C. Shaw, "Preliminary Results From a Round-Robin Study of Ultraviolet Degradation of Spacecraft Thermal-Control Coatings," Symposium on Thermal Radiation of Solids, 4 Mar 1964, San Francisco, Calif., NASA SP-55, edited by S. Katzoff

63. S. A. Greenberg, Private Communication, May 1967

64. G. A. Zerlaut, G. Noble, and F. O. Rogers, Development of Space-Stable Thermal Control Coatings, IITRI, Report IITRI-U6002-55, Sep 1967

Section 9

CONTRACT REPORTS

1. Emissivity Coatings for Low-Temperature Space Radiators, QPR-1, NASA-CR-54807, Lockheed Missiles & Space Company, Sunnyvale, Calif., Sep 1965. Contents: Literature survey, coating selection, description of experimental apparatus.

2. Emissivity Coatings for Low-Temperature Space Radiators, QPR-2, NASA-CR-72059, Lockheed Missiles & Space Company, Sunnyvale, Calif., Dec 1965. Contents: Apparatus description, uv source description, initial properties of coatings.

3. Emissivity Coatings for Low-Temperature Space Radiators, QPR-3, NASA-CR-72060, Lockheed Missiles & Space Company, Sunnyvale, Calif., Mar 1966. Contents: Experimental procedure, spectral band absorptance measurements, initial properties of coatings.

4. Emissivity Coatings for Low-Temperature Space Radiators, QPR-4, NASA-CR-72089, Lockheed Missiles & Space Company, Sunnyvale, Calif., Jun 1966. Contents: Initial properties of coatings, thermal cycling results, experimental procedures, exposure test results on titanium dioxide/silicone (thermatrol).

5. Emissivity Coatings for Low-Temperature Space Radiators, QPR-5, NASA-CR-72130, Lockheed Missiles & Space Company, Sunnyvale, Calif., Sep 1966. Contents: Exposure test results on zinc oxide/silicone (S-13), zinc oxide/silicone (S-13G), zirconium silicate/potassium silicate, and zinc oxide/potassium silicate (Z-93).

6. Emissivity Coatings for Low-Temperature Space Radiators, QPR-6, NASA-CR-72161, Lockheed Missiles & Space Company, Sunnyvale, Calif., Dec 1966. Contents: Exposure test results on aluminum silicate/potassium silicate, and zinc oxide/potassium silicate (Z-93).

7. Emissivity Coatings for Low-Temperature Space Radiators, Interim Summary Report, Lockheed Missiles & Space Company, Sunnyvale, Calif., Report L-23-68-1, Jun 1968. Contents: Results of all tests on coating systems through June 1968.

Appendix A
DESCRIPTION OF CANDIDATE COATINGS

A.1 TITANIUM DIOXIDE/METHYL SILICONE (THERMATROL 2A-100)

Source and Cost – Lockheed Missiles & Space Company; price variable depending on quantity; nominal price is $60 per gallon.

Starting Composition – Polymethyl-vinyl siloxane elastomer plus TiO_2 pigment, 1:1 by weight.

- Vehicle: Dow-Corning proprietary, Q92-009, 33% nonvolatile content by weight, 24 hr at 70°C

Flash Point	60° to 65°F
Viscosity, cps	15,000
Specific Gravity	0.835
Diluted with VM and P Naptha	

- Pigment: Titanox RA-NC, Titanium Pigment Corp., proprietary; calcined rutile TiO_2, 93% TiO_2.

Particle Shape and Size – The weighted average particle size is 0.3 μ. The particles are spherical.

Substrate – 2.54 cm diameter disk, 0.127 cm thick of 6061 T-6 aluminum machined to a 30 rms finish.

Method of Application – The finish is applied by spray techniques conforming to MIL-F-18264 specifications. Prior to applying the top coat, the entire surface is primed with one coat of silicone primer, Dow Corning Corp. A-4094 or equivalent,

to a thickness of approximately 0.2 mils. The primer is air cured 30 min minimum prior to application of top coats. Thickness and cure times for the top coat are as follows:

Total dry film thickness, including primer, 3.5 to 5.0 mils
Curing time; 24 hr minimum after final coat

Coating Thickness – 3.5 to 5.0 mils.

Density – 1.5 gm/cm^3

Weight Loss During Vacuum Testing – Negligible after coating has been fully cured.

A.2 ZIRCONIUM SILICATE/POTASSIUM SILICATE

Source and Cost – Lockheed Missiles & Space Company; price variable depending on quantity; nominal price $740 per gallon.

Starting Composition –

- Pigment to binder ratio: 3.5 to 1 by weight
- Pigment: Metals and Thermit Corp., 1000W grade, "Ultrox" zirconium silicate, acid leached and calcined by LMSC
- Binder: potassium silicate

Particle Shape and Size – Particle shape, angular; particle size, $< 1.0\ \mu$.

Substrate – 2.54 cm diameter disk, 0.127 cm thick of 6061 T-6 aluminum machined to a 30 rms finish.

Method of Application – Standard spray gun techniques, base coat reacts with substrate and serves as primer; room temperature cure, approximately 12 hr.

Coating Thickness – 3.0 to 5.0 mils.

Density – 4.0 gm/cm^3

Weight Loss During Vacuum Testing – Less than 5.0%.

A.3 HUGHES INORGANIC WHITE COATING (ALUMINUM SILICATE/ POTASSIUM SILICATE)

Source and Cost – Hughes Aircraft Co.; cost figures not stated by supplier.

Starting Composition –

- Pigment to binder ratio: 4.4 to 1 by weight
- Pigment: A naturally occurring china clay primarily aluminum silicate; approximately 3.0% impurity level, namely Fe-0.70%, Ti 0.42%, Ca 0.05%, Mg 1.28%, Na 0.47%, and K 0.11%; the clay is calcined at 1275°C, then ball milled for 12 hr with water.
- Binder: Sylvania PS-7 electronic grade potassium silicate

Particle Size – Particle size following milling less than 200 mesh.

Substrate – 2.54 cm diameter disk, 0.127 cm thick of 6061 T-6 aluminum machined to 30 rms finish.

Method of Application – The coating is applied in three coats, each coat being baked for 1 hr at 225°F and the final coating baked for 1 hr at 260°F. An air brush is used for painting.

Coating Thickness – 6.0 to 8.0 mils after curing.

Weight Loss During Vacuum Testing – The procedure is covered by Hughes Materials and Process Specification, HMS 15-1374 and HP 4-135. A typical weight loss is 0.02% when exposed to vacuum at 250°F; the weight loss is water vapor.

A.4 ZINC OXIDE/METHYL SILICONE (S-13 Modification II)

Source and Cost – IIT Research Institute; cost not stated by supplier.

Starting Composition –

Materials	Parts by Weight
New Jersey Zinc SP500 zinc oxide	240
General Electric RTV-602 silicone	100
Toluene	170

Formulation – The zinc oxide, the RTV-602, and 100 parts by weight of the toluene are premixed and charged to a porcelain ball mill in a quantity sufficient to just fill the void space when the mill is one-fourth full of grinding stones 0.5 in. in diameter. The paint is ground for 3 hr at approximately 70% critical speed. The critical speed (rpm) is given by $w_{c_s} = 54.2/\sqrt{R}$, where R is the radius of the mill in feet. The basic charge is then removed, and 70 parts of toluene are added to the mill. The mill residue and the solvent are ground until the contents are uniformly thin, but not for more than 5 min. The contents are then added to the main charge, and the whole charge is mixed thoroughly.

Note: The SRC-05 catalyst is not added until the paint is applied.

Particle Shape and Size – Particle shape not stated by supplier. The weighted average particle size is 0.9 μ.

Substrate – 2.54 cm diameter disk, 0.127 cm thick of 6061 T-6 aluminum machined to a 30 rms finish.

Method of Application

Preparation of Paint for Application – The paint is furnished without the SRC-05 catalyst. The catalyst is added as 1 part SRC-05 in 20 parts of toluene per 670 parts of S-13 (as formulated). This concentration represents 0.76% catalyst based on polymer solids. A lower concentration is recommended in order to ensure optimum stability to uv irradiation in vacuum. A concentration of 0.4% based upon RTV-602 provides optimum stability without greatly sacrificing terminal cure properties, although a coating prepared at this concentration represents the lower limit without sacrificing cure and physical properties. Somewhat better physical properties are obtained with a catalyst concentration of 0.5% based on RTV-602. A catalyst concentration of 0.4% of resin solids corresponds to 1 part SRC-05 per 1275 parts of S-13; 0.5% catalyst requires 1 part catalyst per 1020 parts of S-13. The catalyst should be added as a 20:1 reduction in toluene. The catalyst solution is added only as the paint is used and only to the amount that can be applied in about 30 min. The bulk paint was furnished in 5-gal epoxy-lined metal pails. The paint should be thoroughly stirred before transfer to other containers or before addition of catalyst. Allow the catalyst paint to set for 10 min before application to the primed surfaces.

Preparation of Surfaces for Painting – Standard surface cleaning procedures should be used to prepare the surface for application of the S-13 paint. S-13 paint can, in general, be applied to any surface to which the required primer can be applied. The primer, General Electric's proprietary SS-4044, can be applied to either anodized or zinc chromate-primed surfaces. It is preferable that it be applied to clean bare metal or to anodized surfaces, however. Greasy surfaces should be cleaned with standard detergent and water prior to priming; they should be thoroughly dry.

Application of Paint – The primer can be spray-applied (Binks model 18 or comparable gun) at about 30 psi. Only about 0.5 mil of primer is required (just enough to provide a base for the S-13 paint). The primer should be allowed to air-dry for 1 hr before application of the S-13 paint.

The S-13 paint can be spray-applied with a Binks model 18 spray gun (or comparable gun) at a gas pressure of about 60 psi. Unless clean, dry air is available, prepurified nitrogen or prepurified air must be used. The S-13 paint should be allowed to air cure for 16 hr. It is imperative that dust and debris be kept off the surface during the curing process.

The wet film thickness of the paint can be measured by either the Pfund or the Interchemical wet-film thickness gage, or a suitable bridge-type gage. Dry film thickness can be measured with a Fischer Permascope nondestructive thickness tester, type ECTH.

Reapplication – Soiled or damaged areas can be recoated. Soiled areas must be cleaned thoroughly with detergent and water and dried before application of additional S-13 paint. Damaged or gouged areas can be recoated by making a paste of S-13 in which the bulk of the solvent is omitted. Such a material can be troweled or brushed over the damaged areas and cures can be tack-free within a few hours.

Coating Thickness – 3.5 to 5.5 mils.

Weight Loss During Vacuum Testing – Not stated by supplier.

A.5 ZINC OXIDE/METHYL SILICONE (S-13G)

Source and Cost – IIT Research Institute; cost not given by supplier.

Starting Composition –

Material	Part By Weight
New Jersey Zinc Co., SP 500 zinc oxide, PS7-treated	240
General Electric Co., RTV-602 silicone	100
Toluene, USP	175
	515

Silicate Treated ZnO – The PS7 treated ZnO is used to prepare the S-13G paint. Approximately 600 g of "as received" SP500 zinc oxide are thoroughly mixed with 1200 g of PS7 potassium silicate (Sylvania) in a 2-quart capacity ball-mill jar. Approximately 20 cylindrical grinding stones, 1 × 1/2-in. diameter, are added to the mill, and the slurry is ground at approximately 75% of critical speed for 45 min. The ball-jar is removed from the mill, and the ground mixture is allowed to stand approximately 16 hr. The slurry is then reground for 10 min. The ground slurry is transferred to a 3-liter beaker and diluted with 800 ml of distilled water. The mixture is thoroughly stirred and transferred to a large Buchner funnel and filtered at reduced pressure through a No. 597 filter paper.* The filter cake is washed with 3 liters of distilled water and pumped dry. The filter cake is removed from the funnel and spread on an aluminum foil tray. The contents are placed in a forced-air oven and dried for 16 hr at 100°C. The dried treated-pigment is then placed in a completely dry mill jar and dry ground with approximately 20 grinding stones for 15 min. The resultant treated-pigment is then reheated for 1 hr at 100°C.

The zinc oxide, the RTV-602, and 100 parts by weight of the toluene are premixed and charged to a porcelain ball mill in quantity sufficient to just fill the void space when the mill is one-half full of grinding stones 0.5 in. in diameter. The paint is ground for 4 hr at approximately 70% critical speed. The critical speed (rpm) is given by:

$$W_{C_S} = \frac{54.2}{\sqrt{R}}$$

where R is the radius of the mill in feet. The basic charge is then removed, and the remaining toluene is added to the mill. The mill residue and the solvent are ground until the contents are uniformly thin, but not for more than 5 min. The contents are then added to the main charge, and the whole charge is mixed thoroughly. Note: The SRC-05 catalyst is not added until the paint is applied.

*Schleicher and Schuell Analytical Filter Paper.

Particle Size and Shape – Not stated by supplier.

Substrate – 2.54 cm diameter disk, 0.127 cm thick of 6061 T-6 aluminum machined to a 30-rms finish.

Method of Application

Preparation of Paint for Application – The paint is furnished without the SRC-05 catalyst. The catalyst is added as 1 part SRC-05 in 10 parts of toluene: The catalyst solution is added to the paint with thorough stirring. A low catalyst concentration is recommended to ensure optimum stability to ultraviolet irradiation in vacuum. A concentration of 0.4% based upon RTV-602 provides optimum stability without greatly sacrificing thermal-cure properties, although a coating prepared at this concentration represents the lower limit without sacrificing cure and physical properties. Somewhat better physical properties are obtained with a catalyst concentration of 0.5% based on RTV-602 and still better properties are obtained at 0.75% SRC-05. The SRC-05 catalyst-to-paint ratio is 1 part SRC-05 in 10 parts of toluene to 1030 parts of S-13G (by weight). The catalyst solution is added only as the paint is used and to only the amount that can be applied in a 30-min period. Allow the catalyzed paint to set for 10 to 15 min before application to the primed surfaces. The paint should be thoroughly stirred before transfer to other containers or before addition of catalyst.

Preparation of Surfaces for Painting – Standard surface cleaning procedures should be used to prepare the surface for application of the S-13G paint. The S-13G paint can, in general, be applied to any surface to which the required primer can be applied. The primer, General Electric's proprietary SS-4044, can be applied to either anodized or zinc chromate-primed surfaces. It is preferable that it be applied to clean bare metal or to anodized surfaces, however. Greasy surfaces should be cleaned with standard detergent and water prior to priming; they should be thoroughly dry.

Application of Paint – The primer can be spray-applied (Binks model 18, Paasche Autch, or comparable gun) at about 30 psi. Only about 0.5 mil of primer is required (just enough to provide a base for the S-13 paint). The primer should be allowed to air-dry for 1 to 2 hr before application of the S-13G paint. The S-13G paint can be spray-applied with a Binks model 18 spray gun (or comparable gun) at a gas pressure of about 60 psi. Unless clean, dry air is available, prepurified nitrogen or prepurified air must be used. The S-13G paint should be allowed to air-cure 16 hr before handling. It is imperative that dust and debris be kept off the surface during the curing process.

The wet film thickness of the paint can be measured by either the Pfund or the Interchemical wet-film thickness gage, or a suitable bridge-type gage. Dry film thickness can be measured with a Fischer Permascope nondestructive thickness tester, type ECTH.

Reapplication – Soiled or damaged areas can be recoated. Soiled area must be cleaned thoroughly with detergent and water and dried before application of additional S-13G paint. Damaged or gouged areas can be recoated by making a paste of S-13G in which the bulk of the solvent is omitted. Such a material can be troweled or brushed over the damaged areas and cures tack-free within a few hours.

A.6 ZINC OXIDE/POTASSIUM SILICATE (Z-93)

Source and Cost – IIT Research Institute; cost not stated by supplier.

Starting Composition –

- Pigment to binder ratio: 4.3 to 1 by weight
- Pigment: New Jersey Zinc Co., SP500 zinc oxide; calcined at 600° to 700°C for 16 hr (heating and cooling rates are not critical)
- Binder: Sylvania Electric Products Corp., PS7 potassium silicate

Formulation – The materials are mixed in a PBR of 4.30 and a solids content of 56.9%. A typical batch is 100 g of ZnO, 50 cm^3 of PS7 (35% solution), and 50 cm^3 of distilled water. The ingredients are ball-milled with porcelain balls in a dense alumina mill. The volume ratio of balls to materials is 1:3, and the total charge is <50%. The milling time of 6 hr at 70% critical speed [rpm = 54.2 $\sqrt{\text{mill radius}}$ (ft)] yields a satisfactory consistency for spraying and is recommended.

The paint is prepared just before it is to be used. Shelf life for this composition is limited. Actual shelf time should not exceed 24 hr, and the mixture should be shaken occasionally to maintain the pigment in suspension.

Particle Shape and Size – Particle shape not stated by supplier; mean particle size $\sim 0.6\ \mu$.

Substrate – 2.54 cm diameter disk, 0.127 cm thick of 6061 T6 aluminum machined to a 30-rms finish.

Method of Application –

Application – The formulation is applied by spray-painting. The carrier gas should be clean; prepurified nitrogen is a good source. Aluminum or plastic substrates should be abraded; e.g., with No. 60 Aloxite metal cloth, and thoroughly washed with detergent and water.

The application technique consists of spraying at a distance of 6 to 12 in. until a reflection due to the liquid is apparent. This is followed by air-drying until the gloss is practically gone, at which time the spraying-drying cycle is repeated. A thickness of about 1 mil is achieved per cycle. Coating dimensions can therefore be predictably applied. However, hand-spraying is inherently an art and not a science, and experience must be gained by the individual painter to determine the most satisfactory technique for him.

Reapplication – The porous nature of a cured coating necessitates heavy spraying upon application of a second coat to achieve a satisfactory, finished texture. If the area to be repainted has been contaminated, it should be scrupulously cleaned with detergent and water. If desired, the paint can be removed simply by abrasion, since it is somewhat soft.

Curing – Satisfactory physical properties are obtained by an air-drying cure. Improved hardness is obtained by heat-curing at 140° C. Strict adherence to cleanliness should be observed during this step as in all the other steps. The presence of impurities can greatly decrease the stability of paints to the space environment.

Coating Thickness – 4.5 to 6.0 mils.

Weight Loss During Vacuum Testing – Not stated by supplier.

A.7 OPTICAL SOLAR REFLECTOR (LMSC)

Source and Cost – Optical Coatings Laboratory, Inc.; present large quantity price of $\$2.20/\text{in.}^2$

Composition – Metallic silver, vacuum deposited on one surface of fused silica, silver overcoated by a vacuum-deposited layer of Inconel.

- Fused Silica: Corning Glass Works No. 7940, 8×10^{-3}-in. thick by 1-in. square
- Coatings: Approximately 1000 Å of silver plus 500 Å Inconel overcoat. Both depositions made in same chamber without breaking vacuum

Optical Properties – Solar absorptance from 0.27 to 1.80 μm = 0.05 ± 0.005, total hemispherical emittance at 300°K (80°F) = 0.81 ± 0.02. Spectral reflectance data shown by Fig. A-7, minimum reflectance of 0.87 and 0.380 ± 0.001 μm, 0.95 at 0.475 ± 0.005 μm and 0.98 at 1.00 ± 0.02 μm. The very high reflectance to solar

energy results from the silver second surface as the fused silica is transparent to 4 μm. The high emittance is achieved by the opacity of the fused silica in the spectral region beyond 4.5 μm.

Substrate – 2.54-in. diameter disk, 0.127-in. thick of 6061-T6 aluminum machined to a 30 rms finish.

Method of Application – The OSR is attached to the substrate with an adhesive or a double-coated layer of plastic tape. The test specimen was attached to the aluminum disk with approximately 1-mil thickness of General Electric Co. RTV 615 silicone adhesive (GE No. SS 4120 primer). The adhesive is allowed to air cure for 5 days.

Density – 2.2 gm/cm^3, OSR plus adhesive weight per unit area of 0.49 kg/m^2 (0.10 lb/ft^2).

Weight Loss During Vacuum Testing – Negligible after adhesive is fully cured.

A.8 INITIAL OPTICAL PROPERTIES

The initial optical properties, the solar absorptance (α_s) and the infrared emittance (ϵ), have been determined and are tabulated in Table A-1. Spectral reflectance curves for each coating type are presented in Figs. A-1 through A-7. Data obtained by use of the Cary spectrophotometer and the Gier-Dunkle integrating sphere are presented for comparison. The emittance values reported were obtained by use of the Lion Research Corp. Optical Surface Comparator.

Table A-1

INITIAL ROOM TEMPERATUE OPTICAL PROPERTIES

Sample	Source	Coating	Solar Absorptance		Emittance (Optical Surface Comparator)
			Cary	Gier-Dunkle	
1	LMSC	Titanium Dioxide/	0.15 ± 0.02	0.17 ± 0.01	0.88 ± 0.03
2		Methyl Silicone	0.15 ± 0.02	0.16 ± 0.01	0.82 ± 0.03
3		(LMSC Thermatrol	0.15 ± 0.02		0.91 ± 0.03
4		2A-100)	0.18 ± 0.02[(a)]	0.19 ± 0.01	0.85 ± 0.03
5			0.15 ± 0.02		0.85 ± 0.03
6			0.15 ± 0.02		0.85 ± 0.03
7			0.15 ± 0.02		0.87 ± 0.03
8			0.15 ± 0.02		0.86 ± 0.03
9	LMSC	Zirconium Silicate/	0.11 ± 0.02	0.11 ± 0.01	0.91 ± 0.03
10		Potassium Silicate	0.11 ± 0.02		0.87 ± 0.03
11		(LMSC)	0.14 ± 0.02	0.15 ± 0.01	0.90 ± 0.03
12			0.11 ± 0.02		0.90 ± 0.03
13			0.13 ± 0.02		0.91 ± 0.03
14			0.11 ± 0.02	0.11 ± 0.01	0.90 ± 0.03
15			0.14 ± 0.02		0.90 ± 0.03
16			0.10 ± 0.02		0.90 ± 0.03
19	Hughes	Aluminum Silicate/	0.14 ± 0.02	0.14 ± 0.01	0.90 ± 0.03
20		Potassium Silicate	0.14 ± 0.02	0.14 ± 0.01	0.88 ± 0.03
21		(Hughes)	0.14 ± 0.02		0.90 ± 0.03
22			0.14 ± 0.02		0.90 ± 0.03
23			0.14 ± 0.02		0.89 ± 0.03
24			0.14 ± 0.02		0.88 ± 0.03
25			0.14 ± 0.02		0.90 ± 0.03
26			0.13 ± 0.02		0.90 ± 0.03
27	IITRI	Zinc Oxide/	0.19 ± 0.02	0.20 ± 0.01	0.79 ± 0.03
28		Methyl Silicone	0.19 ± 0.02	0.20 ± 0.01	0.79 ± 0.03
29		(S-13, IITRI)	0.19 ± 0.02		0.81 ± 0.03
30			0.19 ± 0.02		0.80 ± 0.03
31			0.19 ± 0.02		0.81 ± 0.03
32			0.19 ± 0.02		0.87 ± 0.03
33			0.18 ± 0.02		0.85 ± 0.03
34			0.19 ± 0.02		0.80 ± 0.03

Table A-1 (Cont.)

Sample	Source	Coating	Solar Absorptance		Emittance (Optical Surface Comparator)
			Cary	Gier-Dunkle	
35	IITRI	Zinc Oxide/	0.14 ± 0.02	0.15 ± 0.01	0.92 ± 0.03
36		Potassium Silicate	0.14 ± 0.02	0.14 ± 0.01	0.96 ± 0.03
37		(Z-93, IITRI)	0.14 ± 0.02		0.96 ± 0.03
38			0.14 ± 0.02		0.91 ± 0.03
39			0.14 ± 0.02		0.96 ± 0.03
40			0.14 ± 0.02		0.96 ± 0.03
41			0.14 ± 0.02		0.97 ± 0.03
42			0.14 ± 0.02		0.95 ± 0.03
43	IITRI	Zinc Oxide/	0.19 ± 0.02	0.20 ± 0.01	0.85 ± 0.03
44		Methyl Silicone	0.20 ± 0.02	0.20 ± 0.01	0.85 ± 0.03
45		(S-13G, IITRI)	0.20 ± 0.02	0.20 ± 0.01	0.85 ± 0.03
46			0.20 ± 0.02	–	0.85 ± 0.03
47			0.19 ± 0.02	–	0.85 ± 0.03
48			0.16 ± 0.02	–	0.86 ± 0.03
49			0.20 ± 0.02	–	0.84 ± 0.03
50			0.19 ± 0.02	–	0.86 ± 0.03

(a) Coating not of proper thickness (< 5 mil).

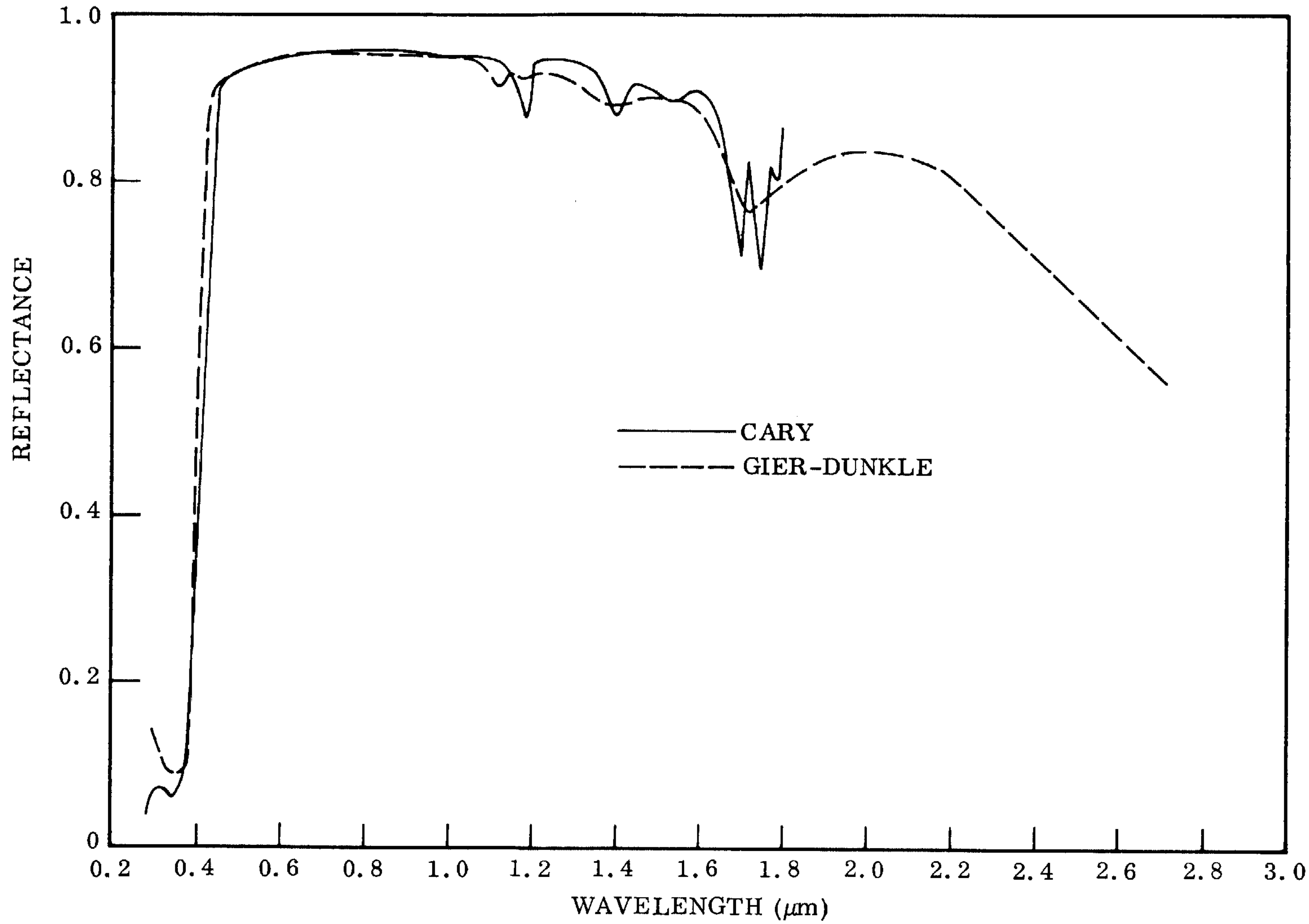

Fig. A-1 Typical Spectral Reflectance of Titanium Dioxide/Methyl Silicone Coating (Thermatrol 2A-100)

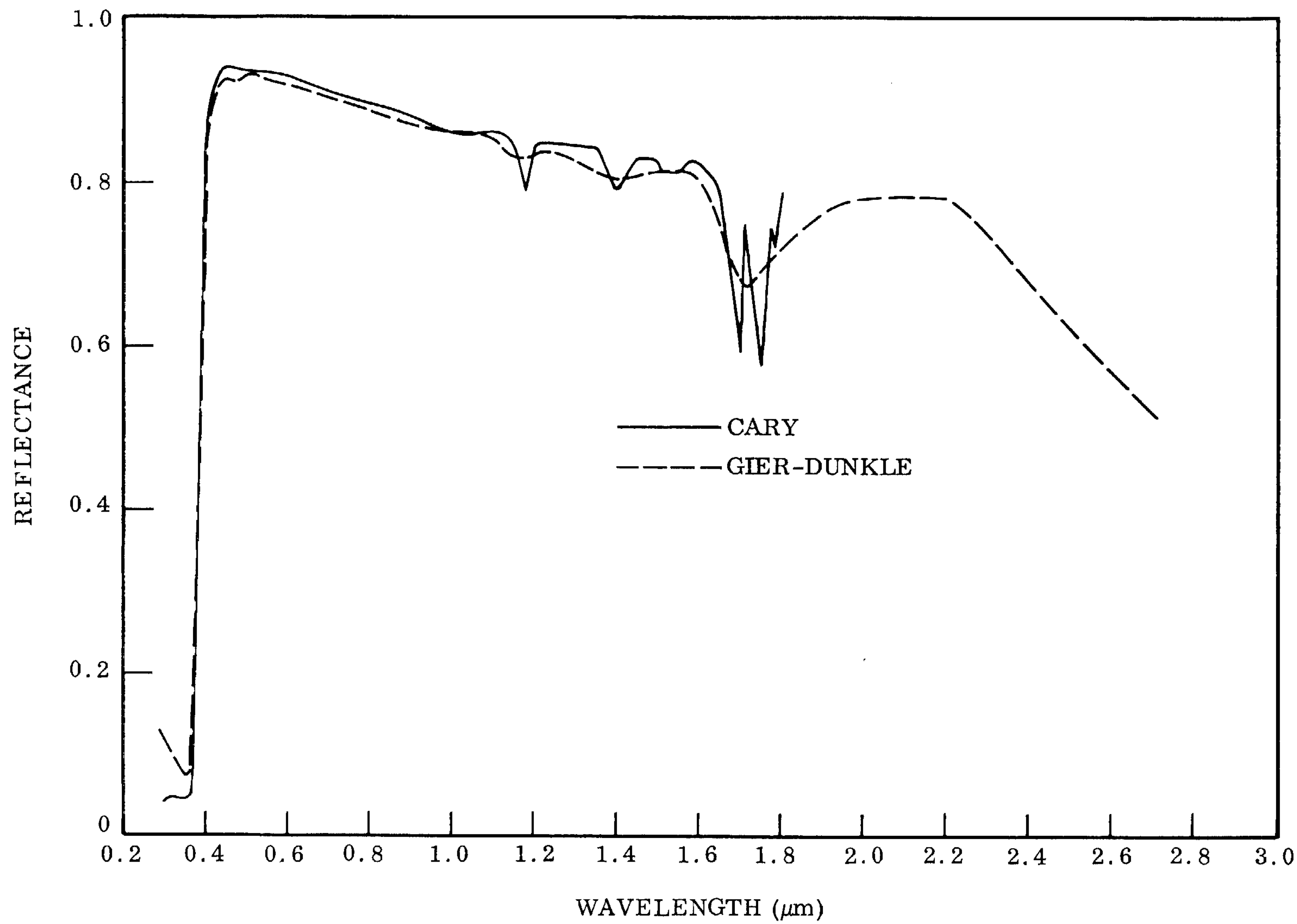

Fig. A-2 Typical Spectral Reflectance of Zinc Oxide/Methyl Silicone Coating (S-13)

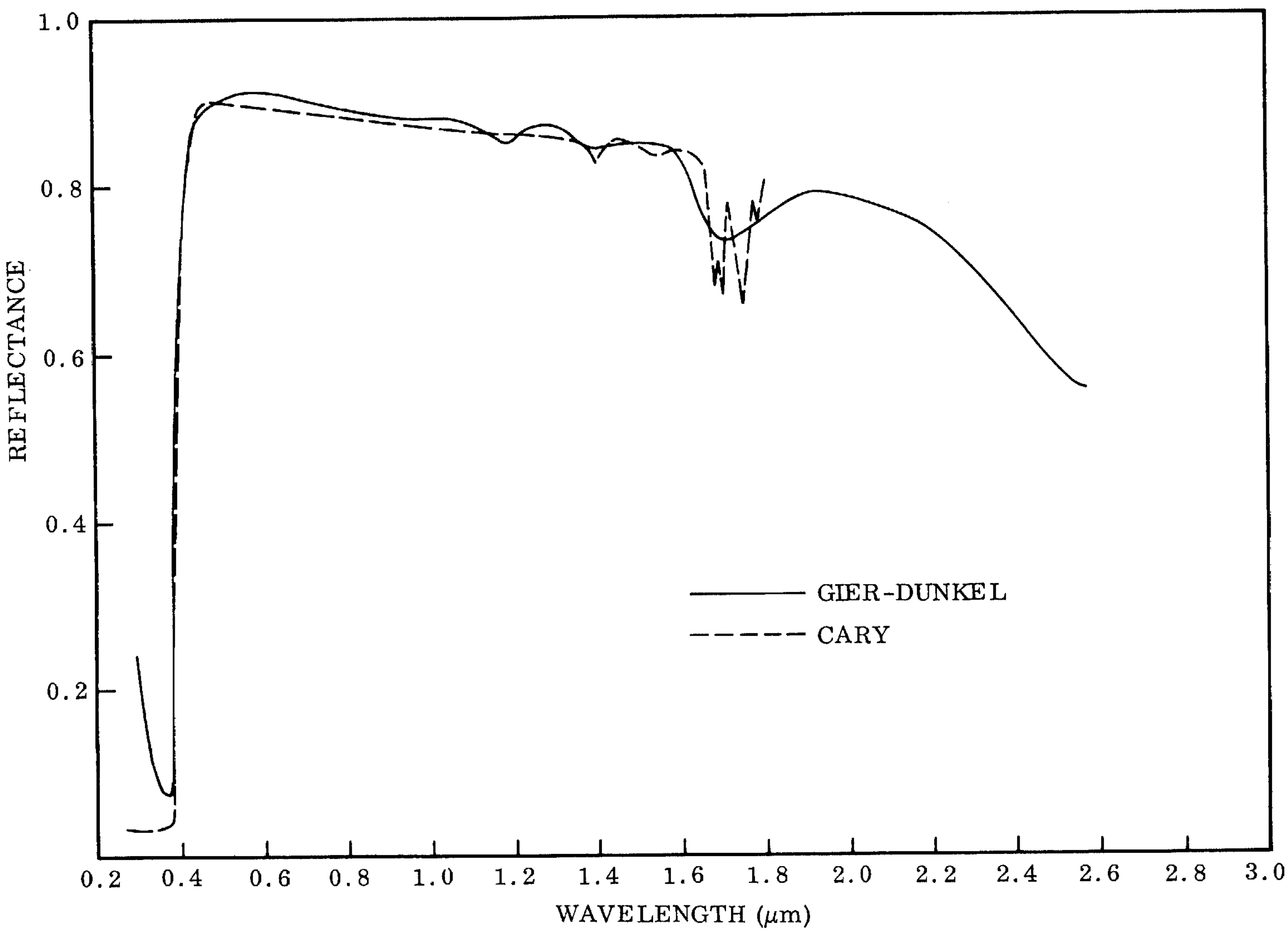

Fig. A-3 Typical Room Temperature Normal Spectral Reflectance of Zinc Oxide/Methyl Silicone (S-13G) Coating

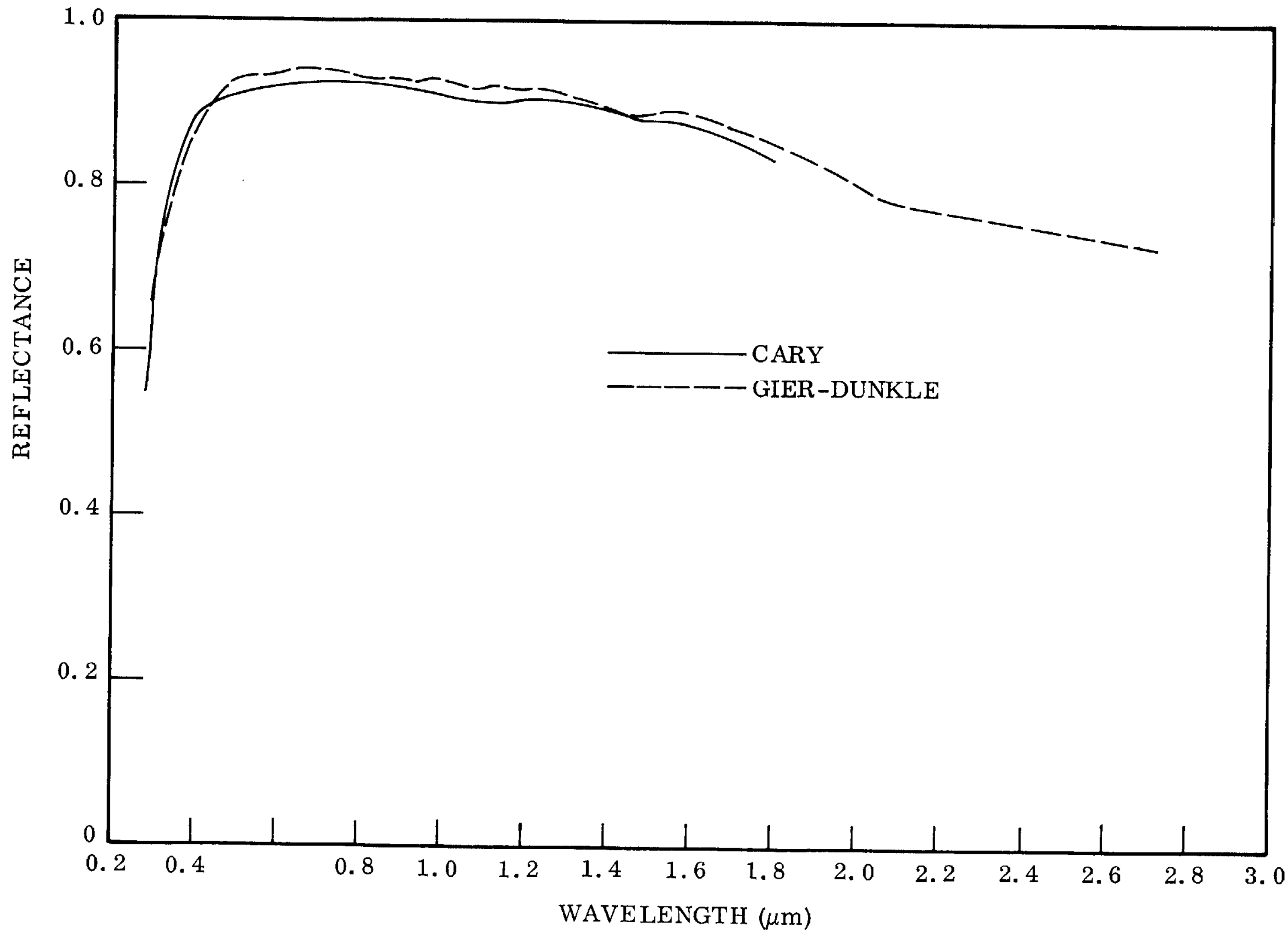

Fig. A-4 Typical Spectral Reflectance of Zirconium Silicate/Potassium Silicate Coating (LMSC)

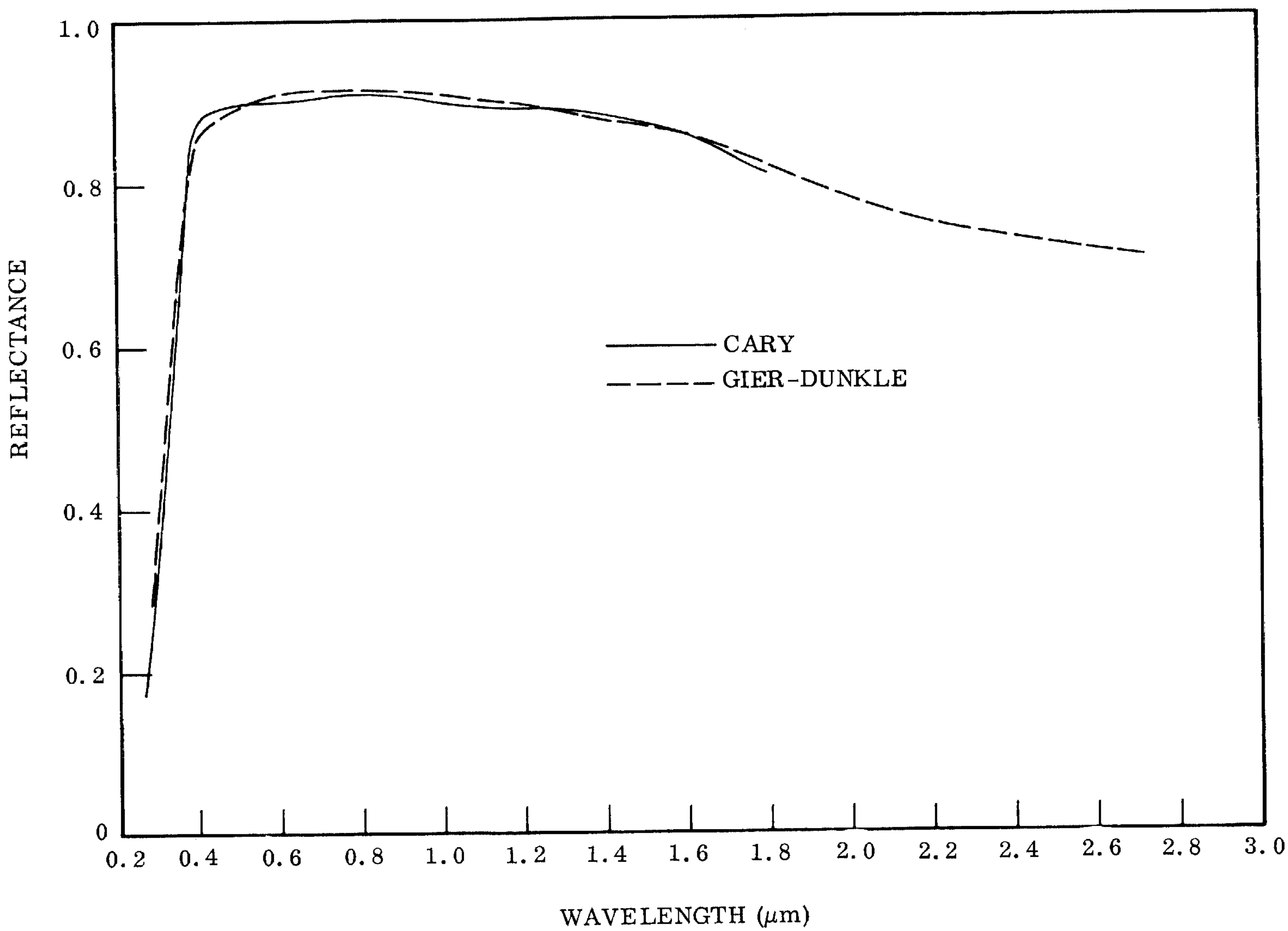

Fig. A-5 Typical Spectral Reflectance of Aluminum Silicate/Potassium Silicate Coating (Hughes)

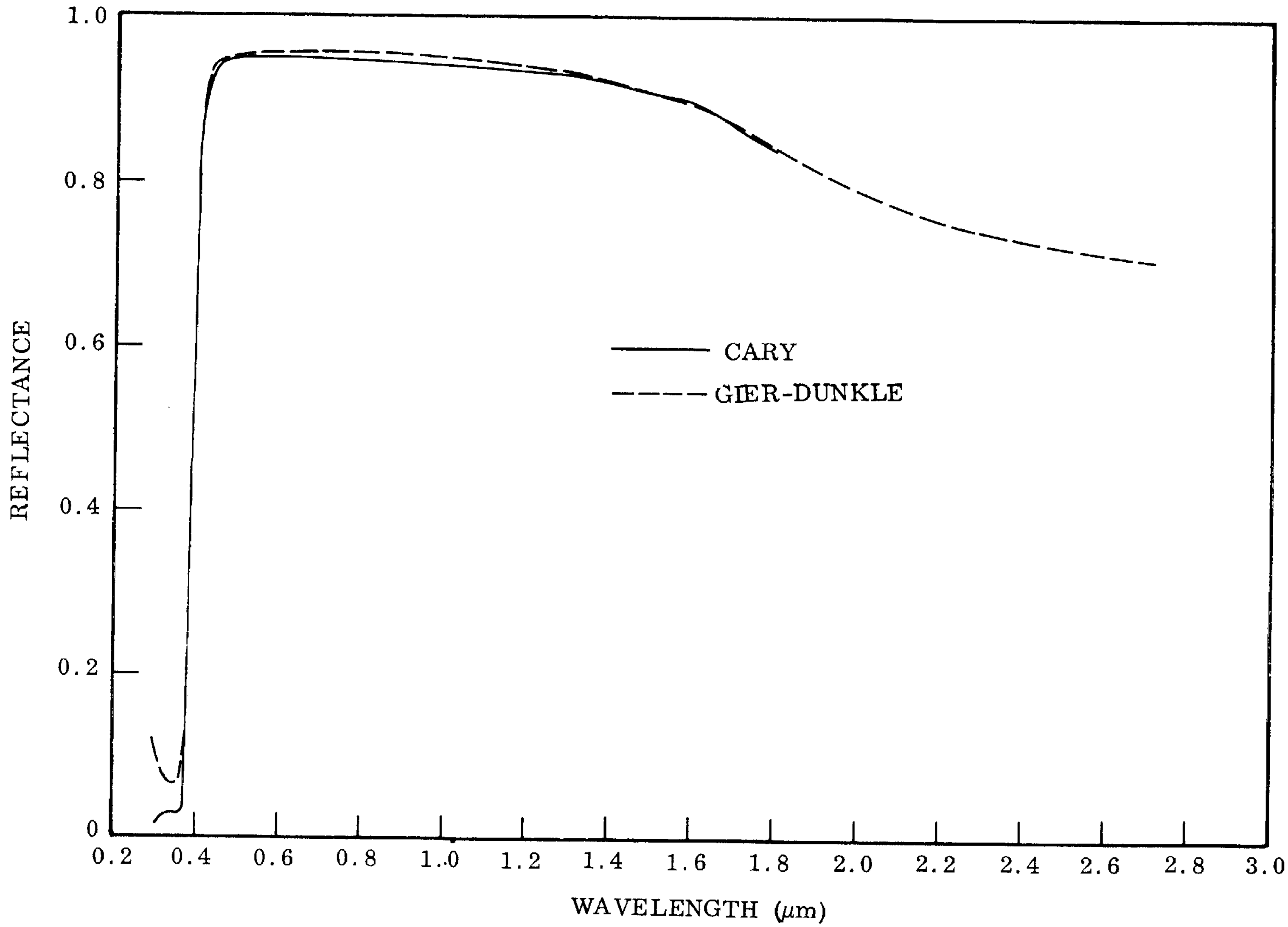

Fig. A-6 Typical Spectral Reflectance of Zinc Oxide/Potassium Silicate Coating (Z-93)

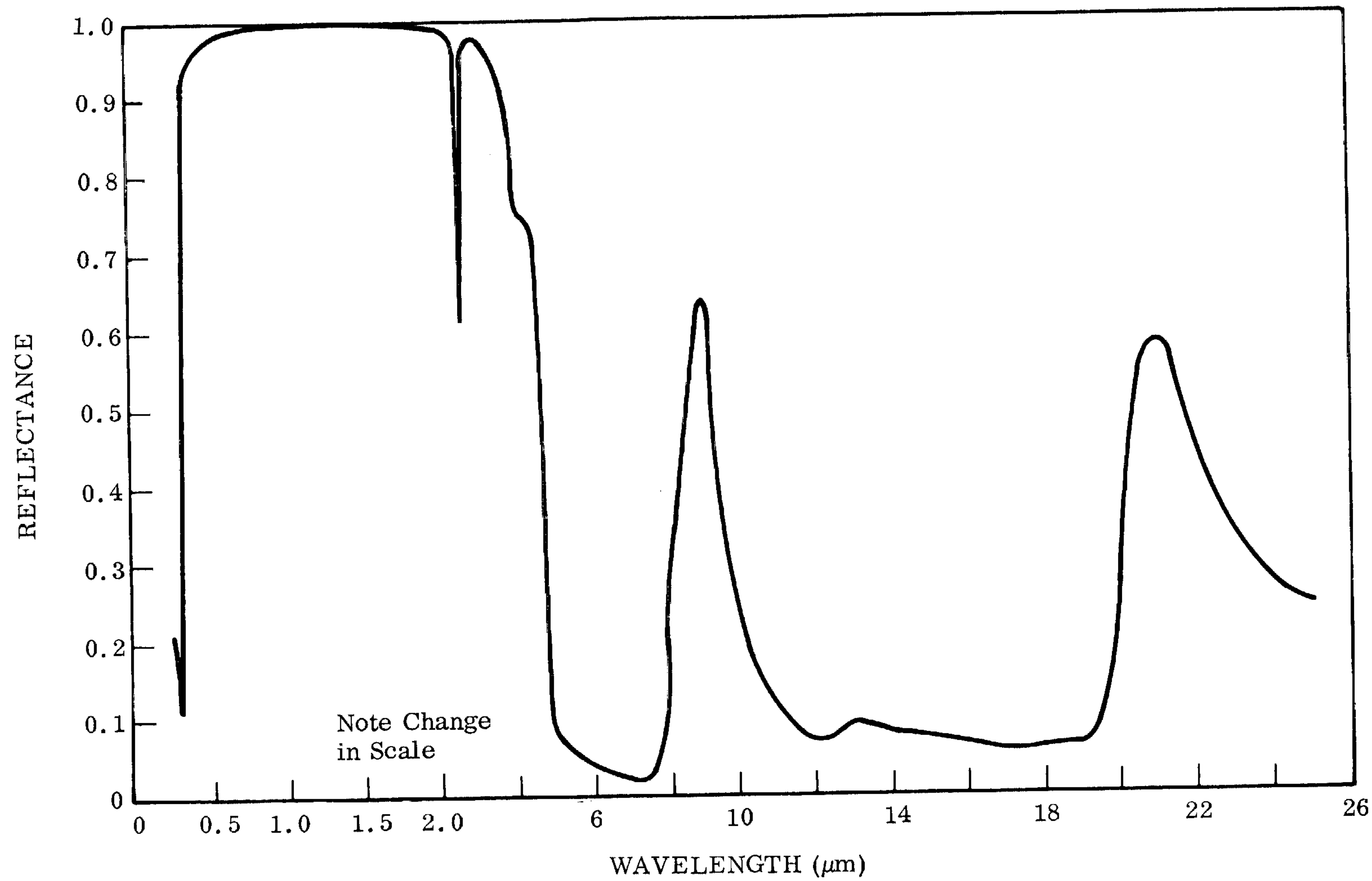

Fig. A-7 Spectral Reflectance of Optical Solar Reflector

Appendix B

CALORIMETRIC ABSORPTANCE AND EMITTANCE DATA

Table B-1

CALORIMETRIC TOTAL HEMISPHERICAL EMITTANCE AND IN SITU ABSORPTANCE DATA FOR TITANIUM DIOXIDE/METHYL SILICONE COATING (THERMATROL 2A-100), SAMPLE 1, AT 395°K (250°F)

Time (hr)	Temp. (°K)	Temp. (°F)	ϵ_{TH}	α_H (a)					α_s (b)
				Total	0.20/0.41	0.41/0.60	0.60/0.85	0.85/-	
1/4	395	250	0.87	0.18	0.70	0.12	0.07	0.13	0.18
5	395	250	0.87	0.21	0.70	0.17	0.07	0.19	0.21
69	395	250	0.87	0.29	0.85	0.25	0.16	0.22	0.29
117	395	250	0.85	0.30	0.85	0.24	0.18	0.26	0.31
168	395	250	0.88	0.31	0.85	0.25	0.18	0.28	0.32
250 (c)	395	250	0.88	0.29	0.85	0.25	0.17	0.24	0.30
360	395	250	0.87	0.29	0.80	0.24	0.17	0.27	0.31
410	395	250	0.85	0.30	0.85	0.25	0.18	0.26	0.31
457	395	250	0.86	0.30	0.85	0.24	0.18	0.26	0.31
486	395	250	0.85	0.31	0.90	0.25	0.18	0.27	0.32
550	395	250	0.85	0.31	0.90	0.25	0.19	0.27	0.32
Before Exposure (d)				0.14	0.69	0.08	0.06	0.07	0.15
After Exposure (d)				0.24	0.79	0.27	0.15	0.13	0.26

(a) Absorptance for xenon source.
(b) Absorptance for solar source.
(c) Vacuum failure at 245 hr; pressure reestablished at 6×10^{-8} Torr at 250 hr; data taken at this time.
(d) From Cary room temperature reflectance measurements.

Table B-2

CALORIMETRIC TOTAL HEMISPHERICAL EMITTANCE AND IN SITU ABSORPTANCE DATA FOR ZINC OXIDE/METHYL SILICONE (S-13) COATING, SAMPLE 27, AT 395°K (250°F)

Hour	Cycle	Temp. (°K)	Temp. (°F)	ϵ_{TH}	α_H (a) Total	α_H (a) 0.2–0.41	α_H (a) 0.41–0.6	α_H (a) 0.6–0.85	α_H (a) 0.85–	α_s (b) Total
0	1	294	80	0.86	0.21	–	–	–	–	–
0	1	339	150	.87	.21	–	–	–	–	–
0	2	395	250	.86	.21	–	–	–	–	–
4	3	395	250	.85	.21	0.65	0.08	0.06	0.24	0.21
53	15	395	250	.86	.23	.65	.10	.06	.27	.23
61	27	395	250	.86	.24	.65	.15	.06	.28	.24
113	42	395	250	.85	.27	.70	.15	.08	.30	.26
158	52	395	250	.86	.26	.70	.19	.08	.28	.26
230	82	395	250	.86	.27	.75	.21	.09	.28	.27
280	94	395	250	.86	.27	.75	.25	.08	.29	.28
330	105	395	250	.87	.26	.70	.26	.10	.28	.28
402	125	395	250	.87	.27	.65	.26	.08	.28	.28
450	136	395	250	.87	.27	.65	.27	.08	.30	.28
500	147	395	250	.86	.27	.70	.27	.10	.28	.28
Before Exposure(c)					.18	.65	.08	.10	.14	.18
After Exposure(c)					.26	.76	.31	.15	.17	.28

(a) Absorptance for xenon source.
(b) Absorptance for solar source.
(c) From Cary room temperature reflectance measurements.

Table B-3

CALORIMETRIC TOTAL HEMISPHERICAL EMITTANCE AND IN SITU ABSORPTANCE DATA FOR ZINC OXIDE/METHYL SILICONE (S-13) COATING, SAMPLE 28, AT 395°K (250°F)

Hour	Cycle	Temp. (°K)	Temp. (°F)	ϵ_{TH}	α_H (a) Total	α_H (a) 0.2−0.41	α_H (a) 0.41−0.6	α_H (a) 0.6−0.85	α_H (a) 0.85−	α_s (b) Total
0	0	290	62	0.85	0.21	–	–	–	–	–
0	0	342	155	.88	.20	–	–	–	–	–
0	1	395	250	.85	.21	0.70	0.10	0.10	0.19	0.20
4	2	395	250	.86	.22	.70	.10	.10	.23	.21
50	12	395	250	.87	.23	.65	.12	.10	.26	.23
146	33	395	250	.86	.26	.65	.18	.10	.28	.26
196	45	395	250	.87	.27	.65	.23	.08	.32	.28
246	57	395	250	.87	.30	.70	.28	.08	.32	.30
296	69	395	250	.87	.29	.70	.26	.09	.31	.30
328[c]	75	395	250	.86	.25	.70	.21	.10	.26	.26
346	81	395	250	.86	.27	.70	.22	.10	.29	.27
396	93	395	250	.87	.28	.70	.22	.10	.31	.28
468	111	395	250	.86	.27	.70	.24	.11	.30	.28
516	123	395	250	.87	.27	.70	.23	.14	.30	.28
564	135	395	250	.87	.27	.70	.24	.14	.30	.28
636	153	395	250	.87	.27	.70	.24	.14	.30	.28
Before Exposure[d]					.19	.65	.08	.10	.14	.19
After Exposure[d]					.28	.78	.32	.17	.21	.31

(a) Absorptance for xenon source.
(b) Absorptance for solar source.
(c) Electronic pump off, pressure increase to > 50 μ.
(d) From Cary room temperature reflectance measurements.

Table B-4

CALORIMETRIC TOTAL HEMISPHERICAL EMITTANCE AND IN SITU ABSORPTANCE DATA FOR ZINC OXIDE/METHYL SILICONE (S-13G) COATING, SAMPLE 43, AT 395°K (250°F)

Hour	Cycle	Temp. (°K)	Temp. (°F)	ϵ_{TH}	α_H (a) Total	α_H (a) 0.2–0.41	α_H (a) 0.41–0.6	α_H (a) 0.6–0.85	α_H (a) 0.85–	α_s (b) Total
0	0	294	70	0.86	0.23	–	–	–	–	–
0	0	339	150	.89	.21	–	–	–	–	–
0	1	395	250	.90	.21	–	–	–	–	–
0	1	395	250	.90	.20	0.85	0.12	0.05	0.15	0.20
4	1	395	250	.93	.21	.90	.12	.05	.16	.21
51	13	395	250	.92	.23	.90	.17	.08	.17	.24
149	46	395	250	.92	.24	.90	.21	.09	.17	.25
195	58	395	250	.92	.26	.92	.27	.10	.17	.27
248	70	395	250	.90	.26	.90	.28	.10	.17	.27
296	81	395	250	.92	.26	.90	.32	.09	.17	.28
344	92	395	250	.92	.26	.85	.35	.11	.17	.28
392	104	395	250	.90	.26	.85	.35	.11	.17	.28
500	125	395	250	.91	.26	.85	.35	.10	.18	.28
Before Exposure(c)					.19	.70	.10	.10	.13	.19
After Exposure(c)					.28	.82	.37	.20	.15	.31

(a) Absorptance for xenon source.
(b) Absorptance for solar source.
(c) From Cary room temperature reflectance measurements.

Table B-5

CALORIMETRIC TOTAL HEMISPHERICAL EMITTANCE AND IN SITU ABSORPTANCE DATA FOR ZINC OXIDE/METHYL SILICONE (S-13G) COATING, SAMPLE 44, AT 395°K (250°F)

Hour	Cycle	Temp. (°K)	Temp. (°F)	ϵ_{TH}	α_H (a) Total	α_H (a) 0.2–0.41	α_H (a) 0.41–0.6	α_H (a) 0.6–0.85	α_H (a) 0.85–	α_s (b) Total
0	0	294	70	0.90	0.24	–	–	–	–	–
0	0	339	150	.93	.22	–	–	–	–	–
0	1	395	250	.91	.19	0.80	0.10	0.08	0.14	0.19
5	1	395	250	.91	.20	.80	.10	.08	.14	.20
75	17	395	250	.91	.20	.80	.16	.09	.15	.21
123	29	395	250	.91	.21	.80	.16	.08	.16	.22
172	41	395	250	.91	.21	.80	.21	.08	.16	.22
227	53	395	250	.92	.22	.75	.27	.08	.16	.23
274	65	395	250	.92	.22	.75	.27	.08	.16	.23
327	77	395	250	.91	.22	.75	.27	.10	.16	.24
423	100	395	250	.91	.22	.75	.27	.10	.17	.24
471	112	395	250	.90	.22	.75	.27	.10	.17	.24
520	125	395	250	.91	.22	.75	.28	.10	.18	.25
Before Exposure (c)					.18	.65	.10	.10	.13	.20
After Exposure (c)					.23	.75	.29	.12	.15	.27

(a) Absorptance for xenon source.
(b) Absorptance for solar source.
(c) From Cary room temperature reflectance measurements.

Table B-6

CALORIMETRIC TOTAL HEMISPHERICAL EMITTANCE AND IN SITU ABSORPTANCE DATA FOR ZIRCONIUM SILICATE/POTASSIUM SILICATE COATING, SAMPLE 9, AT 534°K (500°F)

Hour	Cycle	Temp. (°K) (°F)	ϵ_{TH}	α_H (a)					α_s (b)
				Total	0.2–0.41	0.41–0.6	0.6–0.85	0.85–	Total
0	0	294 80	0.87	0.13	–	–	–	–	–
0	0	339 150	.86	.16	–	–	–	–	–
0	0	395 250	.82	.17	–	–	–	–	–
0	0	534 500	.80	–	–	–	–	–	–
1	1	534 500	.70	.13	0.30	0.12	0.10	0.11	0.13
3	2	534 500	.70	.17	.35	.19	.19	.13	.18
50	14	534 500	.69	.26	.40	.29	.30	.24	.27
100	25	534 500	.71	.33	.50	.39	.36	.30	.36
Before Exposure(c)				.12	.25	.11	.09	.10	.12
After Exposure(c)				.38	.67	.51	.37	.25	.36

(a) Absorptance for xenon source.
(b) Absorptance for solar source.
(c) From Cary room temperature reflectance measurements.

Table B-7

CALORIMETRIC TOTAL HEMISPHERICAL EMITTANCE AND IN SITU ABSORPTANCE DATA FOR ZIRCONIUM SILICATE/POTASSIUM SILICATE COATING, SAMPLE 14, AT 534°K (500°F)

Hour	Cycle	Temp (°K) (°F)	ϵ_{TH}	α_H (a)					α_s (b)
				Total	0.2–0.41	0.41–0.6	0.6–0.85	0.85–	Total
0	0	294 70	0.87	0.16	–	–	–	–	–
0	0	339 150	.87	.15	–	–	–	–	–
0	0	395 250	.87	.14	–	–	–	–	–
1	1	534 500	.71	.12	0.30	0.12	0.10	0.08	0.12
12	5	534 500	.71	.23	.50	.30	.23	.15	.25
24	10	534 500	.71	.31	.50	.31	.35	.23	.31
75	22	534 500	.71	.38	.50	.39	.43	.29	.37
127	33	534 500	.71	.39	.50	.45	.48	.33	.40
171	44	534 500	.70	.39	.50	.46	.46	.34	.41
196	49	534 500	.71	.38	.50	.39	.45	.34	.40
267	65	534 500	.72	.38	.50	.38	.50	.34	.40
315	77	534 500	.72	.40	.55	.39	.50	.37	.41
380	92	534 500	.72	.40	.55	.37	.49	.39	.41
432	104	534 500	.70	.42	.55	.40	.47	.40	.43
500	120	534 500	.71	.41	.55	.45	.48	.43	.42
Before Exposure(c)				.11	.23	.10	.09	.10	.12
After Exposure(c)				.48	.61	.60	.55	.40	.51

(a) Absorptance for xenon source.
(b) Absorptance for solar source.
(c) From Cary room temperature reflectance measurements.

Table B-8

CALORIMETRIC TOTAL HEMISPHERICAL EMITTANCE AND IN SITU ABSORPTANCE DATA FOR ALUMINUM SILICATE/POTASSIUM SILICATE COATING, SAMPLE 19, AT 534°K (500°F)

Hours	Cycle	Temp. (°K)	Temp. (°F)	ϵ_{TH}	α_H (a) Total	α_H (a) 0.2–0.41	α_H (a) 0.41–0.60	α_H (a) 0.60–0.85	α_H (a) 0.85–	α_s (b) Total
0	0	290	62	0.90	0.14	–	–	–	–	–
0	0	342	115	.89	.15	–	–	–	–	–
0	0	395	250	.92	.18	–	–	–	–	–
0	0	534	500	.72	–	–	–	–	–	–
0	1	534	500	.72	.18	0.35	0.22	0.13	0.13	0.20
24	7	534	500	.72	.30	.41	.36	.35	.18	.31
75	19	534	500	.72	.44	.65	.50	.48	.32	.44
122(c)	31	534	500	.72	.46	.60	.55	.50	.38	.46
Before Exposure(d)					.14	.32	.11	.10	.12	.14
After Exposure(d)					.42	.60	.54	.40	.33	.41

(a) Absorptance for xenon source.
(b) Absorptance for solar source.
(c) Test terminated due to thermocouple failure.
(d) From Cary room temperature reflectance measurements.

Table B-9

CALORIMETRIC TOTAL HEMISPHERICAL EMITTANCE AND IN SITU ABSORPTANCE DATA FOR ALUMINUM SILICATE/POTASSIUM SILICATE COATING, SAMPLE 21, AT 534°K (500°F)

Hours	Cycle	Temp. (°K)	Temp. (°F)	ϵ_{TH}	α_H (a) Total	α_H (a) 0.2–0.41	α_H (a) 0.41–0.6	α_H (a) 0.6–0.85	α_H (a) 0.85–	α_S (b) Total
0	0	290	62	0.94	0.15	–	–	–	–	0.15
0	0	342	115	.96	.15	–	–	–	–	.15
0	0	395	250	.93	.15	–	–	–	–	.15
0	0	534	500	.82	.16	0.47	0.11	0.10	0.10	.16
24	3	534	500	.80	.25	.49	.35	.18	.17	.25
72	13	534	500	.80	.37	.61	.38	.38	.19	.37
168	39	534	500	.79	.43	.58	.38	.38	.33	.43
218	52	534	500	.79	.44	.60	.44	.38	.35	.44
290	68	534	500	.80	.48	.64	.48	.41	.39	.48
338	72	534	500	.80	.46	.61	.44	.43	.41	.46
386	82	534	500	.78	.47	.59	.47	.43	.40	.47
458	97	534	500	.80	.51	.60	.51	.45	.42	.50
530	112	534	500	.81	.50	.63	.54	.47	.45	.50
Before Exposure(c)					.13	.40	.11	.09	.11	.14
After Exposure(c)					.46	.65	.55	.46	.38	.45

(a) Absorptance for xenon source.
(b) Absorptance for solar source.
(c) From Cary room temperature reflectance measurements.

Table B-10

CALORIMETRIC TOTAL HEMISPHERICAL EMITTANCE AND IN SITU ABSORPTANCE DATA FOR ZINC OXIDE/POTASSIUM SILICATE (Z-93) COATING, SAMPLE 35, AT 534°K (500°F)

Hour	Cycle	Temp. (°K)	Temp. (°F)	ϵ_{TH}	α_H (a)					α_s (b)
					Total	0.2–0.41	0.41–0.6	0.6–0.85	0.85–	Total
0	0	294	70	0.93	0.12	–	–	–	–	–
0	0	339	113	.94	.12	–	–	–	–	–
0	0	395	252	.91	.11	–	–	–	–	–
0	1	534	500	.81	.11	–	–	–	–	–
0	1	534	500	.81	.11	0.60	0.03	0.05	0.08	0.12
12	5	534	500	.80	.16	.55	.20	.08	.09	.16
60	16	534	500	.80	.20	.55	.27	.10	.12	.20
140	33	534	500	.80	.21	.55	.28	.13	.16	.22
181	43	534	500	.82	.22	.55	.27	.15	.17	.23
256	61	534	500	.82	.23	.55	.25	.20	.16	.24
304	72	534	500	.82	.23	.55	.25	.20	.18	.24
356	83	534	500	.81	.23	.50	.25	.20	.18	.24
404	94	534	500	.81	.24	.50	.25	.23	.19	.25
426	99	534	500	.82	.24	.55	.26	.22	.19	.25
502	120	534	500	.81	.24	.55	.26	.23	.19	.25
Before Exposure (c)					.13	.64	.05	.05	.07	.14
After Exposure (c)					.25	.70	.28	.19	.16	.26

(a) Absorptance for xenon source.
(b) Absorptance for solar source.
(c) From Cary room temperature reflectance measurements.

Table B-11

CALORIMETRIC TOTAL HEMISPHERICAL EMITTANCE AND IN SITU ABSORPTANCE DATA FOR ZINC OXIDE/POTASSIUM SILICATE (Z-93) COATING, SAMPLE 36, AT 534°K (500°F)

Hours	Cycle	Temp. (°K)	Temp. (°F)	ϵ_{TH}	α_H [a] Total	α_H [a] 0.2–0.41	α_H [a] 0.41–0.6	α_H [a] 0.6–0.85	α_H [a] 0.85–	α_s [b] Total
0	0	290	62	0.93	0.13	–	–	–	–	0.14
0	0	342	156	.91	.13	–	–	–	–	.14
0	0	534	500	.82	.11	–	–	–	–	.12
0	0	534	500	.81	.10	0.50	0.05	0.07	0.05	.11
15	12	534	500	.79	.15	.50	.08	.11	.10	.15
87	30	534	500	.81	.23	.55	.20	.20	.19	.24
187	54	534	500	.79	.25	.65	.22	.20	.19	.25
235	66	534	500	.79	.24	.65	.22	.22	.20	.24
282	78	534	500	.79	.24	.65	.22	.22	.20	.24
331[c]	90	534	500	.81	.31	.75	.32	.26	.25	.32
Before Exposure[d]					.13	.60	.05	.05	.06	.14
After Exposure[d]					.42					.42

(a) Absorptance for xenon source.
(b) Absorptance for solar source.
(c) Vacuum failure pressure >100 Torr.
(d) From Cary room temperature reflectance measurements.

Table B-12

CALORIMETRIC TOTAL HEMISPHERICAL EMITTANCE AND IN SITU ABSORPTANCE DATA FOR ZINC OXIDE/POTASSIUM SILICATE (Z-93) COATING, SAMPLE 40, AT 450°K (350°F)

Hour	Temp. (°K)	Temp. (°F)	ϵ_{TH}	α_H (a) Total	α_H (a) 0.2-0.41	α_H (a) 0.41-0.6	α_H (a) 0.6-0.85	α_H (a) 0.85→	α_s (b) Total
0	450	350	0.87	0.12	0.50	0.10	0.04	0.08	0.12
20	450	350	.87	.16	.75	.15	.07	.08	.16
58	450	350	.86	.18	.80	.17	.08	.08	.18
106	450	350	.87	.18	.84	.23	.09	.09	.20
154	450	350	.87	.19	.85	.23	.10	.10	.20
226	450	350	.87	.20	.91	.23	.12	.10	.22
274	450	350	.87	.21	.90	.23	.11	.11	.22
322	450	350	.87	.21	.94	.29	.10	.11	.24
394	450	350	.87	.20	.95	.27	.10	.11	.24
488	450	350	.87	.22	.87	.28	.13	.11	.24
560	450	350	.87	.20	.87	.24	.14	.12	.23
608	450	350	.88	.22	.85	.30	.14	.13	.24
656	450	350	.88	.22	.88	.28	.18	.13	.24
728	450	350	.87	.24	.85	.31	.16	.13	.26
776	450	350	.87	.25	.80	.31	.16	.14	.25
824	450	350	.87	.25	.75	.35	.20	.14	.26
896	450	350	.87	.25	.80	.30	.20	.14	.26
944	450	350	.87	.25	.80	.30	.19	.14	.25
1004	450	350	.87	.25	.85	.30	.20	.14	.26
Before Exposure(c)				.12	.60	.05	.05	.07	.14
After Exposure(c)				.21	.90	.25	.15	.10	.23

(a) Absorptance for xenon source.
(b) Absorptance for solar source.
(c) From Cary room temperature reflectance measurements.

Table B-13

CALORIMETRIC TOTAL HEMISPHERICAL EMITTANCE AND IN SITU ABSORPTANCE DATA FOR ZINC OXIDE/POTASSIUM SILICATE (Z-93) COATING, SAMPLE 38, AT 422°K (300°F)

Hour	Temp. (°K)	Temp. (°F)	ϵ_{TH}	α_H (a) Total	α_H (a) 0.2−0.41	α_H (a) 0.41−0.6	α_H (a) 0.6−0.85	α_H (a) 0.85→	α_S (b) Total
0	422	300	0.87	0.14	0.63	0.12	0.06	0.08	0.14
19	422	300	.87	.15	.64	.20	.06	.10	.16
95	422	300	.87	.16	.62	.24	.09	.10	.18
145	422	300	.87	.16	.62	.23	.08	.10	.18
193	422	300	.87	.16	.57	.23	.08	.11	.18
265	422	300	.86	.17	.61	.23	.10	.10	.19
313	422	300	.87	.16	.63	.23	.09	.10	.18
361	422	300	.87	.16	.58	.24	.09	.10	.18
433	422	300	.87	.16	.60	.26	.08	.11	.18
500	422	300	.88	.17	.57	.30	.08	.11	.19
Before Exposure(c)				.12	.60	.05	.05	.07	.14
After Exposure(c)				.18	.70	.25	.10	.08	.20

(a) Absorptance for xenon source.
(b) Absorptance for solar source.
(c) From Cary room temperature reflectance measurements.

Table B-14

CALORIMETRIC TOTAL HEMISPHERICAL EMITTANCE AND IN SITU ABSORPTANCE DATA FOR ZINC OXIDE/POTASSIUM SILICATE (Z-93) COATING, SAMPLE 39, AT 422°K (300°F)

Hour	Cycle	Temp. (°K)	Temp. (°F)	ϵ_{TH}	α_H (a) Total	α_H (a) 0.2–0.41	α_H (a) 0.41–0.6	α_H (a) 0.6–0.85	α_H (a) 0.85 →	α_S (b) Total
0	0	294	70	0.92	0.12	–	–	–	–	0.12
0	0	348	162	.91	.11	–	–	–	–	.11
0	0	422	300	.91	.11	–	–	–	–	.11
0	1	422	300	.91	.11	0.70	0.06	0.06	0.06	.12
0	4	422	300	.91	.10	.70	.06	.06	.06	.11
24	8	422	300	.90	.10	.70	.07	.07	.08	.11
48	13	422	300	.89	.10	.70	.07	.07	.07	.11
98	25	422	300	.90	.10	.75	.07	.08	.09	.11
148	37	422	300	.89	.10	.75	.07	.07	.08	.11
198	50	422	300	.85	.11	.75	.08	.09	.10	.12
248	62	422	300	.89	.10	.75	.08	.08	.09	.11
298	74	422	300	.89	.12	.85	.08	.08	.10	.13
322	80	422	300	.89	.13	.85	.08	.07	.09	.14
400	95	422	300	.89	.13	.90	.07	.07	.09	.14
450	107	422	300	.89	.14	.90	.09	.07	.08	.15
475	113	422	300	.89	.13	.90	.08	.07	.09	.14
550	128	422	300	.89	.13	.90	.09	.07	.08	.14
625		422	300	.87	.14	.90	.09	.07	.09	.15
700		422	300	.90	.13	.90	.09	.08	.10	.14
750		422	300	.88	.13	.90	.10	.07	.10	.14
846		422	300	.89	.12	.90	.09	.09	.10	.13
921		422	300	.89	.13	.90	.10	.09	.10	.14
1017		422	300	.88	.14	.90	.10	.09	.10	.15
1089		422	300	.88	.13	.90	.10	.09	.10	.14
1161		422	300	.88	.13	.90	.09	.09	.10	.14

Table B-14 (Cont.)

Hour	Cycle	Temp. (°K)	Temp. (°F)	ϵ_{TH}	α_H (a) Total	α_H (a) 0.2–0.41	α_H (a) 0.41–0.6	α_H (a) 0.6–0.85	α_H (a) 0.85 →	α_s (b) Total
1210		422	300	0.88	0.13	0.90	0.10	0.09	0.10	0.14
1260		422	300	.89	.13	.90	.10	.09	.10	.14
1332		422	300	.88	.13	.90	.11	.08	.10	.14
1404		422	300	.88	.13	.90	.10	.09	.10	.14
1524		422	300	.89	.13	.90	.10	.08	.10	.14
1596		422	300	.88	.14	.90	.11	.09	.10	.15
1668		422	300	.87	.14	.90	.11	.08	.10	.15
1710		422	300	.87	.14	.90	.11	.09	.10	.15
1764		422	300	.87	.14	.90	.10	.10	.10	.15
1836		422	300	.88	.14	.90	.11	.10	.10	.15
1890		422	300	.88	.14	.90	.11	.09	.10	.15
1932		422	300	.88	.14	.90	.11	.09	.10	.15
2004		422	300	.88	.14	.90	.12	.09	.10	.15
2100		422	300	.88	.15	.90	.12	.09	.10	.16
2172		422	300	.87	.14	.90	.11	.09	.10	.15
2268		422	300	.87	.14	.90	.12	.10	.11	.15
2340		422	300	.87	.14	.90	.11	.10	.10	.15
2436		422	300	.87	.14	.90	.10	.09	.10	.15
2556		422	300	.86	.13	.90	.11	.09	.10	.14
2604		422	300	.86	.13	.90	.10	.09	.10	.15
2676		422	300	.87	.14	.90	.12	.09	.10	.15
2772		422	300	.87	.14	.90	.11	.09	.10	.15
2844		422	300	.86	.13	.90	.11	.09	.10	.15
2892		422	300	.86	.13	.90	.11	.10	.10	.14
2940		422	300	.86	.13	.90	.10	.09	.11	.14
3012		422	300	.86	.13	.90	.10	.09	.09	.15
3060		422	300	.87	.13	.90	.09	.09	.10	.15

Table B-14 (Cont.)

Hour	Cycle	Temp. (°K)	Temp. (°F)	ϵ_{TH}	α_H [a] Total	0.2−0.41	0.41−0.6	0.6−0.85	0.85→	α_s [b] Total
3108		422	300	0.87	0.13	0.90	0.09	0.10	0.10	0.15
3180		422	300	.88	.13	.90	.10	.09	.10	.15
3228		422	300	.88	.14	.90	.10	.10	.10	.16
3276		422	300	.87	.13	.90	.10	.09	.10	.15
3348		422	300	.87	.13	.90	.10	.10	.10	.15
3444		422	300	.88	.14	.90	.11	.10	.10	.16
3516		422	300	.88	.13	.90	.10	.10	.11	.16
3516		422	300	.88	.13	.76	.10	.07	.04	.15
3564		422	300	.88	.13	.79	.08	.09	.12	.15
3612		422	300	.86	.13	.73	.10	.08	.12	.15
3684		422	300	.87	.12	.67	.09	.05	.11	.14
3732		422	300	.87	.12	.65	.13	.10	.11	.16
3780		422	300	.87	.12	.65	.08	.06	.11	.15
3852		422	300	.87	.12	.70	.08	.08	.10	.15
3900		422	300	.87	.13	.66	.10	.10	.10	.16
3948		422	300	.88	.12	.66	.08	.06	.11	.15
4020		422	300	.88	.12	.67	.10	.10	.10	.16
4068		422	300	.88	.12	.67	.10	.10	.10	.16
4116		422	300	.87	.12	.60	.10	.05	.10	.14
4188		422	300	.87	.12	.65	.11	.05	.10	.15
4236		422	300	.88	.12	.65	.11	.05	.11	.15
4284		422	300	.88	.12	.63	.10	.07	.10	.15
4356		422	300	.88	.12	.65	.08	.09	.10	.15
4404		422	300	.88	.12	.67	.10	.06	.10	.15
4452		422	300	.88	.12	.65	.10	.07	.10	.15

Table B-14 (Cont.)

Hour	Cycle	Temp. (°K)	Temp. (°F)	ϵ_{TH}	α_H [a] Total	0.2–0.41	0.41–0.6	0.6–0.85	0.85 →	α_s [b] Total
4524		422	300	0.88	0.12	0.65	0.10	0.07	0.10	0.15
4574		422	300	.88	.12	.67	.10	.05	.11	.15
After Vacuum Failure[c]					.26	.75	.45	.25	.13	.14

(a) Absorptance for xenon source.
(b) Absorptance for solar source.
(c) From Cary room temperature reflectance measurements.

Table B-15

CALORIMETRIC IN SITU SOLAR ABSORPTANCE AND TOTAL HEMISPHERICAL EMITTANCE OF ZINC OXIDE/POTASSIUM SILICATE (Z-93) COATING, SAMPLE 59, AT 422°K (300°F)

Hour	Temp. (°K)	(°F)	ϵ_{TH}	α_H					α_s
				Total	0.2−0.41	0.41−0.6	0.6−0.85	0.85→	Total
0	422	300	0.88	0.126	0.75	0.11	0.05	0.05	0.137
22	422	300	.89	.15	.90	.16	.05	.05	.16
96	422	300	.87	.17	.92	.16	.07	.07	.18
144	422	300	.88	.16	.87	.17	.07	.07	.18
192	422	300	.88	.16	.80	.20	.07	.07	.18
264	422	300	.88	.16	.80	.18	.10	.07	.19
312	422	300	.88	.16	.78	.20	.07	.08	.18
360	422	300	.89	.16	.80	.17	.08	.09	.18
432	422	300	.88	.16	.76	.19	.07	.08	.18
480	422	300	.89	.16	.76	.20	.09	.08	.18
528	422	300	.90	.16	.76	.19	.08	.08	.18
600	422	300	.89	.16	.80	.17	.10	.08	.19
648	422	300	.90	.16	.80	.19	.09	.08	.19
768	422	300	.88	.15	.77	.18	.07	.08	.18
816	422	300	.88	.15	.80	.17	.08	.08	.19
864	422	300	.88	.14	.75	.18	.07	.08	.17
936	422	300	.88	.14	.78	.16	.08	.08	.17
984	422	300	.90	.15	.78	.18	.08	.08	.18
1032	422	300	.89	.14	.78	.18	.08	.08	.18
1152	422	300	.88	.14	.70	.16	.08	.08	.17
1200	422	300	.88	.15	.72	.17	.09	.08	.17
1272	422	300	.89	.14	.73	.17	.08	.08	.17
1320	422	300	.88	.14	.72	.18	.08	.08	.17
1488	422	300	.90	.14	.70	.19	.08	.08	.17
1536	422	300	.88	.15	.68	.21	.09	.09	.18

Table B-15 (Cont.)

Hour	Temp. (°K)	Temp. (°F)	ϵ_{TH}	α_H Total	α_H 0.2–0.41	α_H 0.41–0.6	α_H 0.6–0.85	α_H 0.85→	α_s Total
1608	422	300	0.87	0.15	0.66	0.18	0.09	0.09	0.17
1656	422	300	.88	.15	.65	.18	.10	.08	.17
1704	422	300	.88	.15	.67	.18	.10	.08	.17
1776	422	300	.88	.15	.68	.20	.09	.08	.18
1824	422	300	.89	.16	.70	.18	.11	.08	.18
1872	422	300	.88	.16	.70	.19	.09	.09	.18
1944	422	300	.90	.16	.70	.18	.09	.09	.18
2016	422	300	.88	.16	.68	.19	.10	.08	.18
2256	422	300	.88	.16	.69	.19	.09	.08	.17
2424	422	300	.87	.15	.69	.17	.11	.08	.17
2472	422	300	.88	.15	.66	.19	.10	.08	.17
2560	422	300	.88	.15	.68	.17	.11	.08	.18
2644	422	300	.85	.15	.67	.18	.10	.09	.17
2736	422	300	.88	.15	.68	.18	.10	.08	.17
2784	422	300	.88	.15	.68	.18	.11	.09	.18
				Xenon lamp off 2832 to 3335 hr					
3336	422	300	.88	.16	.66	.17	.10	.09	.17
3408	422	300	.87	.15	.64	.16	.11	.09	.17
3508	422	300	.88	.15	.64	.18	.10	.09	.17
3580	422	300	.88	.15	.64	.18	.11	.09	.17
3678	422	300	.88	.16	.62	.16	.12	.09	.17
3676	422	300	.89	.16	.64	.20	.11	.09	.18
3798	422	300	.88	.16	.63	.17	.12	.09	.18
3866	422	300	.87	.16	.66	.17	.11	.09	.18
3914	422	300	.87	.16	.64	.20	.12	.09	.18
3962	422	300	.87	.16	.61	.17	.13	.09	.17
4034	422	300	.87	.17	.65	.20	.12	.09	.18
4082	422	300	.87	.17	.66	.21	.12	.09	.18

Table B-15 (Cont.)

Hour	Temp. (°K)	(°F)	ϵ_{TH}	α_H Total	0.2–0.41	0.41–0.6	0.6–0.85	0.85–	α_s Total
4202	422	300	0.86	0.16	0.65	0.20	0.13	0.09	0.19
4298	422	300	.87	.17	.66	.20	.12	.09	.19
4370	422	300	.87	.17	.65	.20	.12	.09	.18
4466	422	300	.88	.17	.63	.20	.13	.09	.18
4530	422	300	.89	.17	.62	.21	.13	.09	.19
4634	422	300	.87	.17	.61	.20	.13	.10	.19
4706	422	300	.88	.17	.61	.25	.12	.09	.19
4754	422	300	.88	.17	.66	.22	.12	.09	.19
4802	422	300	.88	.17	.65	.23	.12	.09	.19
4874	422	300	.88	.17	.62	.21	.12	.10	.20
4921	422	300	.86	.17	.63	.22	.11	.10	.19
4969	422	300	.87	.17	.66	.20	.11	.10	.19
5089	422	300	.88	.17	.62	.22	.10	.11	.18
5137	422	300	.88	.17	.59	.24	.11	.09	.18
5209	422	300	.89	.17	.63	.24	.10	.10	.19
5329	422	300	.88	.17	.60	.25	.11	.10	.19
5401	422	300	.88	.17	.61	.25	.11	.11	.19
5449	422	300	.88	.17	.64	.25	.13	.09	.20
5497	422	300	.89	.17	.59	.26	.12	.09	.20
5617	422	300	.86	.18	.62	.25	.12	.10	.20
5665	422	300	.87	.17	.58	.25	.11	.10	.19
5737	422	300	.88	.17	.59	.26	.12	.09	.19
5785	422	300	.88	.17	.58	.26	.14	.09	.20
5833	422	300	.88	.17	.59	.25	.11	.10	.19
5905	422	300	.87	.17	.58	.22	.14	.10	.19
5953	422	300	.89	.17	.58	.25	.11	.10	.19
6001	422	300	.88	.17	.61	.25	.11	.10	.19

Table B-15 (Cont.)

Hour	Temp. (°K)	Temp. (°F)	ϵ_{TH}	α_H Total	α_H 0.2–0.41	α_H 0.41–0.6	α_H 0.6–0.85	α_H 0.85–	α_s Total
6073	422	300	0.87	0.17	0.62	0.22	0.11	0.10	0.19
6121	422	300	.86	.17	.60	.26	.09	.10	.19
6169	422	300	.88	.17	.63	.22	.11	.09	.19
6241	422	300	.88	.17	.64	.23	.09	.10	.19
6289	422	300	.87	.16	.64	.22	.08	.10	.19
6457	422	300	.88	.17	.68	.20	.10	.10	.19
6505	422	300	.86	.17	.64	.23	.08	.10	.19
6577	422	300	.88	.17	.63	.22	.11	.09	.19
6625	422	300	.86	.17	.65	.20	.11	.10	.19
6673	422	300	.89	.17	.62	.24	.10	.09	.19
6745	422	300	.88	.16	.62	.22	.11	.10	.19
6793	422	300	.88	.16	.62	.22	.10	.09	.19
6913	422	300	.88	.17	.62	.23	.10	.09	.19
6961	422	300	.88	.16	.62	.23	.10	.10	.19
7009	422	300	.87	.16	.62	.20	.10	.10	.19
7081	422	300	.88	.16	.66	.19	.10	.10	.18
7129	422	300	.87	.16	.63	.19	.09	.10	.19
7177	422	300	.88	.16	.65	.21	.09	.10	.18
7249	422	300	.89	.16	.65	.18	.10	.10	.18
7345	422	300	.89	.16	.60	.18	.11	.10	.18
7417	422	300	.88	.16	.62	.18	.10	.10	.18
7465	422	300	.87	.16	.63	.19	.09	.10	.18
7513	422	300	.88	.16	.65	.20	.11	.10	.19
7585	422	300	.88	.16	.62	.22	.10	.10	.19
7633	422	300	.87	.17	.65	.20	.10	.10	.19
7681	422	300	.88	.16	.63	.17	.10	.10	.18
7753	422	300	.87	.16	.64	.18	.72	.10	.18

Table B-15 (Cont.)

Hour	Temp. (°K)	Temp. (°F)	ϵ_{TH}	α_H Total	α_H 0.2–0.41	α_H 0.41–0.6	α_H 0.6–0.85	α_H 0.85–	α_s Total
7801	422	300	0.87	0.16	0.60	0.19	0.10	0.10	0.18
7849	422	300	.86	.17	.62	.20	.11	.09	.18
7921	422	300	.88	.17	.63	.20	.09	.09	.18
8017	422	300	.88	.16	.62	.21	.09	.10	.18
8029	422	300	.88	.16	.62	.20	.10	.10	.18
8125	422	300	.88	.16	.62	.20	.10	.10	.18
8251	422	300	.88	.16	.57	.17	.12	.10	.18
8301	422	300	.88	.16	.56	.17	.12	.10	.18
8349	422	300	.88	.16	.57	.18	.11	.10	.18
8421	422	300	.88	.16	.55	.17	.13	.10	.18
8517	422	300	.87	.16	.54	.17	.12	.10	.18
8589	422	300	.88	.16	.57	.17	.12	.10	.18
8781	422	300	.87	.16	.59	.19	.13	.10	.18
9021	422	300	.90	.17	.54	.21	.11	.11	.18
9093	422	300	.86	.16	.57	.19	.11	.10	.17
9189	422	300	.88	.15	.50	.20	.09	.10	.17
9285	422	300	.86	.16	.53	.21	.11	.10	.18
9357	422	300	.87	.17	.54	.23	.14	.10	.19
9424	422	300	.86	.17	.54	.21	.12	.10	.18
9501	422	300	.88	.16	.52	.20	.09	.10	.17
9597	422	300	.86	.16	.54	.19	.13	.10	.18
9645	422	300	.87	.15	.52	.21	.11	.10	.18
9693	422	300	.87	.16	.52	.19	.11	.10	.18
9789	422	300	.88	.16	.59	.19	.09	.11	.18
9861	422	300	.87	.15	.50	.19	.11	.11	.17
9885	422	300	.86	.15	.53	.20	.12	.10	.18
9975	422	300	.86	.16	.50	.18	.11	.11	.17

Table B-15 (Cont.)

Hour	Temp. (°K)	(°F)	ϵ_{TH}	α_H Total	0.2–0.41	0.41–0.6	0.6–0.85	0.85–	α_s Total
10071	422	300	0.88	0.15	0.48	0.19	0.10	0.11	0.17
10143	422	300	.86	.14	.50	.17	.13	.10	.17
10239	422	300	.88	.15	.49	.19	.12	.10	.17
10431	422	300	.88	.15	.49	.21	.11	.10	.17
10454	422	300	.88	.14	.49	.19	.12	.10	.17
10517	422	300	.87	.15	.45	.19	.13	.10	.17
10517	corrected for window transmission			.17	.62	.22	.14	.12	.19
Before Exposure(c)				.13	.60	.06	.06	.07	.15
After Exposure(c)				.20	.66	.23	.14	.10	.21

(a) Absorptance for xenon source.
(b) Absorptance for solar source.
(c) From Cary room temperature reflectance measurements.

Table B-16

CALORIMETRIC IN SITU SOLAR ABSORPTANCE AND TOTAL HEMISPHERICAL EMITTANCE OF ZINC OXIDE/POTASSIUM SILICATE COATING (Z-93), SAMPLE 56, AT 366°K (200°F)

Hour	Temp. (°K)	Temp. (°F)	ϵ_{TH}	α_H(a) Total	α_H(a) 0.2−0.41	α_H(a) 0.41−0.6	α_H(a) 0.6−0.85	α_H(a) 0.85→	α_s(b) Total
0	366	200	0.89	0.14	0.84	0.05	0.04	0.08	0.14
17	366	200	.89	.16	.88	.10	.06	.08	.16
70	366	200	.89	.17	.89	.14	.08	.08	.18
93	366	200	.89	.17	.89	.16	.06	.08	.18
161	366	200	.90	.17	.90	.14	.09	.08	.18
233	366	200	.89	.18	.90	.16	.07	.08	.18
329	366	200	.89	.18	.91	.16	.10	.08	.19
377	366	200	.89	.18	.90	.16	.10	.08	.19
425	366	200	.89	.18	.90	.16	.09	.08	.19
497	366	200	.89	.18	.89	.16	.09	.09	.19
545	366	200	.89	.17	.85	.17	.10	.09	.19
593	366	200	.89	.18	.85	.20	.09	.09	.20
665	366	200	.89	.18	.82	.18	.08	.09	.18
713	366	200	.90	.19	.87	.18	.10	.09	.20
761	366	200	.89	.19	.87	.19	.10	.09	.20
833	366	200	.89	.18	.85	.19	.11	.09	.20
881	366	200	.89	.18	.85	.18	.11	.09	.19
939	366	200	.88	.19	.80	.20	.12	.09	.20
1011	366	200	.88	.17	.80	.19	.10	.09	.20
1059	366	200	.89	.18	.83	.19	.10	.09	.19
1179	366	200	.88	.17	.84	.18	.09	.09	.19
1227	366	200	.88	.19	.85	.19	.13	.09	.20
1275	366	200	.88	.181	.82	.21	.12	.08	.19
1347	366	200	.88	.183	.84	.21	.11	.09	.20

Table B-16 (Cont.)

Hour	Temp. (°K)	Temp. (°F)	ϵ_{TH}	α_H [a] Total	α_H [a] 0.2–0.41	α_H [a] 0.41–0.6	α_H [a] 0.6–0.85	α_H [a] 0.85 →	α_S [b] Total
1395	366	200	0.89	0.187	0.84	0.19	0.13	0.09	0.20
1443	366	200	.90	.173	.85	.18	.11	.09	.19
1575	366	200	.88	.173	.85	.18	.10	.09	.19
1621	366	200	.88	.183	.82	.19	.12	.09	.20
1693	366	200	.89	.183	.82	.19	.12	.09	.20
1741	366	200	.88	.187	.81	.22	.11	.09	.20
1909	366	200	.88	.183	.80	.22	.11	.09	.20
1957	366	200	.88	.183	.80	.22	.12	.085	.20
2024	366	200	.88	.185	.80	.22	.11	.085	.20
After Exposure[c]				.18	.75	.25	.12	.10	.21

(a) Absorptance for xenon source.
(b) Absorptance for solar source.
(c) From Cary room temperature reflectance measurements.

Table B-17

CALORIMETRIC IN SITU SOLAR ABSORPTANCE AND TOTAL HEMISPHERICAL EMITTANCE OF ZINC OXIDE/POTASSIUM SILICATE COATING (Z-93), SAMPLE 42, AT 300°K (80°F)

Hour	Temp. (°K)	Temp. (°F)	ϵ_{TH}	α_H (a) Total	α_H (a) 0.2–0.41	α_H (a) 0.41–0.6	α_H (a) 0.6–0.85	α_H (a) 0.85 →	α_s (b) Total
0	300	80	0.90	0.14	0.72	0.10	0.05	0.08	0.14
43	300	80	.88	.14	.70	.09	.05	.09	.14
293	300	80	.89	.15	.67	.11	.06	.08	.14
365	300	80	.87	.14	.67	.15	.04	.09	.15
461	300	80	.88	.15	.66	.15	.05	.09	.15
509	300	80	.88	.15	.65	.14	.06	.09	.15
605	300	80	.89	.15	.69	.14	.06	.09	.16
701	300	80	.90	.15	.70	.16	.07	.09	.16
773	300	80	.90	.16	.67	.19	.09	.08	.16
821	300	80	.88	.15	.71	.18	.05	.09	.17
869	300	80	.89	.16	.70	.19	.08	.09	.17
941	300	80	.89	.15	.65	.19	.08	.09	.17
989	300	80	.88	.16	.70	.15	.09	.08	.17
1039	300	80	.88	.15	.65	.19	.09	.08	.17
1109	300	80	.89	.16	.66	.20	.08	.08	.17
1157	300	80	.87	.16	.73	.19	.10	.08	.17
1205	300	80	.89	.16	.69	.20	.09	.08	.18
1277	300	80	.88	.16	.68	.20	.07	.09	.17
1325	300	80	.88	.16	.63	.23	.07	.09	.18
1373	300	80	.87	.16	.65	.22	.10	.08	.17
1445	300	80	.90	.16	.66	.23	.10	.08	.18
1545	300	80	.88	.16	.65	.22	.08	.09	.13
1617	300	80	.88	.16	.68	.22	.10	.08	.19
1665	300	80	.87	.16	.67	.24	.08	.08	.18

Table B-17 (Cont.)

Hour	Temp. (°K)	Temp. (°F)	ϵ_{TH}	α_H (a) Total	0.2–0.41	0.41–0.6	0.6–0.85	0.85→	α_s (b) Total
1713	300	80	0.87	0.16	0.67	0.22	0.08	0.09	0.18
1785	300	80	.88	.17	.69	.22	.09	.09	.18
1953	300	80	.85	.17	.69	.21	.09	.08	.18
2001	300	80	.88	.17	.68	.21	.09	.09	.18
After Exposure(c)				.16	.75	.17	.06	.08	.17

(a) Absorptance for xenon source.
(b) Absorptance for solar source.
(c) From Cary room temperature reflectance measurements.

Table B-18

CALORIMETRIC TOTAL HEMISPHERICAL EMITTANCE AND IN SITU ABSORPTANCE DATA FOR OPTICAL SOLAR REFLECTOR, SAMPLE 60, AT 339°K (150°F)

Hour	Temp. (°K)	Temp. (°F)	ϵ_{TH}	α_H (a) Total	α_H (a) 0.2–0.41	α_H (a) 0.41–0.6	α_H (a) 0.6–0.85	α_H (a) 0.85–	α_s (b) Total
0	339	150	0.80	0.056	0.26	0.05	0.03	0.03	0.061
122	339	150	.80	.054	.23	.05	.02	.04	.058
170	339	150	.78	.057	.25	.05	.03	.03	.060
242	339	150	.79	.057	.26	.05	.04	.03	.062
338	339	150	.80	.055	.23	.07	.03	.03	.062
410	339	150	.80	.056	.25	.06	.04	.03	.062
458	339	150	.80	.055	.25	.06	.02	.03	.059
528	339	150	.80	.057	.26	.05	.02	.04	.059
648	339	150	.78	.057	.26	.06	.04	.03	.063
696	339	150	.79	.055	.23	.07	.03	.03	.061
768	339	150	.78	.057	.27	.05	.03	.03	.061
816	339	150	.80	.056	.25	.05	.03	.03	.059
864	339	150	.81	.057	.25	.05	.04	.03	.061
936	339	150	.79	.058	.24	.05	.04	.03	.058
984	339	150	.80	.057	.25	.05	.05	.03	.063
1032	339	150	.80	.056	.25	.05	.04	.03	.061

(a) Absorptance for xenon source.
(b) Absorptance for solar source.

Table B-18 (Cont.)

Hour	Temp. (°K)	Temp. (°F)	ϵ_{TH}	α_H (a) Total	α_H (a) 0.2−0.41	α_H (a) 0.41−0.6	α_H (a) 0.6−0.85	α_H (a) 0.85−	α_s (b) Total
1104	339	150	0.78	0.057	0.26	0.04	0.04	0.03	0.059
1152	339	150	.77	.055	.23	.07	.03	.03	.062
1200	339	150	.79	.056	.26	.05	.03	.03	.059
1272	339	150	.80	.056	.24	.06	.03	.03	.060
1320	339	150	.78	.056	.23	.08	.03	.03	.064
1468	339	150	.80	.054	.22	.08	.02	.03	.061
1536	339	150	.80	.052	.20	.07	.02	.03	.060
1608	339	150	.80	.054	.22	.08	.03	.03	.063
1656	339	150	.78	.056	.25	.05	.03	.03	.059
1704	339	150	.77	.057	.25	.06	.03	.03	.061
1776	339	150	.78	.056	.24	.07	.03	.03	.063
1824	339	150	.79	.057	.23	.07	.05	.03	.057
1944	339	150	.78	.058	.24	.06	.05	.03	.063
1994	339	150	.79	.056	.25	.04	.04	.03	.058
2040	339	150	.78	.059	.24	.06	.05	.03	.063
—	387	232	.74	—	—	—	—	—	—
—	354	177	.76	—	—	—	—	—	—
—	326	122	.79	—	—	—	—	—	—
—	307	93	.79	—	—	—	—	—	—
Before Exposure(c)				.052	.25	.05	.03	.01	.055
After Exposure(c)				.055	.27	.06	.03	.01	.061

(a) Absorptance for xenon source.
(b) Absorptance for solar energy.
(c) From Cary room temperature reflectance measurements.

NASA-Langley, 1969 —— 17 E-5088